

Syntheis and Characterization of a Substituted Benzothiazole Derivatives As Murd Inhibitors Evaluation for their Anti-Microbial Activity

Prof. Dr. Mr. Venkatachalam T¹, Mx. Elakkiya R²

¹Professor, Pharmaceutical Chemistry, Jkkmmrf's Annai Jkk Sampoorani Ammal College Of Pharmacy Komarapalayam - 638 18

²Assistant Professor, Pharmaceutical Chemistry, Jkkmmrf's Annai Jkk Sampoorani Ammal College Of Pharmacy Komarapalayam - 638 18

Abstract:

Resistance to antimicrobials agent among the pathogens has emerged as a worldwide problem in the past 20 years and has escalated in the past decade [1]. From 1962-2000 no new major class of antibiotics has been reported has been stated as innovation gap in antibiotic discovery. The screening of natural products from extract and formation from microorganism has been known as 'Golden Age' of antibacterial. This era is also known as empirical screening as those agents has been selected without knowing their mechanism of action. In order to limit the hits the screening method from 1960 has been modified to subset all the possibilities.

1. INTRODUCTION

Resistance to antimicrobials agent among the pathogens has emerged as a worldwide problem in the past 20 years and has escalated in the past decade [1]. From 1962-2000 no new major class of antibiotics has been reported has been stated as innovation gap in antibiotic discovery. The screening of natural products from extract and formation from microorganism has been known as 'Golden Age' of antibacterial. This era is also known as empirical screening as those agents has been selected without knowing their mechanism of action. In order to limit the hits the screening method from 1960 has been modified to subset all the possibilities.

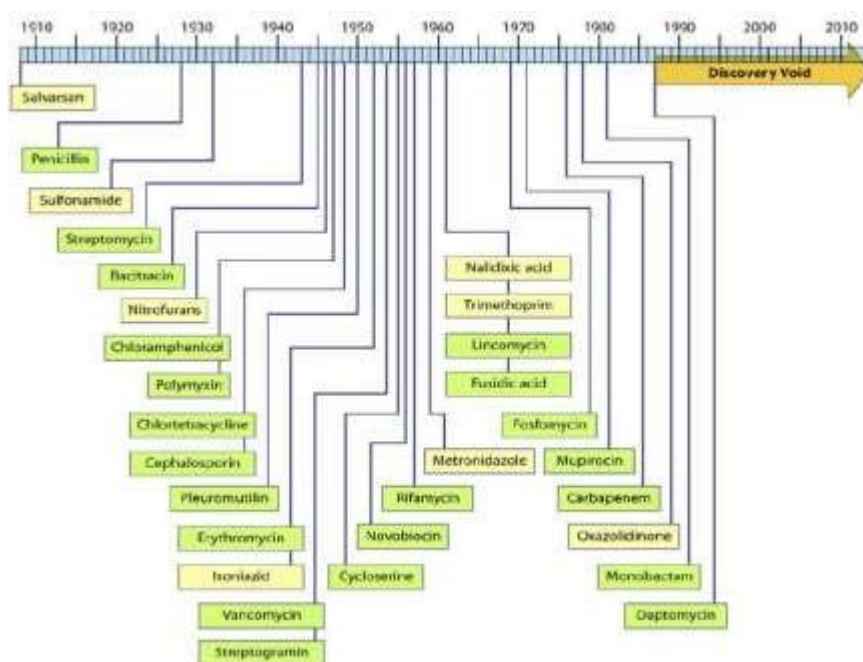


Figure 1: The discovery void are those from the dates indicated by the reported discovery or patent.

The direction of novel antibacterial discovery research (as opposed to that of improving up on established classes) in the past 20 years has been to deploy an array of new technologies, based on genomics, bioinformatics, structural biology, and various high- throughput methods, in an effort to transform the giant leap of novel discovery into doable quantum steps. The fact that successful systemic antibacterial have multiple molecular targets ortargets encoded by multiple genes has been evident for the past 20years (**Figure 1**).

These antibacterial are not subject to high-level target-based resistance by single genetic changes in the host. The hypothesis is that these agents are successful mono therapeutics and not subject to such resistance because they are multi targeted. During the hearing of the Antibiotic Development to Advance Patient Treatment Act (ADAPT), Boston University Law Professor Kevin Outterson said, “In the movies, heroic research scientists discover the cure before the credits roll; in real life, research programs require at least a decade and generally longer to deliver an effective antibiotic” [2].

In an analysis of expenditure on health care, the World Bank report (2014) mentioned that high-income countries invested 12.26% of their gross domestic product (GDP), whereas upper-middle-income countries invested only 6.17% of GDP and low-income countries only 5.75%. Global expenditure for health care was 9.9% of total global GDP [3] Europe is a resource-rich economic setting. Most countries are either high-income or upper-middle- income countries. The region also suffers from high rates of antibiotic resistance. In a report published by the London School of Hygiene and Tropical Medicine, in the European Union, Iceland and Norway the burden of additional hospital care costs due to antibiotic-resistant infections was estimated to be approximately 1.6 billion in the year 2012 [4]. Novel business model: a new business model is necessary in fostering the development of new vaccines and anti-invectives. It is also crucial to strengthen a sustainable market for increasing R&D investment by companies. World over ‘tax credits’ to be given to companies working in new anti-infective development [5].

Urgent Threats

- Carbapenem-resistant *Acinetobacter*
- *Candida auris* (*C.auris*)
- *Clostridioides difficile* (*C.difficile*)
- Carbapenem-resistant *Enterobacteriaceae* (CRE)
- Drug-resistant *Neisseria gonorrhoeae* (*N.gonorrhoeae*) Serious Threats
- Drug-resistant *Campylobacter*
- Drug-resistant *Candida*
- Extended-spectrum beta-lactamase (ESBL)-producing *Enterobacteriaceae*
- Vancomycin-resistant *Enterococci* (VRE)
- Multidrug-resistant *Pseudomonas aeruginosa* (*P.aeruginosa*)
- Drug-resistant non typhoidal *Salmonella*
- Drug-resistant *Salmonella* serotype Typhi
- Drug-resistant *Shigella*
- Methicillin-resistant *Staphylococcus aureus* (MRSA)
- Drug-resistant *Streptococcus pneumoniae* (*S.pneumoniae*)
- Drug-resistant Tuberculosis (TB) Concerning threats
- Erythromycin-resistant group A *Streptococcus*
- Clindamycin-resistant group B *Streptococcus*
- Watch List
- Azole-resistant *Aspergillus fumigatus* (*A. fumigatus*)
- Drug-resistant *Mycoplasma genitalium* (*M. genitalium*)
- Drug-resistant *Bordetella pertussis* (*B. pertussis*)

In 2020, United States of Centers for disease control and prevention (CDC) assessed those antibiotic resistant threats which have been summarized below:

Resistant Germ	Threat Estimate, 2019 report	What CDC Counted, 2019 report	Year-to-Year Comparison Provided, 2019 Report	Resistant Infection Increase/ Decrease, 2019 report
Drug-resistant <i>Neisseria Gonorrhoeae</i>	550,000 infections	All infections	Resistance over from 2000– 2017	Increase
<i>Candida auris</i>	3 clinical cases	Clinical cases	Cases over time from 2015–2018	Increase
EBL-producing <i>Enterobacteriaceae</i>	197,400 cases & 9,100 deaths	Incident hospitalized positive clinical cultures, including hospital- & community-onset	Cases over time from 2012–2017	Increase
Erythromycin- resistant	5,400	Invasive infections	Invasive infection	Increase

group A streptococcus	infections & 450 deaths		rates over time from 2010–2017	
Carbapenem resistant <i>Enterobacteriaceae</i>	13,100 cases & 1,100 deaths	Incident hospitalized positive clinical cultures, including hospital- & community-onset	Cases over time from 2012–2017	Stable
Carbapenem-resistant <i>Acinetobacter</i> (formerly multidrug-resistant <i>Acinetobacter</i>)	cases & 700 deaths	Incident hospitalized positive clinical cultures, including hospital- & community-onset	Cases over time from 2012–2017	Decrease
Drug resistant <i>candida</i> (formerly known as fluconazole resistant <i>candida</i>)	34,800 cases & 1,700 deaths	Incident hospitalized positive clinical cultures, including hospital- & community-onset	Cases over time from 2012–2017	Decrease
Vancomycin-resistant <i>Enterococcus</i>	54,500 cases & 5,400 deaths	Incident hospitalized positive clinical cultures, including hospital- & community-onset	Cases over time from 2012–2017	Decrease
Multidrug-resistant <i>Pseudomonas</i> <i>aeruginosa</i>	32,600 cases & 2,700 deaths	Incident hospitalized positive clinical cultures, including hospital- & community-onset	Cases over time from 2012–2017	Decrease

Methicillin-resistant Staphylococcus aureus	323,700 cases & 10,600 deaths	Incident hospitalized positive clinical cultures, including hospital- & community-onset	Cases over time from 2012–2017	Decrease
Drug-resistant Tuberculosis	847 cases & 62 deaths	Cases	Cases over time from 2012–2017	Stable

Clostridioides difficile	223,900 estimated cases in hospitalized patients & 12,800 deaths	Infections requiring hospitalizations or in already hospitalized patients	Cases over time from 2012–2017	Decrease*
Drug-resistant Campylobacter	448,400 infections & 70 deaths	All infections	Percentage of resistance over time from 1997–	N/A
Drug-resistant non-typhoidal Salmonella	212,500 infections & 70 deaths	All infections	2017	N/A
Drug-resistant Salmonella Serotype Typhi	4,100 infections & <5 deaths	All infections	Percentage of resistance over time from 2009–	Increase
Drug-resistant Shigella	77,000 infections & <5 deaths	All infections	2017	N/A
Drug-resistant Streptococcus Pneumoniae	900,000 infections & 3,600 deaths	All infections	Percentage of resistance over time from 1999–	N/A
Clindamycin-resistant group B Streptococcus	13,000 infections & 720 deaths	Invasive infections	2017	N/A

Methicillin-resistant *Staphylococcus aureus* (MRSA) is one of the most important pathogens worldwide, accounting for more than 80 000 severe infections in the USA alone in 2011 and for more than one-half of hospital-related *S. aureus* infections in most Asian countries. The Asia-Pacific region is the most populous region in the world, with one-third of the world's population with rapid urbanization, a significant proportion of people in this region live in high-density cities, which increases the risk of the development and spread of AMR. As MRSA remains an important cause of nosocomial and community-acquired infections in the region, and antimicrobial susceptibility patterns may differ between HA-MRSA and CA-MRSA strains, knowledge of their respective distributions in the population is important for the treatment and management of MRSA infections. In addition to infections, there have also been increasing reports of MRSA carriage in various population groups in the region, including in young children and adults. Whilst MRSA carriers do not experience clinical symptoms as a result of carriage, they may be at higher risk of MRSA infection especially in the event of hospitalization.

or major invasive procedures. Hospital-associated MRSA is a serious problem worldwide, including in Asia. In an investigation regarding the spread of MRSA between the community and hospitals in Asian countries, MRSA accounted for 25.5% of community-associated (CA) *S. aureus* infections and 67.4% of Hospital-associated infections [6]. In India among the gram positive organisms, 42.6% are *S. aureus* were methicillin resistant and 10.5% *E. faecium* were vancomycin-resistant [7]. Most of the resistance proportions of MRSA infections reported in the Asia-Pacific region in this study (range: 0–98.4%) were comparable with resistance proportions reported in Europe (19.7–21.5%) and the Middle East (12.4–30%) and lower than those reported in the USA (29–43.2%) and Africa (16–55%). East Asian locations reported the highest resistance proportions (>40%) in the region, followed by Southeast Asian locations (20% and 30%). MRSA prevalence's reported in the Asia-Pacific region are similar to those reported in other regions and are typically between 1% and 25% [8–15]. As *S. aureus* most commonly causes skin and soft tissue, respiratory tract and bloodstream infections, most studies reported prevalence and resistance proportions of MRSA infections in isolates sampled from one or more of these sites (**Figure 2**). No statistically significant differences in prevalence or resistance proportions of MRSA infections in blood, respiratory tract, or skin and wound samples were found.

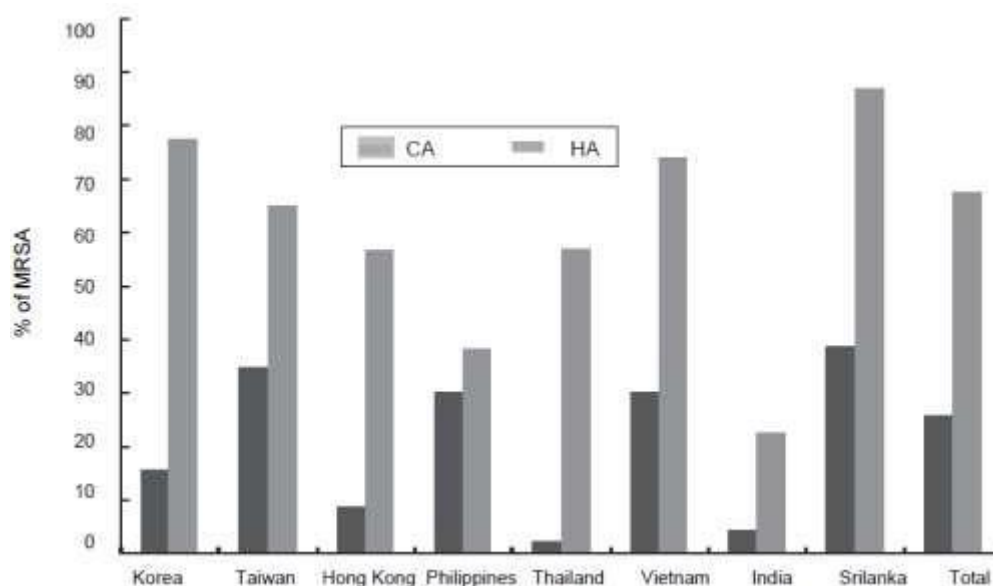


Figure 2: Distribution of community-acquired (CA) and hospital-acquired (HA) infections caused by methicillin-resistant *S. aureus* (MRSA) in selected countries in Asia. Korea refers to South Korea.

Healthcare-associated infection with MDR *Enterobacteriaceae* is greatly heterogeneous. Specifically, *Escherichia coli* and *K. pneumoniae* raise key therapeutic problems due to their rapid development of resistance and high incidence of multidrug resistance, particularly as few therapeutic options remain [16]. The most clinically relevant resistance mechanisms in these species, namely the production of ESBLs that hydrolyze most β lactam antibiotics except carbapenems and β -lactamase inhibitor combinations, are typically associated with unrelated resistance determinants for fluoroquinolones, aminoglycosides and tetracyclines. MDR phenotypes among *E. coli* strains producing ESBLs may reach rates of >80% [17]. *Escherichia coli* is one of the major etiologies causing bacteremia, urinary tract infections (UTIs) and intra-abdominal infections (IAIs). This pathogen causing UTI in the Asia-Pacific

region in 2009 and 2010 showed that only ca. 54.6– 76.7% of 995 *E. coli* isolates were susceptible to third- and fourth-generation cephalosporin's, and the susceptible rates to ciprofloxacin and levofloxacin were 43.1% and 44.3%, respectively [18] (**Figure 3**). It also has an important reservoir in animals and the environment. Owing to the almost exclusive use of fluoroquinolones in CA-UTIs in many European countries, this drug class lost its efficacy against *E. coli* at an unprecedented speed (EARS-Net 2008). Fluoroquinolones resistance combined with the growing prevalence of ESBLs has narrowed the therapeutic options for patients with enterobacterial infections and has increased dependence on carbapenems even in outpatients [19]. *K. pneumoniae* can cause various types of infections, including pneumonia, intra-abdominal infections, bacteraemia and UTIs. In Asian countries such as Taiwan and South Korea, *K. pneumoniae* is an important cause of some community-acquired syndromes, in contrast to Europe and the USA. Moreover, the drug resistance pattern of *K. pneumoniae* may be different in the setting of community- acquired infection and healthcare-associated infections. In China, an investigations of 1025 *K. pneumoniae* isolates revealed that ertapenem, imipenem, amikacin and TZP remained active against *K. pneumoniae* isolates regardless of whether the source was HA or CA and regardless of ESBL production. Another Asia-Pacific surveillance study of 243 *K. pneumoniae* causing UTIs showed similar findings that >90% of isolates were susceptible to ertapenem, imipenem and amikacin. In addition, the susceptible rates to cefepime, ceftazidime and ceftriaxone were only 67.5%, 66.3% and 59.3%, respectively. Overall, most of the *K. pneumoniae* isolates in Asia are still susceptible to carbapenems and aminoglycosides [20].

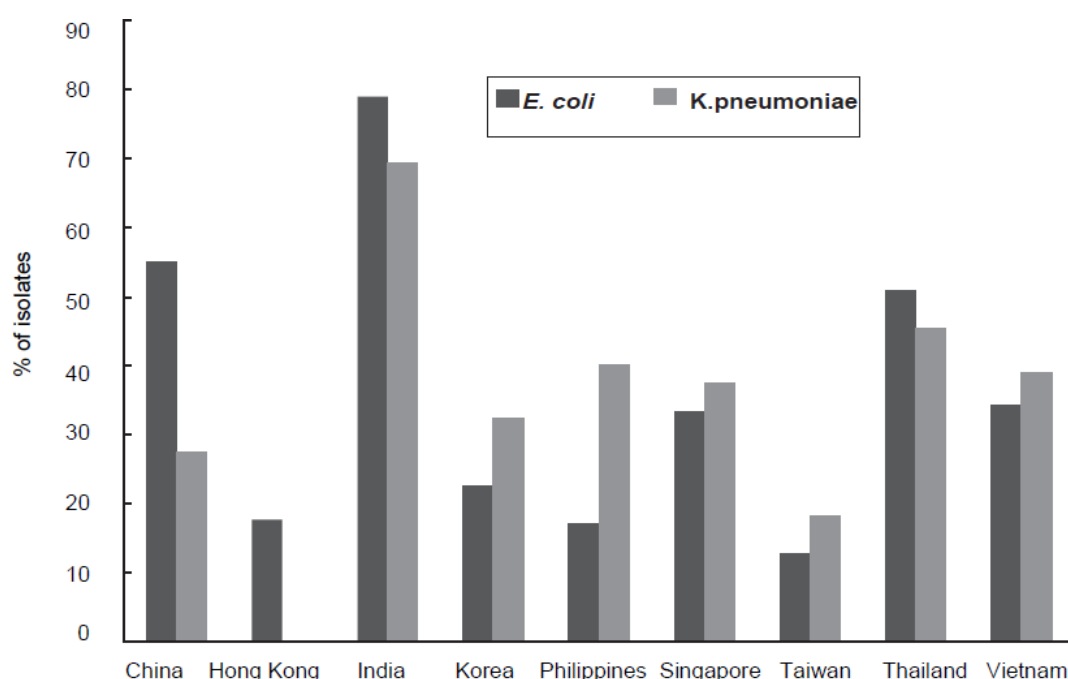


Figure 3: Extended-spectrum β-lactamase (ESBL)-positive rates (% of isolates on y-axis) among *E. coli* and *K. pneumoniae* isolates in selected countries in Asia. Korea refers to South Korea.

ESBL-producing *Enterobacteriaceae* have become a critical issue worldwide, and Asia is no exception, even in the setting of community-acquired infection. The percentage of ESBL- producers among *E. coli* was 79% (India), 55% (China), 50.8% (Thailand), 34.4% (Vietnam), 17.8% (Hong Kong), 33.3% (South Korea and Singapore),

17.0% (The Philippines) and 12.7% (Taiwan). Among *K. pneumoniae* isolates, the ESBL-positive rate was 69.4% (India), 45.5% (Thailand), 40.0% (The Philippines), 39.1% (Vietnam), 37.5% (Singapore), 32.4% (South Korea), 27.5% (China) 18.3% (Taiwan) and 0% (Hong Kong) (Fig. 3). For *K. oxytoca*, the overall ESBL-positive rate was 40.5%, which was highest in India (77.4%) and lowest in Taiwan (14.8%) [21, 22].

As per the ‘scoping report on antimicrobial resistance in India (2017)’, under the aegis of government of India, among the Gram-negative bacteria, more than 70 per cent isolates of *E. coli*, *K. pneumoniae* and *A. baumannii* and nearly half of all *P. aeruginosa* were resistant to fluoroquinolones and third generation cephalosporins. Although the resistance to drug combination of piperacillin-tazobactam was still <35 per cent for *E. coli* and *P. aeruginosa*, the presence of multiple resistance genes including carbapenemases made 65 per cent *K. pneumoniae* resistant. Increasing rates of carbapenem resistance to the tune of 71 per cent in *A. baumannii* led to frequent use of colistin as the last resort antimicrobial. The resistance to colistin has also emerged in India. Although the rate of colistin resistance was <1 per cent, except for 4.1 per cent reported by Gandra et al [12], high mortality of 70 per cent was associated with colistin resistant *K. pneumoniae* [7]. *S. pneumoniae* is one of main etiologies of pneumonia, meningitis, otitis media and sinusitis. The antibiotic resistance pattern can be affected by many factors, such as serotypes, vaccination, disease patterns and patient group [23-26]. In a surveillance of 2184 *S. pneumoniae* isolates from 60 hospitals in 11 Asian countries from 2008 to 2009, the overall resistance to erythromycin was 72.7% and the highest rates were noted for China (96.4%), Taiwan (84.9%) and Vietnam (80.7%). In Malaysia, 35.2% of pneumococcus isolates were erythromycin-susceptible, 4.2% were intermediate and 60.6% were resistant in a multicenter surveillance study [24].

All of the above results indicate that an increase in macrolide resistance among pneumococci developed in Asia, particularly in China and Sri Lanka, and these findings are consistent with previous studies in western countries [25-27]. Furthermore, the level of macrolide resistance has increased, with very high MIC₉₀ values (minimum inhibitory concentration required to inhibit 90% of the isolates) (64 mg/mL to ≤128 mg/mL) in China, Hong Kong, Japan, South Korea, Malaysia, Sri Lanka, Taiwan, Thailand and Vietnam [24]. Among non-meningeal isolates, the non-susceptible rate of pneumococci to penicillin (MIC

≤ 4 mg/mL) was 4.6%, and penicillin resistance (MIC ≤ 8 mg/mL) was extremely rare (0.7%) [24]. In addition, the non-susceptible rate to ceftriaxone was 8.6% and was highest in Sri Lanka and China (Fig. 3) [24]. In Saudi Arabia, the prevalence and rate of penicillin resistance and non-susceptibility among *S. pneumoniae* isolates have significantly increased with time [28]. For fluoroquinolones, the overall resistance rates remained as low as 1.7%, 0.4%, 1.5% and 13.4% for levofloxacin, moxifloxacin, gatifloxacin and ciprofloxacin, respectively [24]. In contrast, the overall rate of multidrug resistance (defined as resistance to more than any three antimicrobial agents of different classes) was 59.3%, with the highest rate in China (83.3%), followed by Vietnam (75.5%), South Korea (63.9%), Hong Kong (62.2%) and Taiwan (59.7%) [24] (**Figure 2**).

Among different serotypes, serotype 19A and 6A had high erythromycin resistance rates of 86.0% and 85.7%, respectively [24]. In addition, 19.1% of serotype 19A isolates were not susceptible to penicillin, and serotype 19A isolates had a higher prevalence of multidrug resistance than non-19A isolates (79.8% vs. 58.0%), especially in Hong Kong (100%), China (94.7%), Taiwan (90.9%) and South Korea (90.6%) [30]. Although most pneumococci are susceptible to penicillin and fluoroquinolones, close monitoring of the drug resistance pattern for each serotype is still indicated.

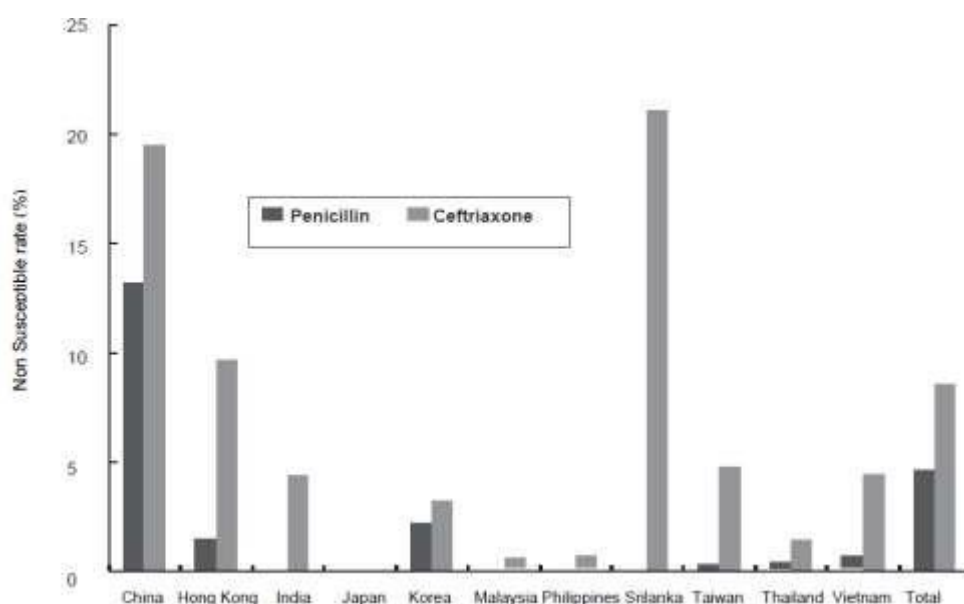


Figure 4: Non-susceptible rates (including intermediate-resistant and resistant) to penicillin and ceftriaxone of *S. pneumoniae* in selected Asian countries. Korea refers to South Korea.

In the past two decades, acquired multi-drug resistant infections have increased due to the production of β -lactamases (eg, extended spectrum β -lactamases [ESBLs] enzymes, carbapenemases, and metallo- β -lactamases), leading to third generation cephalosporin and carbapenem resistance [29]. Among 21 known AMR genes, the important genes responsible for MDR *Salmonella* and *E. coli* are AmpC, bla-TEM-1, bla-CTXM-15, VIM-1, NDM-1, floR, tetG, and the recent mcr-1 gene coding colistin drug resistance [30-32].

Bacteria mainly use two mechanisms for resistance: 1) Intrinsic resistance and 2) acquired resistance. The ability of a bacterium to resist the action of a specific antibiotic due to inherent structural or functional properties is known as intrinsic resistance. *Pseudomonas* displays a very good example of intrinsic resistance mechanism, due to the absence of a susceptible target site for a particular antibiotic [25]. Triclosan which is a broad-spectrum biocide especially against Gram-positive bacteria and several Gram-negative bacteria as well is incapable of preventing the growth of *Pseudomonas*. Initially, it was supposed that active efflux is the reason behind this resistance, but recently the presence of fab I (insensitive allele) encoding an extra enoyl-acyl carrier protein reductase enzyme, which is a target site for triclosan, has been reported [33, 34]. This intrinsic mechanism may also help bacteria to acquire resistance including antibiotic efflux or poor drug penetration resulting in the reduction of the intracellular concentration of antibiotic, modification of the antibiotic target site due to posttranslational target modification or genetic mutation of the target, and inactivation of the antibiotic by modification or hydrolysis [35-38]. Plasmid coding colistin-resistant (mcr-1 dependent) *E. coli* was first isolated from raw meat, animals, and humans in China [39].

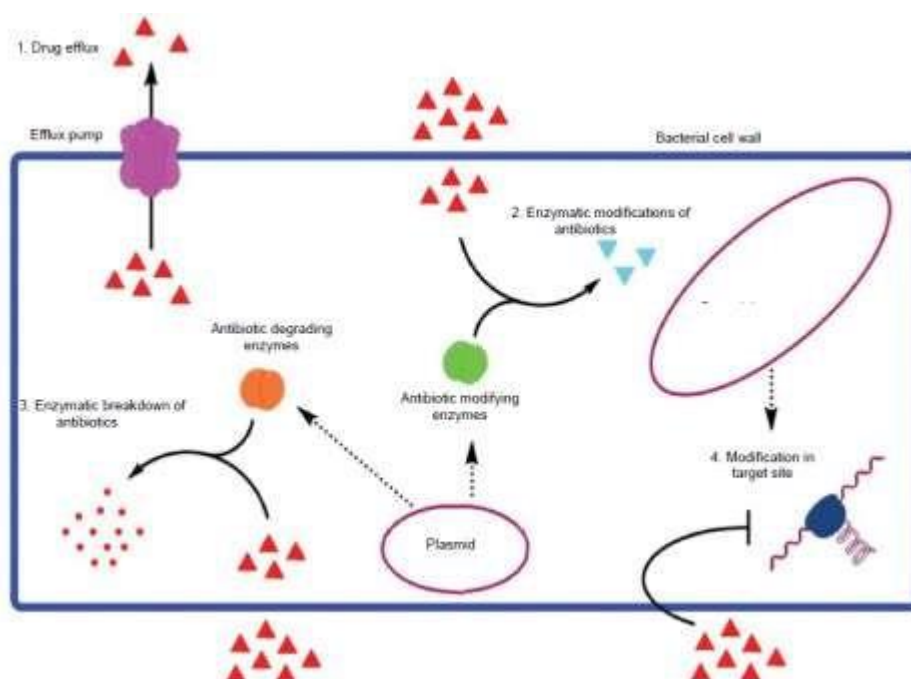


Figure 5: Various mechanisms of antibiotic resistance, including drug efflux with the help of efflux pump, enzymatic modifications of the antibiotic, enzymatic breakdown of the antibiotics, and modification in the target sites.

There are four main molecular mechanisms by which bacteria may resist the effects of antibiotics; modification of the target site, modification or destruction of the antibiotic, antibiotic efflux via efflux transporters and reduced antibiotic influx through decreased membrane permeability (**Figure 5**) [40]. These resistance mechanisms can be present together in different combinations in one bacterial cell, potentially allowing high level resistance to multiple antibiotic compounds simultaneously [41]. Some bacteria possess an innate insensitivity towards certain classes of antibiotics (intrinsic resistance), either through naturally possessing any of the above mechanisms in the absence of artificial antibacterial selection pressure (ampicillin resistance in *Klebsiella* spp.), lack of the antibiotic target (vancomycin resistance in lactobacilli) or lack of a metabolic pathway or enzyme necessary for the activation of the drug (metronidazole resistance in aerobic bacteria) [42,43].

The genes encoding different resistance mechanisms are often located on transposons, which makes it easier for them to be transmitted between different bacteria, and some transposons may contain specialized regions called integrons able to include different resistant genes, thereby making a bacterial species resistant to multiple different antibiotics [44]. In addition, bacteria can also have physical states which aid in resisting antibacterial pressure. A variety of both Gram-positive and Gram-negative bacterial species are known to assemble in biofilms [45] hydrated matrices of extracellular polymeric substance in which the bacterial cells are embedded allowing adherence to both each other and external surfaces. Such structures become problematic when located in urinary catheters or on medical implants; since biofilms are harder for antibiotics to penetrate at lethal concentrations, the biofilm provides resistance to antibiotic action [46]. The bacterial population within the biofilm can also enter into a dormant state where they are not actively growing, and this can also contribute to antibiotic resistance [47,48].

The occurrence of resistance in microbes is a natural process (**Figure 6**); until now, antibiotic

resistance selection is driven using different antibiotics in health care systems, environment, and in agriculture/livestock. Additional important factors which are potent drivers of antibiotic resistance include sanitation settings, infection control standards, water hygiene systems, drug quality, diagnostics and therapeutics, and travel or migration quarantine. In addition to the mutation in various genes residing on the chromosome of the microorganism, exchange of genetic material between organisms plays a vital role in the distribution of antibiotic resistance [49]. Plasmid transmission is the most important phenomenon which may transfer genes of antibiotic resistance to the host cell. Antibiotics may influence this process by inducing the transmission of resistance elements; these antimicrobials may additionally exert a selective pressure to the emergence of resistance [40, 50]. Demonstration of transmission dynamics of resistance has increased the awareness and understanding of how resistant pathogens transmit from human to human [51]. At the community level, feco–oral route is the most important route of transmission especially for resistant pathogens of the family *Enterobacteriaceae*, usually due to sanitation failure. Community-acquired (CA)-MRSA is also a good example to understand the transmission dynamics of resistance at the human–human level, which is usually transmitted due to prolonged hospital stay or unhygienic hospital settings. Sexual contact is also a source of transmission for resistant *N. gonorrhea* [52–54]. Another very important facet known as “one health” also plays a significant role in the transmission dynamics of antibiotic resistance [48]. Irrational use of antimicrobial growth promoters in farm animals is associated with the transmission of resistance to humans via animal products; important pathogens under consideration in this aspect are *Salmonella* spp. and *Campylobacter* spp. additionally, indistinguishable resistant mechanisms have been found in bacteria isolated from humans or animals. Resistant bacteria and mobile genetic elements (MGEs) may make their way from animals to humans through various means [55–57]. The influence of the environment toward antibiotic resistance is also a concern. In the agriculture sector, metals are used as microbicides and may contribute critically to resistance development. The role of sewage systems, pharmaceutical industry pollution, and waste management procedures in human– environment transmission are also well documented. A number of resistant pathogens have been isolated from pre- and post-treatment sewage systems [52, 58].

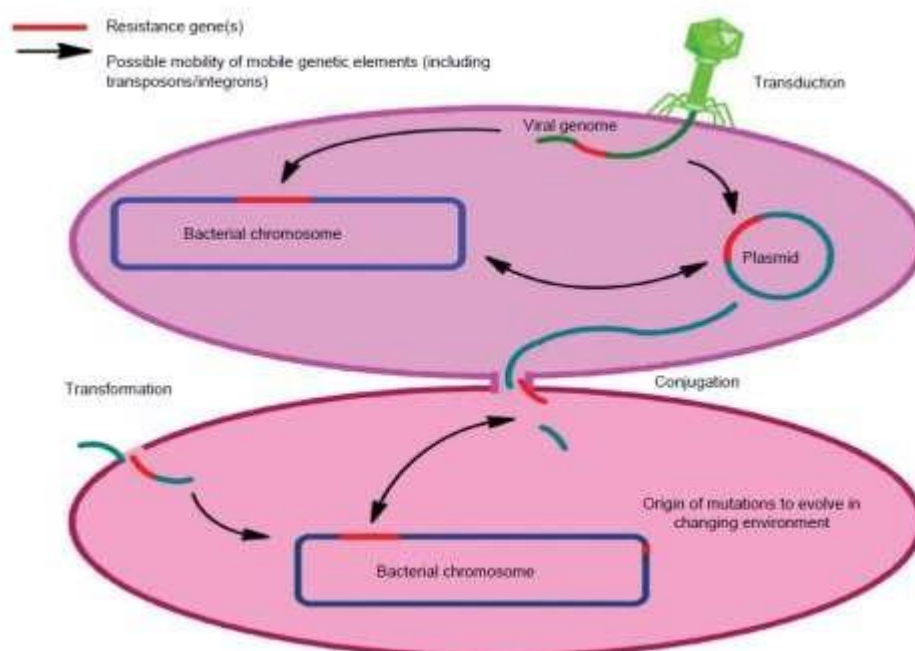


Figure 6: Drivers of antibiotic resistance transmission.

Staphylococcus aureus is a major human pathogen that causes a wide range of clinical infections. It is a leading cause of bacteremia and infective endocarditis as well as osteoarticular skin and soft tissue bacterial meningitis pleuropulmonary and device-related infections. A major cause of concern has been the emergence of methicillin-resistant strains of *S. aureus* (MRSA). Despite, antibacterial therapy methicillin-resistant *S. aureus* (MRSA) is still one of the most widespread and virulent nosocomial pathogens in the world causing a major public health concern. An approach to combat this situation is to discover and develop novel antibiotics with new mechanism of action. MRSA pneumonia has become much more widespread responsible for a significant number of the over 18,500 deaths attributed to MRSA in 2005. In the industrialized world, the population incidence of *S. aureus* bacteremia (SAB) ranges from 10 to 30 per 100,000 person-years. The HIV-infected population has a significantly increased incidence of SAB. Two studies reported incidences of SAB in HIV-infected patients of 494 per 100,000 person-years and 1,960 per 100,000 person-years, or 24 times that of the non-HIV- infected population. The overall incidence of IE was estimated to be 1.5 to 6 per 100,000 person-years. *S. aureus* causes a variety of skin and soft tissue infections (SSTIs), ranging from the benign (e.g., impetigo and uncomplicated cellulitis) to the immediately life- threatening. Emergence of a worldwide epidemic of community-associated (CA) MRSA SSTIs is reported in the past 15 year.

The essential component of the bacterial cell wall is peptidoglycan, which is responsible for maintaining the cell shape and exert mechanical resistance to the higher internal osmotic pressure. Thus, the effective antimicrobial agents are those which can interfere with the assembly and proper biosynthesis of peptidoglycan. As these peptidoglycan- structure are unique to the prokaryotic cells and not present in eukaryotic cells, so, selecting the vital microbial pathways for drug target is optimal. Peptidoglycan consists of linear glycan chains interlinked by short peptides. The glycan chains are composed of alternating units of N- acetylglucosamine and N-acetyl muramic acid. Muramyl residues bear short pentapeptides, a proportion of which are cross-linked either directly or through a second short peptide. It is this cross-linkage that joins the glycan chains into a macromolecular network of high tensile strength and rigidity. A recent review extensively discussed the genetic, biochemical and physiological data concerning the biosynthesis of peptidoglycan monomer unit [59]. The biosynthetic pathway of peptidoglycan is a complex two-stage process. The first stage, which occurs in the cytoplasm, is the formation of the monomeric building block N-acetylglucosamine–N-acetyl muramyl pentapeptide. The first committed step in the pathway is the transfer of an enolpyruvate residue from phosphoenol pyruvate (PEP) to position 3 of UDPN- acetylglucosamine. This reaction is catalyzed by MurA. This is followed by a MurB-catalysed reduction of the enolpyruvate moiety to D-lactate, yielding UDPN-acetyl muramate. A series of ATP-dependent amino acid ligases (MurC, MurD, MurE and MurF) catalyse the stepwise addition of the pentapeptide side-chain on the newly reduced D-lactyl group, resulting in the formation of UDPN-acetyl muramoyl pentapeptide. A large number of antibiotics in clinical use, mostly β -lactams and glycopeptides, act by inhibiting the later steps in peptidoglycan biosynthesis. However, the earlier steps of the biosynthesis of cytoplasmic peptidoglycan precursor are poorly exploited as antibacterial targets: none of the enzymes involved in these steps is inhibited by known antibiotics or synthetic chemicals of therapeutic usefulness, except for MurA, which is inhibited by fosfomycin. The MurA to MurF genes are all essential in bacteria. In addition, Mur proteins are highly conserved among various bacterial species, and common structural motifs can be identified. For this reason, a potential Mur

inhibitor would be expected to be bactericidal and to have a wide spectrum, which validates the choice of these important bacterial enzymes as targets for the development of new inhibitors [60]. The pathway where Mur enzymes are involved in the early stage of peptidoglycan synthesis of bacterial cell has been shown in **Figure 7**.

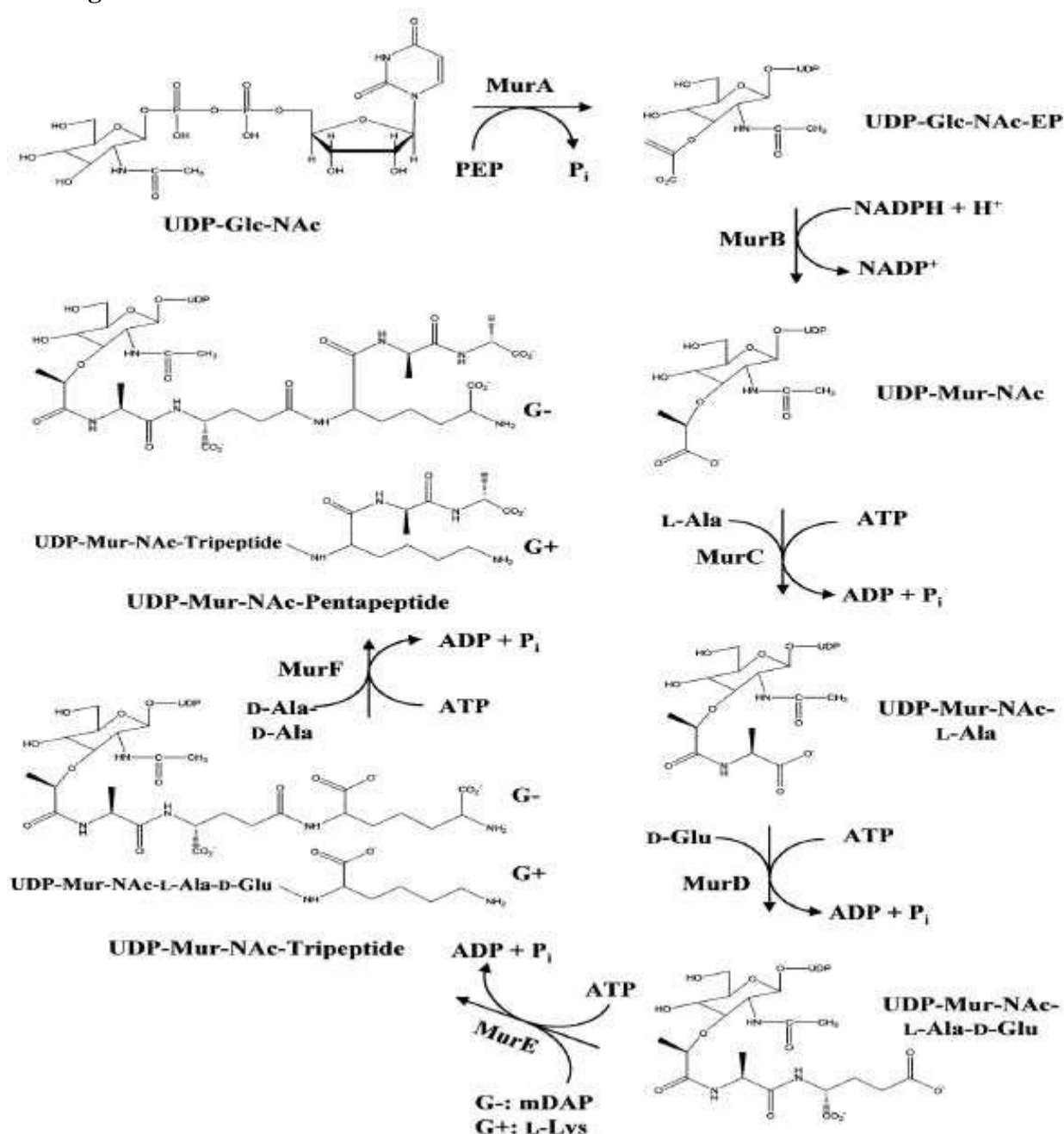


Figure 7: Conversion of UDPN-glucosamine to UDPN-acetyl muramoyl pentapeptide by the sequential action of MurA to MurF enzymes. UDP-Glc- NAc, UDPN-acetyl glucosamine; UDP-Glc-NAc-EP, UDPN-acetyl glucosamine enolpyruvate; UDP-Mur-NAc, UDPN-acetyl muramic acid; mDAP, meso-diaminopimelic acid; G+, Gram-positive bacteria; G–, Gram- negative bacteria.

1.2. MurD enzyme

Early stages of its biosynthetic pathway, specially topologically similar adenosine triphosphate (ATP)

dependent MurC-F ligases are considered one of the most important targets for the discovery of new antibacterial agents [60, 61]. Using the site-directed mutagenesis study, seven residues and the GXXGKT/S ATP-binding consensus sequence has been identified as common invariants among Mur ligases from various bacterial organisms [62]. However, differences are observed in topologies and amino acid sequences of the catalytic pockets of MurD ligases from *Streptococcus pneumoniae*, *Mycobacterium tuberculosis*, *Escherichia coli*, *Staphylococcus aureus* and *Borrelia burgdorferi*. 46973 DaMurD ligase catalyzes the second step in the biosynthesis of peptidoglycan and incorporate D-glutamic acid (D-Glu) to an alanyl residue of the UDP-N-acetylmuramoyl-L-alanine precursor. Its high specificity for D-amino acid substrate, ubiquity among bacteria and its absence in mammals [61, 63] makes this enzyme a promising target. The binding pocket of MurD comprises three globular domains; N-terminal domain which accounts for the fixation of the UDP moiety of UMA, a well conserved central domain and C-terminal domain also known as D-Glu binding site. N-terminal domain consists of five stranded parallel β -sheet surrounded by four helices while the central domain comprises six stranded parallel β -sheet surrounded by seven α -helices and three stranded antiparallel β -sheet. C-terminal domain comprises a six stranded β -sheet surrounded by five α -helices [64]. The ATP binding pocket of MurD is formed in a cleft between the C-terminal and central domains (Fig. 1). It is evident from the structural characteristics that the catalytic pocket amino acids that interact with the UMA and ATP could be exploited to improve the binding affinity of MurD inhibitors [65]. Conformational changes are induced in the C and N-terminal domains and loops after substrate binding with the enzyme. Due to these changes, UMA and ATP are brought together and oriented properly in the cleft by MurD ligase for the formation of an acyl phosphate intermediate. D-Glu is also oriented by this enzyme for the nucleophilic attack and thus stabilizes the tetrahedral intermediate and promotes catalysis [66]. MurD enzyme from *Escherichia coli* showed sequence identities of 31% with *Bacillus subtilis* and 62% with *Haemophilus influenza* [64]. Further, sequence alignment of MurD proteins from *Escherichia coli* and *Staphylococcus aureus* showed conserved amino acid residues in both the organisms [67]. These findings have aroused intense interest to explore different scaffolds as potent inhibitors against MurD active site.

The inhibition of substrate UDP-N-acetyl muramyl-L-alanine was investigated in MurD enzymes from *Enterococcus faecalis*, *Staphylococcus aureus*, *Escherichia coli* and *Haemophilus influenza* [63]. It is observed that for the optimal activity MurDs of Gram-negative bacteria require NH_4^+ and/or K^+ , but not Na^+ , while SO_4^{2-} and Cl^- did not exhibit any effect on the tested enzyme activities. It is concluded that at the early stage of peptidoglycan biosynthesis pathway two Gram-negative bacteria i.e., *Escherichia coli* and *Haemophilus influenza* use more stringent regulation of cell wall biosynthesis compared to the other two studied Gram-positive bacteria. The 3D structure of MurD with N-terminal, central-domain and C-terminal has been shown in **Figure 8**.

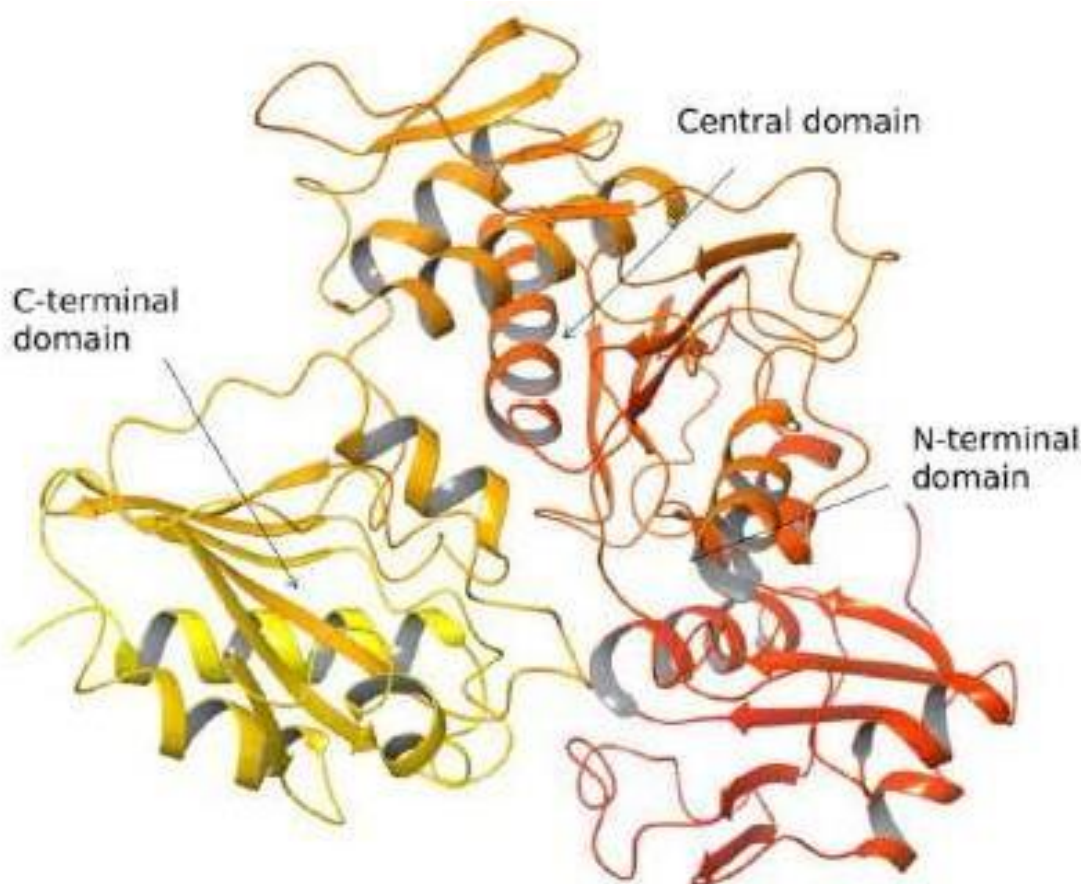
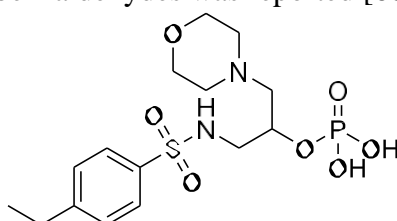


Figure 8: Represents catalytic domains of *E. coli* MurD enzyme (2JFF.pdb)

2. LITERATURE REVIEW

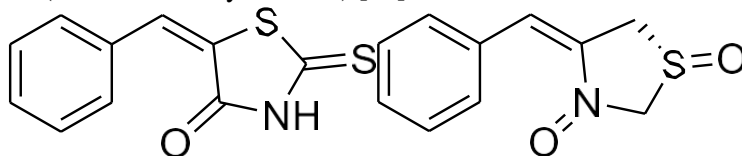
1. **Frlan et al., (2008)** studied the Design and Synthesis of Novel N- Benzyldenesulfonohydrazide Inhibitors of MurC and MurD as Potential Antibacterial Agents. In this study a series of novel N-benzylidene sulfonohydrazide compounds were designed and synthesized as inhibitors of UDP-N-acetylmuramic acid:L-alanine ligase (MurC) and UDP-N-acetylmuramoyl-L-alanine:D-glutamate ligase (MurD) from *E. coli*, involved in the biosynthesis of bacterial cell-walls. Some compounds possessed inhibitory activity against both enzymes with IC₅₀ values as low as 30 μ M. In addition, a new, one-pot synthesis of amidobenzaldehydes was reported [68].



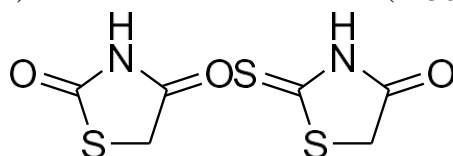
2. **Sova et al., (2008)** described Phosphorylated hydroxyethylamines as novel inhibitors of the bacterial cell wall biosynthesis enzymes MurC to MurF. In search of potent MurD inhibitors, four series of Nacylhydrazones were synthesized and evaluated for their inhibition of MurD. These compounds were also tested for their in vitro antibacterial activities. This compound also exhibited weak antibacterial activity against *Escherichia coli* 1411, *Escherichia coli* SM1411 and *Staphylococcus*

aureus 8325-4 with MIC value of 128 $\mu\text{g/ml}$ in all cases. In this compound removal or replacement of one hydroxy group with a methoxy group resulted in decrease of inhibitory activity against MurC and complete loss of activity against MurD. Phosphorylated hydroxyethylamine have also been developed as inhibitors of MurC to MurF ligases [85]. The IC_{50} values in the micro molar range make these inhibitors good candidates for the development of multiple inhibitors of Mur ligases. Among the series, 1-(4-ethylphenylsulfonamido)-3- morpholinopropan-2-yl dihydrogen phosphate (2) was discovered as most potent inhibitor of *E. coli* MurD with 28% inhibition at 500 μM concentration [69].

3. **Tosmic et al., (2009)** studied Synthesis and biological evaluation of new glutamic acid- based inhibitors of MurD ligase. In this study the glutamic acid substituted 5- benzylidene-2-thioxothiazolidin-4-ones and 5-benzylidene-2,4-thiazolidin-2,4-diones constitute another large family of MurD inhibitors. Structural modification of glutamic acid possessing quinazoline-2,4-diamine based virtual hit resulted in benzylidene-2- thioxothiazolidin-4-ones and 5- benzylidene-2,4-thiazolidin-2,4-diones as potential inhibitors of MurD from *Escherichia coli*. Among all synthesized compounds, 5- benzylidenetherhodanines (S)-17 and (R)-17 exhibited the highest inhibitory activity against *Escherichia coli* MurD (IC_{50} values 206 and 174 μM , respectively). While compounds bearing 5-benzylidene-2,4-thiazolidin-2,4-dione moiety showed residual activity in the range 68-88% when tested at concentration of 250 μM . 5- benzylidenetherhodanines (S)-17 and (R)-17 also exhibited inhibitory activity against MurC-F (residual activity 76-96%) [70].

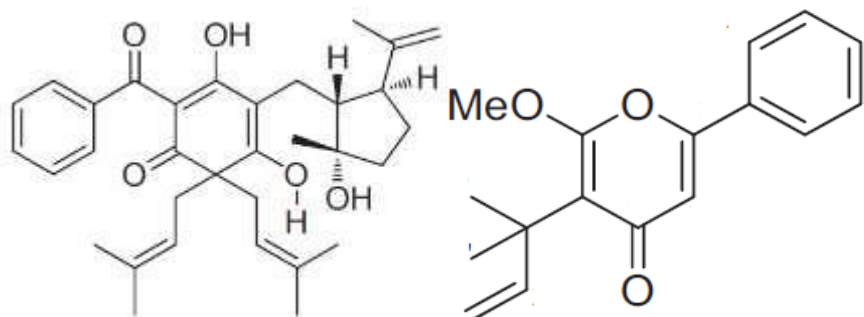


4. **Tomasic et al., (2011)** studied the Novel 2-thioxothiazolidin-4-one inhibitors of bacterial MurD ligase targeting D-Glu-and diphosphate-binding sites. In continuation of the previous work further structural modifications of compounds was attempted to improve the activity. But no improvement in activity was observed against MurD when a short linker between the glutamic acid moiety and 2,4-thiazolidin-dione or 2- thioxothiazolidin-4-one scaffolds was introduced. Among all synthesized compounds, the **20(S)** was observed to be most potent against *Escherichia coli* MurD with an IC_{50} value of 10 μM . It is important to note that the most potent compound contained L-Glu, while the D-Glu-containing derivative **20 (R)** was found to be less active (IC_{50} 45 μM) [71].

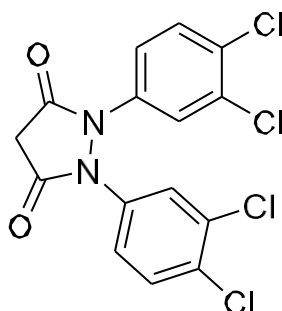


5. **Osman et al., (2012)** studied the antibacterial from *Hypericum acmosepalum* inhibits ATP-dependent MurE ligase from *Mycobacterium tuberculosis*. In this project project to characterise new antibacterial chemotypes from plants, hyperenone A and hypercalin B were isolated from the hexane and chloroform extracts of the aerial parts of *Hypericum acmosepalum*. Hyperenone A and hypercalin B exhibited antibacterial activity against multidrug-resistant strains of *Staphylococcus aureus*, with minimum inhibition concentration ranges of 2–128 mg/L and 0.5–128 mg/L, respectively. Hyperenone A also showed growth-inhibitory activity against *Mycobacterium*

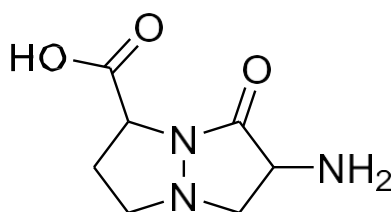
tuberculosis H37Rv and Mycobacterium bovis BCG at 75 mg/L and 100 mg/L. Neither hyperenone A nor hypercalin B inhibited the growth of Escherichia coli and both were non-toxic to cultured mammalian macrophage cells. Both compounds were tested for their ability to inhibit the ATP-dependent MurE ligase of M. tuberculosis, a crucial enzyme in the cytoplasmic steps of peptidoglycan biosynthesis. Hyperenone A inhibited MurE selectively, whereas hypercalin B did not have any effect on enzyme activity [72].



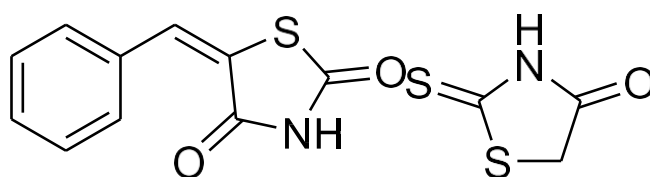
6. **Barreteau et al., (2012)** studied MurD enzymes from different bacteria: evaluation of inhibitors. Biochemical pharmacology. In present work 20 Escherichia coli MurD inhibitors have been tested against the MurD enzymes from Streptococcus pneumoniae, Borrelia burgdorferi, Staphylococcus aureus, and Mycobacterium tuberculosis. Most of the tested inhibitors exhibited less activity against the four other orthologues. This may be due to the differences in topologies of the active sites and the amino acid sequences of the MurD ligases studied [73].
7. **Yang et al., (2012)** described 3,5-Dioxypyrazolidines, Novel Inhibitors of UDP-N-Acetylenolpyruvylglucosamine Reductase (MurB) with Activity against Gram-Positive Bacteria. A series of 3,5-dioxypyrazolidines was identified as novel inhibitors of UDP- N-acetylenolpyruvylglucosamine reductase (MurB). Compounds 1 to 3, which are 1,2- bis(4-chlorophenyl)-3,5-dioxypyrazolidine-4-carboxamides, inhibited Escherichia coli MurB, Staphylococcus aureus MurB, and E. coli MurA with 50% inhibitory concentrations (IC₅₀s) in the range of 4.1 to 6.8 M, 4.3 to 10.3 M, and 6.8 to 29.4 M, respectively. Compound 4 showed moderate inhibitory activity against E. coli MurB, S. aureus MurB, and E. coli MurC (IC₅₀s, 24.5 to 35 M). A fluorescence binding assay indicated tight binding of compound 3 with E. coli MurB, giving a dissociation constant of 260nM. Structural characterization of E. coli MurB was undertaken, and the crystal structure of a complex with compound 4 was obtained at 2.4 Å resolution. The crystal structure indicated the binding of a compound at the active site of MurB and specific interactions with active-site residues and the bound flavin adenine dinucleotide cofactor [74].



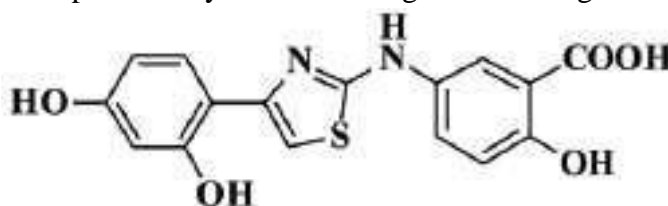
8. **Novak et al., (2013)** studied the Synthesis of pyrazolo [1, 2-a] pyrazole-based peptide mimetics. In this study the peptides based 3-amino-2-oxo-1,5- diazabicyclo[3.3.0]octane-8-carboxylic acids were synthesized and evaluated for their inhibitory activity against Escherichia coli MurD. Among them inhibitors 24-27 (Figure 20) exhibited 50% residual activity [75].



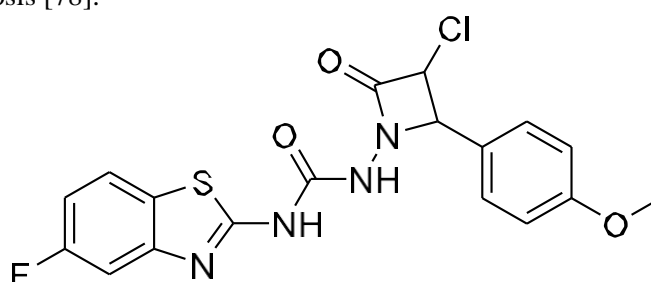
9. **Perdih et al., (2013)** Molecular dynamics simulation and linear interaction energy study of d-Glu-based inhibitors of the MurD ligase. In this work the high resolution X- ray crystal structures of MurD with benzylidene-2,4-thiazolidindione and 2- thioxothiazolidin-4-one based inhibitors revealed their binding modes within the catalytic pockets which were observed to be similar. 2-Thioxothiazolidin-4-one based inhibitor 21 occupied the uracil binding site with an IC₅₀ value of 8.20 μ M against E.coli MurD. This inhibitor exhibited interactions with Arg35, Thr36 and Asp37 residues, while the carboxylic groups of the D-Glu moiety occupied the same position as the carboxylic groups of UDP-MurNAc-L-Ala-D-Glu. Further, molecular dynamics simulations in conjunction with the linear interaction energy (LIE) studies of benzylidene-2,4-thiazolidin-diones/2-thioxothiazolidin-4-ones having D-Glu analogues 12, 21 and 22 were performed to evaluate the inhibitory mechanism of MurD. It is observed that non-polar van der Waals interaction is the main driving force for the inhibitor binding, while electrostatic interactions play minor role [76].



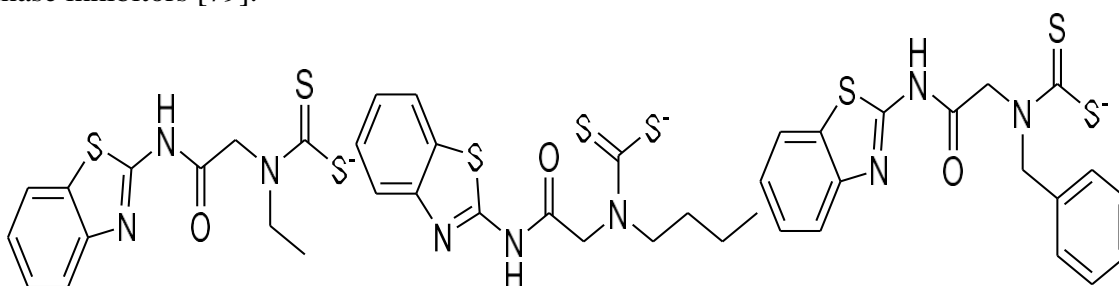
10. **Perdih et al., (2014)** studied Inhibitor Design Strategy Based on an Enzyme Structural Flexibility: A Case of Bacterial MurD Ligase. In this study, we present a drug design strategy using multiple protein structures for the identification of novel MurD ligase inhibitors. Our main focus was the ATP binding site of the MurD enzyme. In the first stage, three MurD protein conformations were selected based on the obtained OPS/TMD data as the initial criterion. Subsequently, a two-stage virtual screening approach was utilized combining derived structure-based pharmacophores with molecular docking calculations. Selected compounds were then assayed in the established enzyme binding assays, and compound 3 from the aminothiazole class was discovered to act as a dual MurC/MurD inhibitor in the micromolar range. A steady- state kinetic study was performed on the MurD enzyme to provide further information about the mechanistic aspects of its inhibition. In the final stage, all used conformations of the MurD enzyme with compound 3 were simulated in classical molecular dynamics (MD) simulations providing atomistic insights of the experimental results. Overall, the study depicts several challenges that need to be addressed when trying to hit a flexible moving target such as the presently studied bacterial MurD enzyme and show the possibilities of how computational tools can be proficiently used at all stages of the drug discovery process [77].



11. **Sarkar et al., (2018)** design, synthesis, and evaluate the antitubercular activity of a novel benzothiazole-containing an azetidinone ring. In this study, new compounds of benzothiazole-containing azetidinone derivatives were designed and synthesized using substituted benzaldehyde. The structures of the synthesized compounds were characterized by TLC, IR, elemental analysis, and ^1H NMR. *In vitro* screening data revealed that all the synthesized compounds A6–A10 exhibited the ability to inhibit the growth of *Mycobacterium tuberculosis* in terms of MIC. Variable and modest activity was observed against the investigated strains of bacteria; however, the compound A6 exhibited significant antitubercular activity against *M. tuberculosis* H37Rv (MTCC 200) compared to that of the reference drugs isoniazid and rifampicin. These experimental data were consistent with our computational predictions in terms of the compound A6 that exhibited a satisfactory backbone for the antitubercular activity, perhaps due to an increase in hydrophobicity resulting in better penetration through the cell wall of *M. tuberculosis* [78].

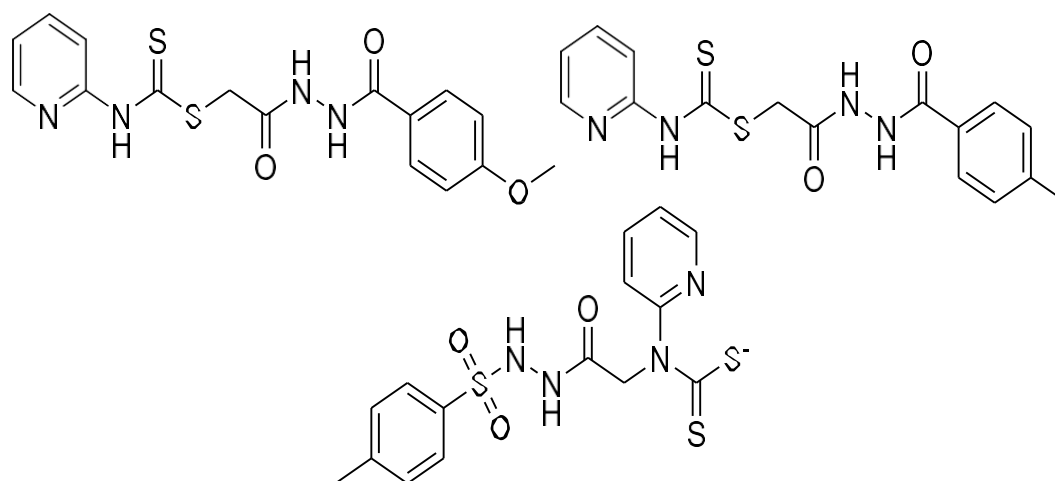


12. **Harshita et al., (2020)** described design synthesis and biological evaluation of dithiocarbamate substituted 2-aminobenzothiazole derivatives as proviral integration site of moloney murine leukaemia virus 1 kinase inhibitors. A novel series of derivatives containing dithiocarbamate moiety as a side chain at the second position of 2-amino benzothiazole nucleus were synthesized and characterized by spectral analysis. From the 3-(4,5-dimethylthiazol-2-yl)-2,5-diphenyl tetrazolium bromide Assay performed, compounds 4a, 4c and 4h of the series emerged as potent anticancer agents against SK-OV-3 cell lines. From the anti-mitotic activity studies all the compounds showed good to moderate activity with half-maximal inhibitory concentration. The evaluation of *in silico* absorption, distribution, metabolism, excretion, and toxicity and molecular descriptors, proved that the synthesized compounds possess drug like properties and are safer to the normal cells. From the molecular docking studies, compounds 4a, 4c, 4h showed good binding affinity with PIM 1 Kinase protein and retained required amino acid interaction similar to the co-crystal. Hence, this study proves 2 amino benzothiazole dithiocarbamate derivatives can be used as encouraging leads as PIM 1 Kinase inhibitors [79].



13. **Kumar et al., (2020)** studied Synthesis, Molecular Docking and Antibacterial Activity of Some Novel Pyridin-2-yl-Carbamodithioates. In the present study a series of pyridin- 2-yl-

carbamodithioates were synthesized and characterized by the spectral data. The Compounds were synthesized by heating together a mixture of triethyl ammonium N- (2-pyridyl)-dithiocarbamate and the corresponding N'-(chloroacetyl)arylhydrazide/2- chloro- N'(arylsulfonyl) acetohydrazide in refluxing absolute ethanol. Synthesized compounds were evaluated for their in vitro activity against selected Gram-positive and Gram-negative bacterial strains by disk diffusion and two-fold serial dilution methods. All other tested compounds, except 1 exhibited significant activity against the tested strain of Gram-negative bacteria *P. aeruginosa* 2200 with MIC values in the range of 31.25-62.50 µg/ml. Most of the tested compounds did not show activity against the tested Gram-positive bacteria *Staphylococcus aureus* NCIM 5022. Compound 2 and 3 exhibited significant activity against Gram-negative bacteria *E. coli* with MIC value of 15.62 µg/ml. Results are compared with the standard drug ciprofloxacin [80].



3. AIM AND OBJECTIVES

Aim

To design, synthesis of a novel substituted benzothiazole derivatives and evaluation for their biological activity.

Objectives

- Designed the novel set of substituted benzothiazole derivatives.
- The designed compounds were synthesized in the laboratory by the conventional methods.
- Synthesized compounds were characterized by IR, ¹HNMR, ¹³C NMR, LC-MS.
- Molecular docking studies
- *In vitro* cell line studies

4. PLAN OF WORK

The work has been divided into five stages

Stage I : Literature survey

A thorough literature survey was carried on prodrug used in the treatment of potential anti- cancer activity. The literature was carried out from 2000 to till date and review article has been prepared for the peer review submission.

Stage II : Optimization of reaction condition and synthesis of designed benzimidazole derivatives.

Stage III : Characterization of synthesized compounds by spectral data like FT- IR, ¹HNMR, ¹³CNMR

and Mass Spectroscopy.

Stage IV : *In vitro* anti-bacterial screening.

5. MATERIALS AND METHODS

5.1. Reagents and Instrumentation

- Oven dried glass wares were used to perform all the reactions. Procured reagents were of analytical grade and solvents of laboratory grade and purified as necessary according to techniques mentioned in Vogel's Textbook of Practical Organic Chemistry.
- In an open glass capillary tubes using Veego VMP-1 apparatus, melting points have been determined in °C and are uncorrected.
- Ascending TLC on precoated silica-gel plates (MERCK 6 F254) visualized under UV light was utilized to routinely monitor the progress and purity of the synthesized compounds. Solvents used during TLC are n-hexane, ethyl acetate, methanol, petroleum ether, chloroform and dichloromethane.
- The Infrared Spectra was plotted by Perkin-Elmer Fourier Transform-Infrared Spectrometer and in reciprocal centimeters the band positions are noted.
- Nuclear magnetic spectra (¹H NMR) were obtained from Bruker DRX-300 (300 MHz FT-NMR) spectrophotometer using DMSO as solvent with TMS as the internal standard ¹³C NMR have been recorded utilizing Bruker with Dimethyl sulphoxide as solvent. Shimadzu LC-MS was employed to record Mass Spectra.

5.2. *In-silico* molecular docking studies

5.2.1. Devices and materials

In the molecular scenario in the modern drug design, the docking is commonly used to understand the interaction between the target ligand-receptor and the target lead molecule's binding orientation with its protein receptor and is quite frequently used to detect the associations between the target components. The research work was done in-silico by utilizing bioinformatics tools. Also, we utilize some of the offline programming's like protein data bank (PDB) www.rcsb.org/pdb, PubChem database, Marvin sketch. The molecular docking studies were carried out through Discovery studio42.

5.2.2. Preparation of protein

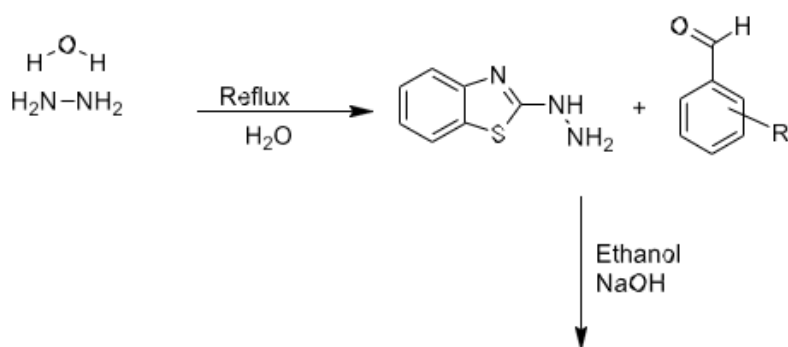
By utilizing the offline program protein data bank (PDB), we take the Topoisomerase II (PDB ID: 4FM7) was obtained from PDB website. From the protein (4FM7) we removed the crystal water, followed by the addition of missing hydrogens, protonation, ionization, energy minimization. The SPDBV (swiss protein data bank viewer) force field was applied for energy minimization. Prepared protein is validated by utilizing the Ramachandran plot 43.

5.2.3. Identification of active sites

Identification of active amino acid present in the protein is detected by using Protein- ligand interaction profile (PLIP) <https://plip-tool.biotec.tu-dresden.de/plipweb/plip/index> offline tool in google. From this, I found the active amino acid present in the protein44.

5.2.4. Preparation of Ligands

By utilizing the Marvin sketch tool, the molecules are designed in two and three- dimensional structures. After designed molecule, the structure was optimized in 3D optimization in Marvin sketch and saved as a pdb format.



5.3. Synthesis of designed compounds (Scheme 1)

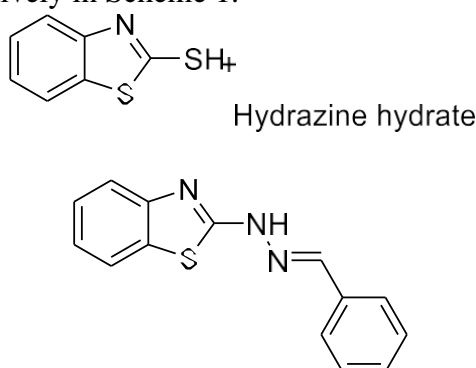
5.3.1. Synthesis of 2-hydrazinylbenzo[d]thiazole (A)

A solution of 2-mercaptobenzothiazole (70) (3.0 g, 17.9 mmol) in absolute EtOH (60 mL) was treated with hydrazine hydrate (10 mL). The reaction mixture was refluxed on water bath for 5 h. The mixture was cooled and the solvent was evaporated in vacuo. The separated product was filtered and crystallized from EtOH to give pale yellow crystals (2.70 g, 92% yield); m.p. 194°C.

5.3.2. General procedure for the synthesis of N'-(1,3-benzothiazol-2-yl)-4-substituted benzohydrazide.

2-Hydrazino-1,3-benzothiazole (71) (0.242 g, 0.0014 mol) and hydroxybenzotriazole (HOBt) (0.450 g, 0.0029 mol) was successively added to the corresponding substituted benzoic acid (0.2 g, 0.0014 mol) in N,N-dimethylformamide (DMF) (15 mL). The mixture was cooled to 0

°C in an ice bath with stirring and then 1-ethyl-3-(3-dimethylaminopropyl)carbodiimide hydrochloride (EDC. HCl) (0.563 gm, 0.00294 mol) was added. The reaction mixture was then slowly allowed to reach the room temperature over 1 hour and then stirring was further continued at this temperature till completion of reaction. Progress of reaction was monitored with TLC using n-hexane:ethylacetate (1:4) as eluent, spots are detected by using UV spectroscopy. The reaction was quenched by saturated NaHCO₃ solution and then extracted with EtOAc (20 ml x 3). The organic layer was dried with anhydrous Na₂SO₄, filtered and concentrated under reduced pressure. The synthetic route for compounds are presented, respectively in Scheme 1.



Scheme 1: progress for synthesis of Title compounds

5.4. In vitro studies

5.4.1. In vitro antibacterial screening of synthesized compounds

5.4.1.1. Determination of minimum inhibitory concentration (MIC)

The newly synthesized compounds were screened against two bacterial strains, *Staphylococcus aureus* NCIM 5021 and *Staphylococcus epidermidis* NCIM 2493 following the guidelines of Clinical

Laboratories Standard Institute (CLSI 2007) [173]. The tests were performed in Mueller Hinton medium (Hi-media) by broth micro dilution method, in 96-well micro titer plates. All the compounds were dissolved in sterile dimethyl sulfoxide (DMSO) to screen their antibacterial activity. Ciprofloxacin was dissolved in sterile DMSO and used as positive control, while sterile DMSO served as a negative control. The final volume for MIC protocols was 100 μ L, whereas DMSO concentration in assays well was less than 1%. Synthesized compounds were tested in the concentration range of 19.74 to 221.98 μ M. The bacterial suspensions at 105 Colony Forming Unit/mL (CFU/mL) concentrations were inoculated to the corresponding wells. Following inoculation 96- well microtitre plates was incubation at 37 °C for 24 h. Plates were then agitated and read for the absorbance at a wavelength of 600 nm. All tests were performed in triplicate and the results were taken as a mean. After MIC determination, 50 μ L aliquot from each well was sub-cultured on Mueller- Hinton agar plates and were further incubated at 37 °C for 24 h. All experiments were performed in triplicate. The wells are visually inspected for turbidity under black background to determine the growth of the organism. The wells containing the antimicrobial agent in concentration sufficient to inhibit the growth remain clear. In experimental terms the MIC is the concentration of the drug present in the last clear well, i.e. the well having the lowest antibiotic concentration in which growth is not observed.

5.4.1.2. Determination of Minimum bactericidal concentration (MBC)

The Minimum Bactericidal Concentration (MBC) is the lowest concentration of an antibacterial agent required to kill a bacterium over a fixed, somewhat extended period, such as 18 hours or 24 hours, under a specific set of conditions. It can be determined from the broth dilution of MIC tests by sub-culturing to agar plates that do not contain the test agent. The MBC is identified by determining the lowest concentration of antibacterial agent that reduces the viability of the initial bacterial inoculum by a pre-determined reduction such as $\geq 99.9\%$. The MBCs were determined by sub-culturing aliquots (20 μ l) from the bacterial suspension wells with no visible bacterial growth at concentrations greater than the defined MIC and from control wells onto nutrient agar plates. The plates were incubated aerobically at 37 °C for 24 hours and colonies were comparatively counted with the starting inoculum. MBC was determined as the concentration at which a $\geq 99.9\%$ decrease in bacterial counts (i.e., 3 log 10 reduction in cfu/ml) was achieved or the lowest concentrations that did not produce any bacterial growth in the agar plates were regarded as MBC values. All experiments were repeated in triplicate for each strain. The ratio $MBC/MIC \leq 2$ indicates bactericidal activity, while MBC/MIC ratio ≥ 4 shows bacteriostatic activity of test compound.

6. RESULT AND DISCUSSION

6.1. Molecular docking

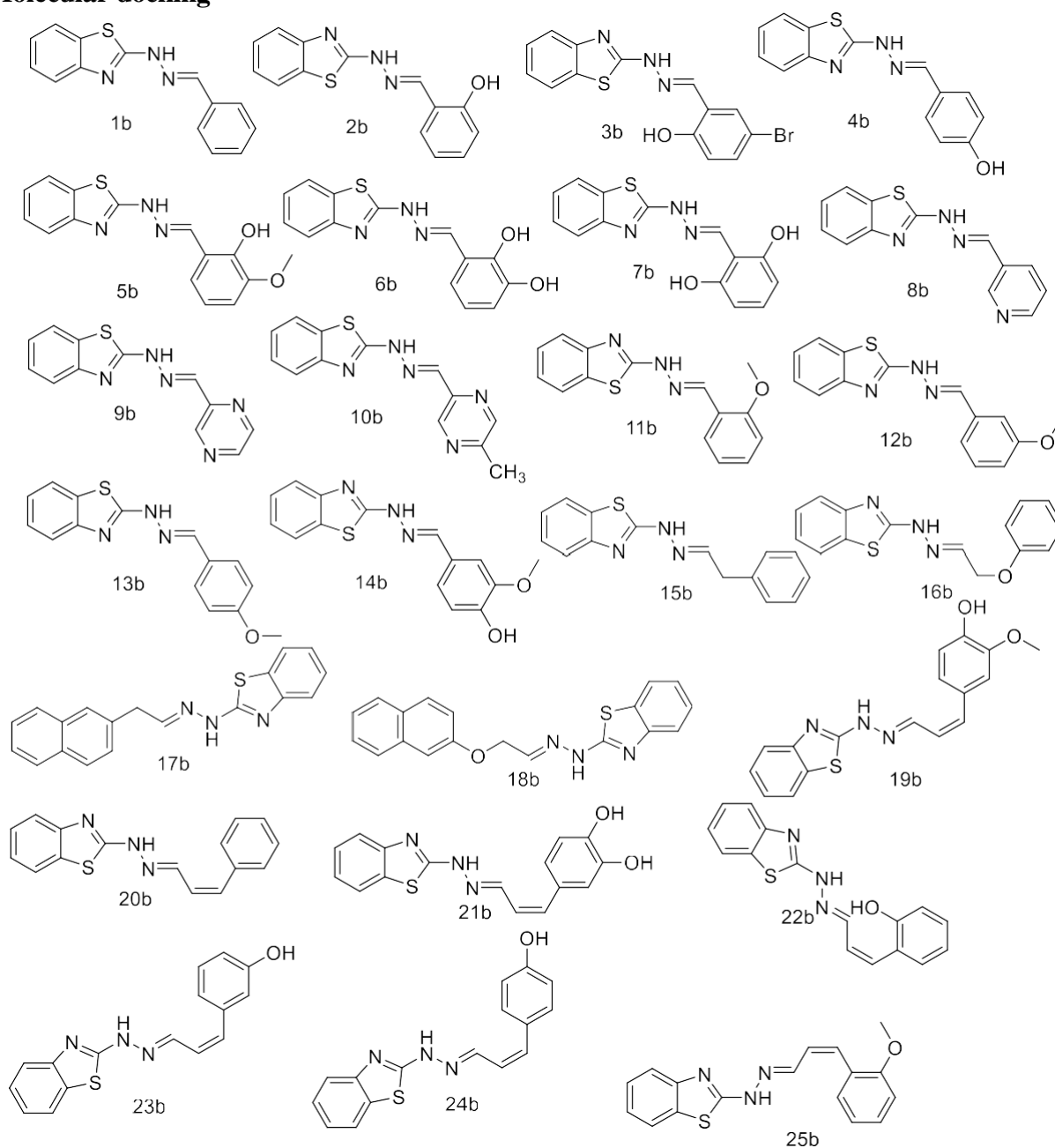


Figure 9. Chemical structure of newly designed compounds

The *in-silico* docking study of the 25 designed molecules (**Figure 9**) to the enzyme's active sites was performed by the C dock module of Discovery studio to determine the binding affinities of the ligands. The designed compounds were docked towards MurD (PDB ID: 2JFF) in order to ascertain their MurD inhibition activity against inflammation. All the compounds were exhibited good affinity for the receptor when compared with ciprofloxacin with MurD (PDB ID: 2JFF) inhibitory activity as an anti-cancer agent. The Docking scores of docking studies against MurD (PDB ID: 2JFF) are shown in **Table 1**.

From the in-silico docking results, it is evident that the interactions are mainly lipophilic factors due to the presence of aromatic heterocyclic rings.

Among the docked compounds, compound 17b possesses significant docking score --

9.2 K/cal when compared to standard drug ciprofloxacin. The compound 17b shows 2 hydrogen bonds between the amino acids MET145 and LEU147. The compound 18b shows a significant docking score of **- 9. K/cal** along with 2 hydrogen bonds with amino acids MET145 and LEU147. The remaining docked compound shows a docking score range from 6 to 9 K/cal along with one or two hydrogen bond interactions. **Figures 10 - 19** shows the docking pose of the designed compounds. Based on the docking score the derivatives 5b, 6b, 7b, 14b, 17b 18b, 21b, 22b, 23b and 24b are selected for the synthesis by conventional method.

Table 1. Docking score of designed compounds

Compound code	Binding Affinity
1b	-7.1
2b	-7.6
3b	-7.7
4b	-7.7
5b	-8.1
6b	-8
7b	-7.8
8b	-7
9b	-7.3
10b	-7.3
11b	-7.8
12b	-7.4
13b	-7.5
14b	-7.8
15b	-7.6
16b	-7.7
17b	-9.2
18b	-9
19b	-7.9
20b	-7.6
21b	-8.3

22b	-8
23b	-8
24b	-8.1
25b	-7.7
Ciprofloxacin	- 9.5

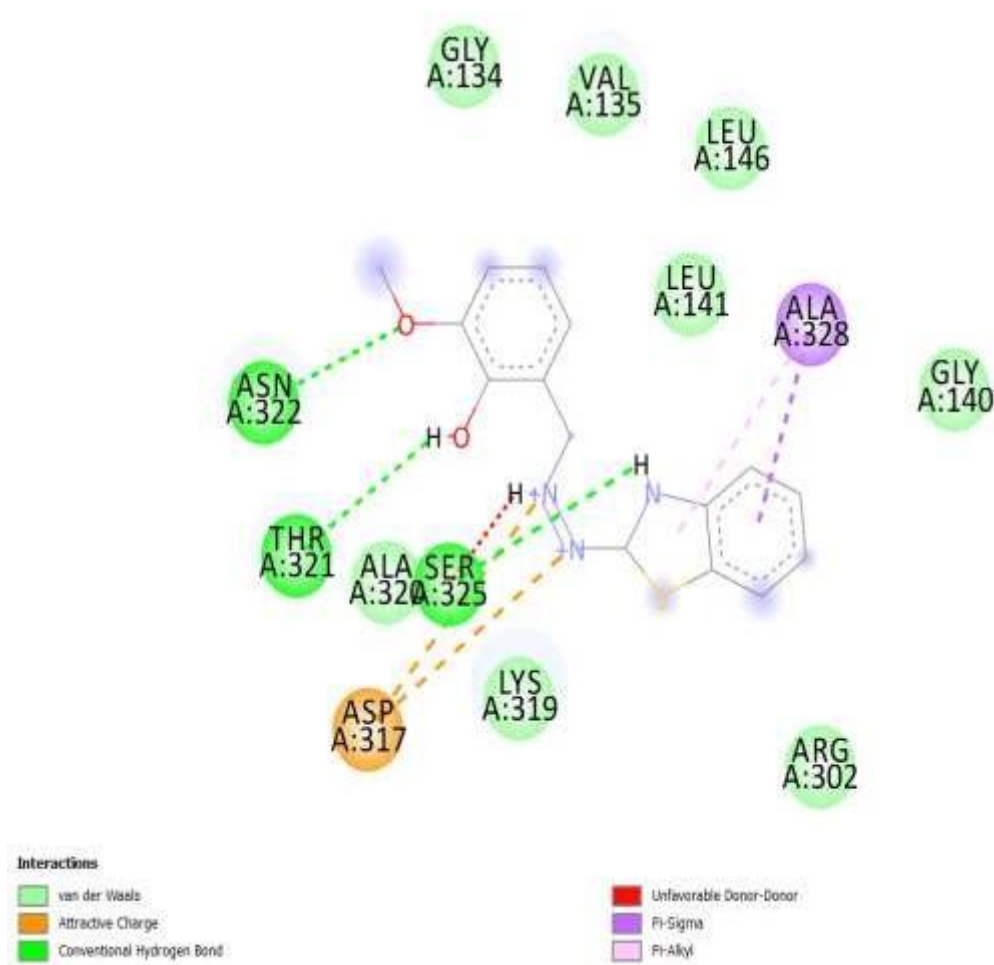


Figure 10. 2D docking pose of compound 6

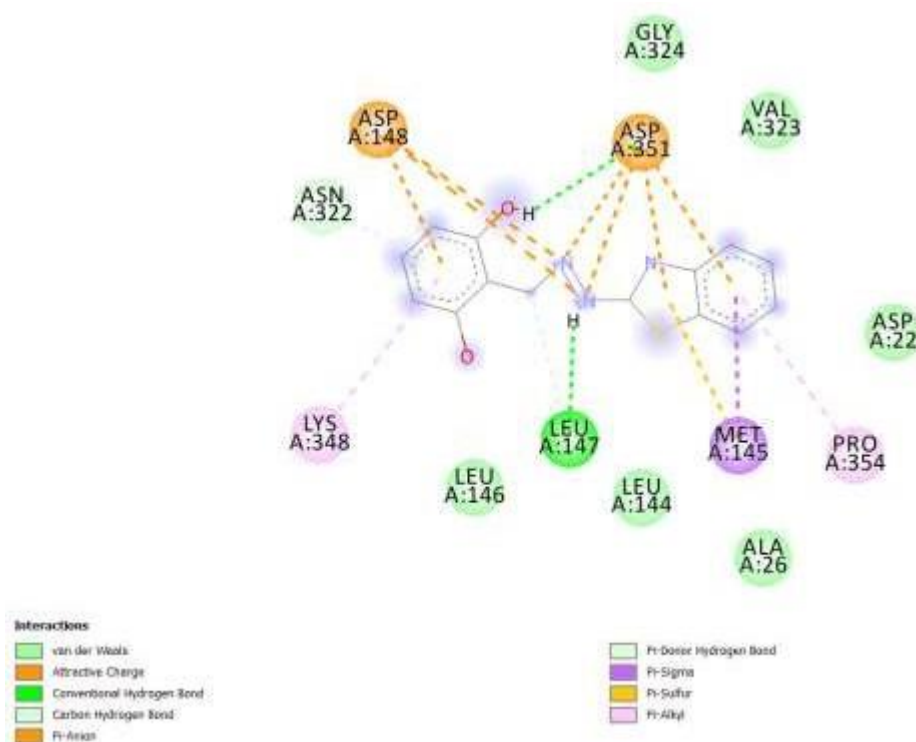


Figure 11. 2D docking pose of compound 7

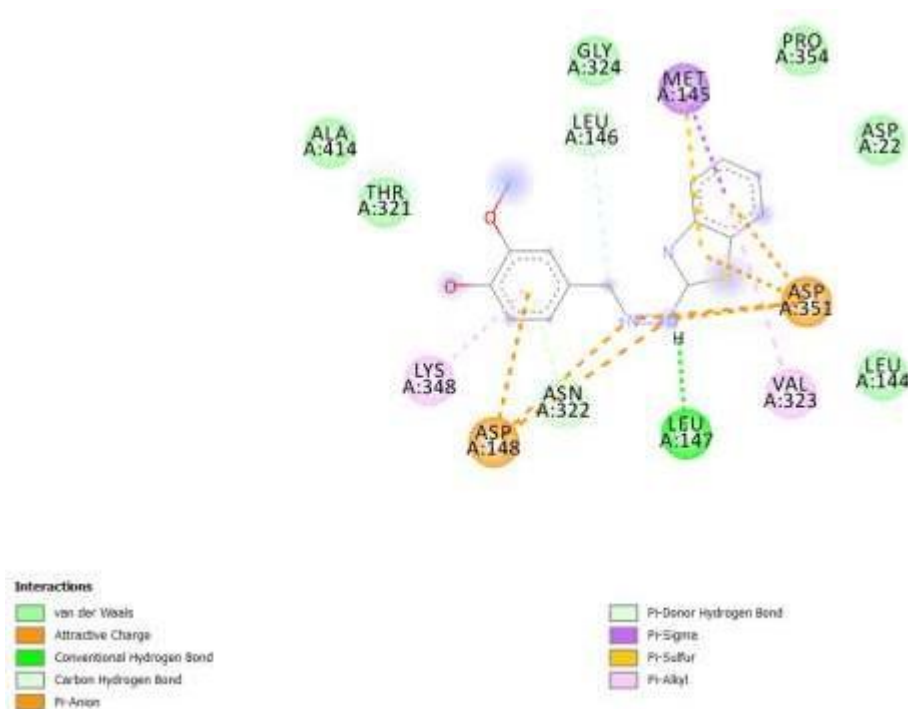


Figure 12. 2D docking pose of compound 14

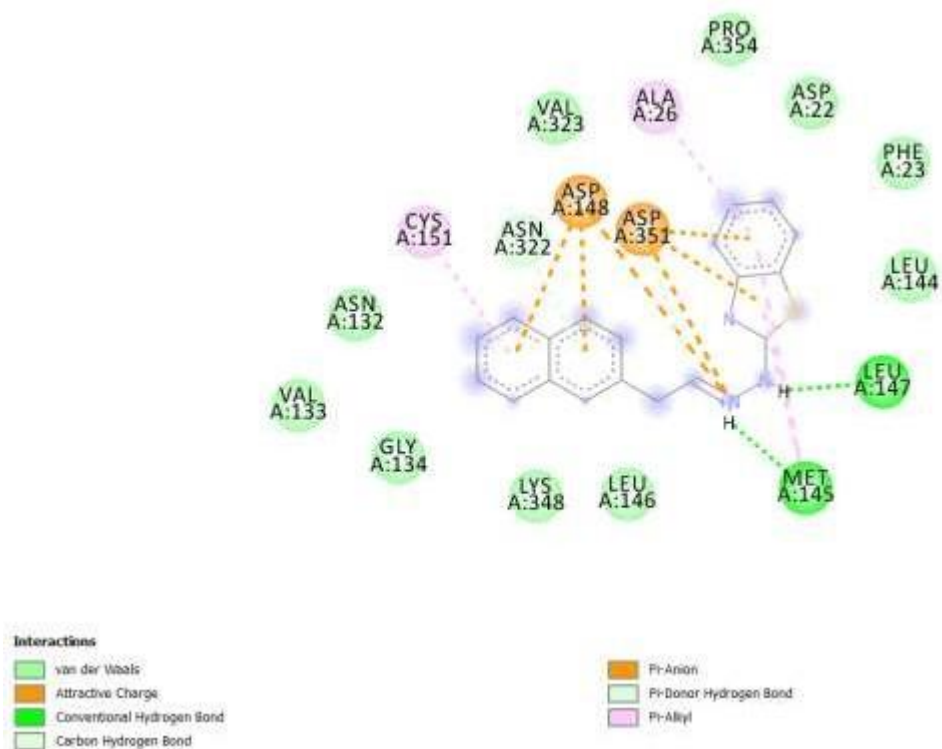


Figure 13. 2D docking pose of compound 17

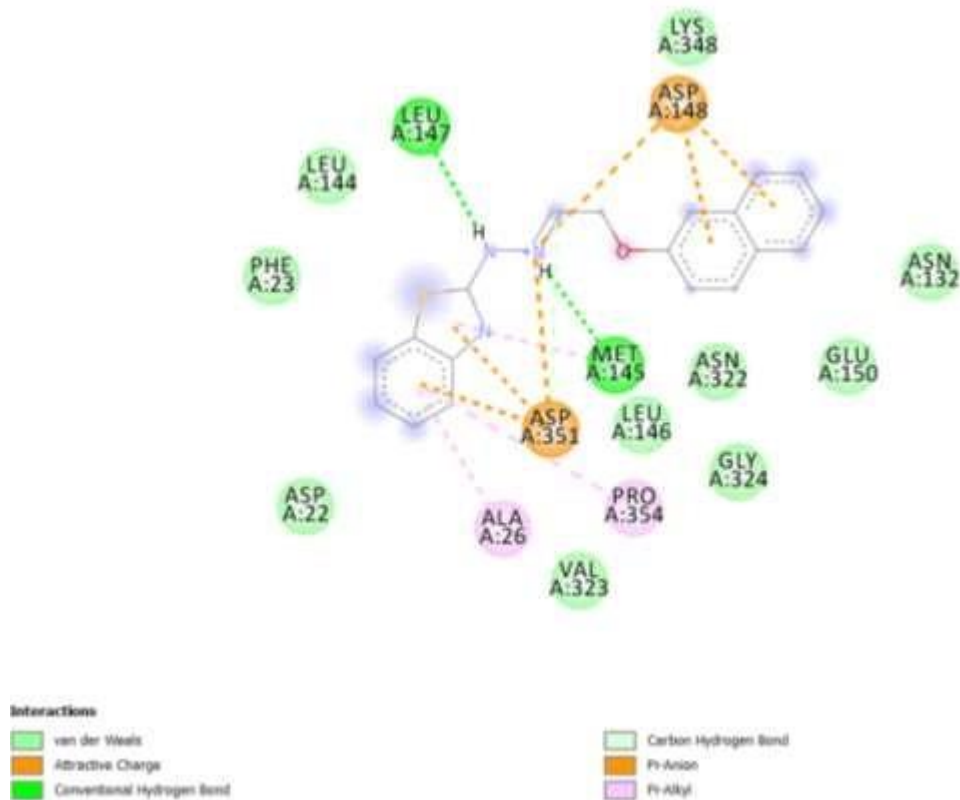


Figure 14. 2D docking pose of compound 17

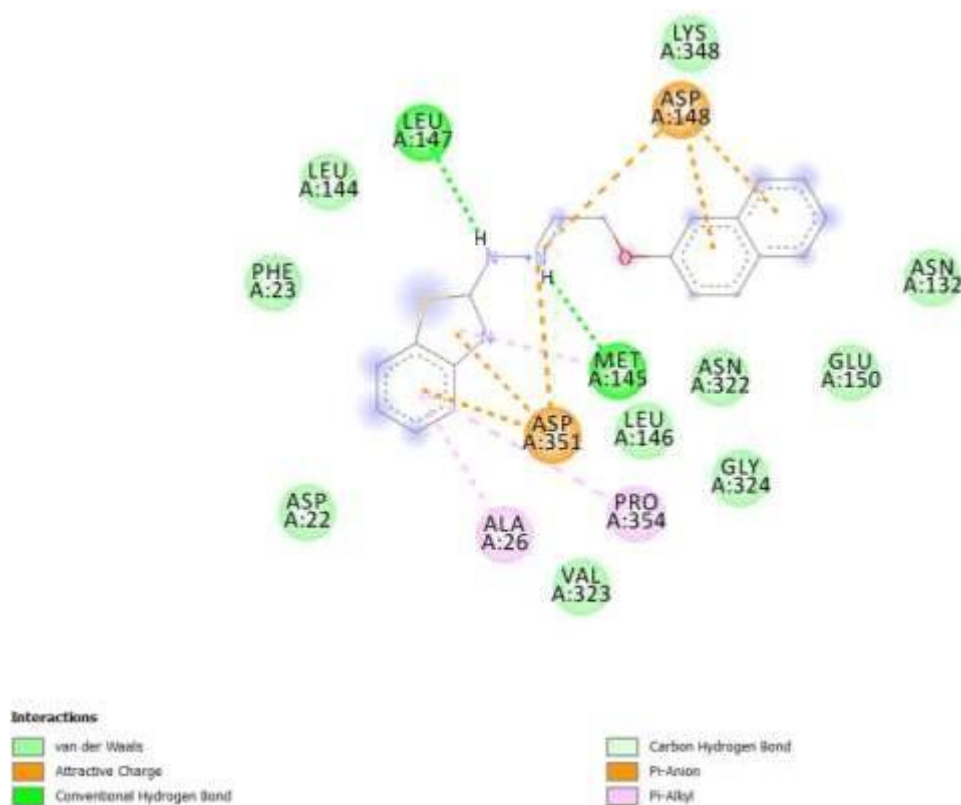


Figure 15. 2D docking pose of compound 18

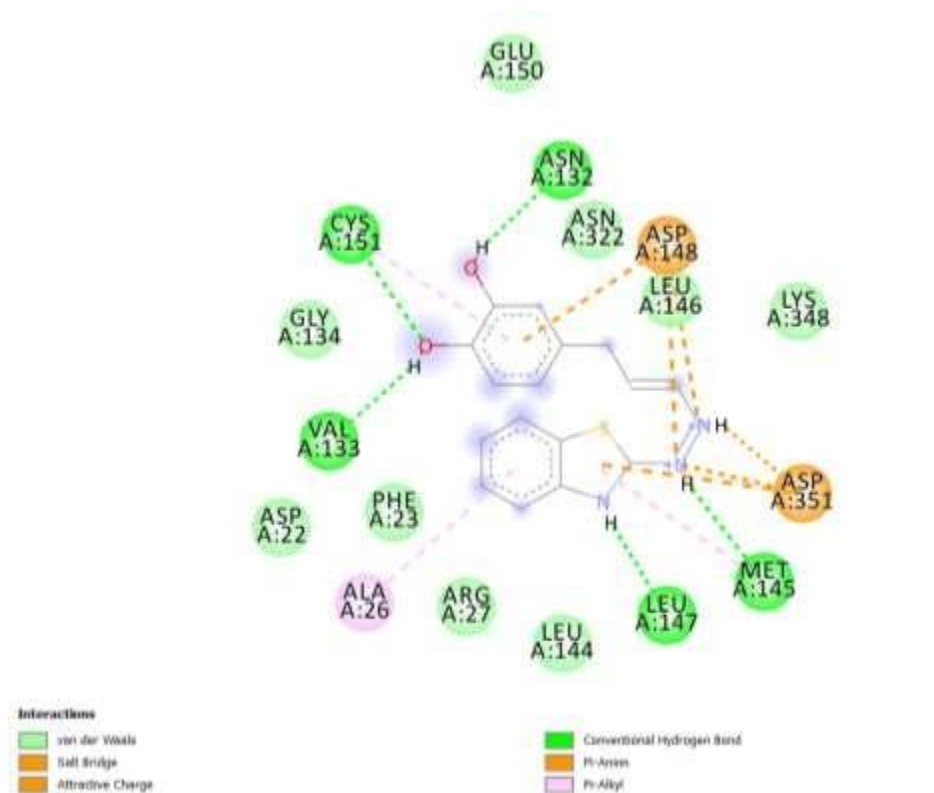


Figure 16. 2D docking pose of compound 21

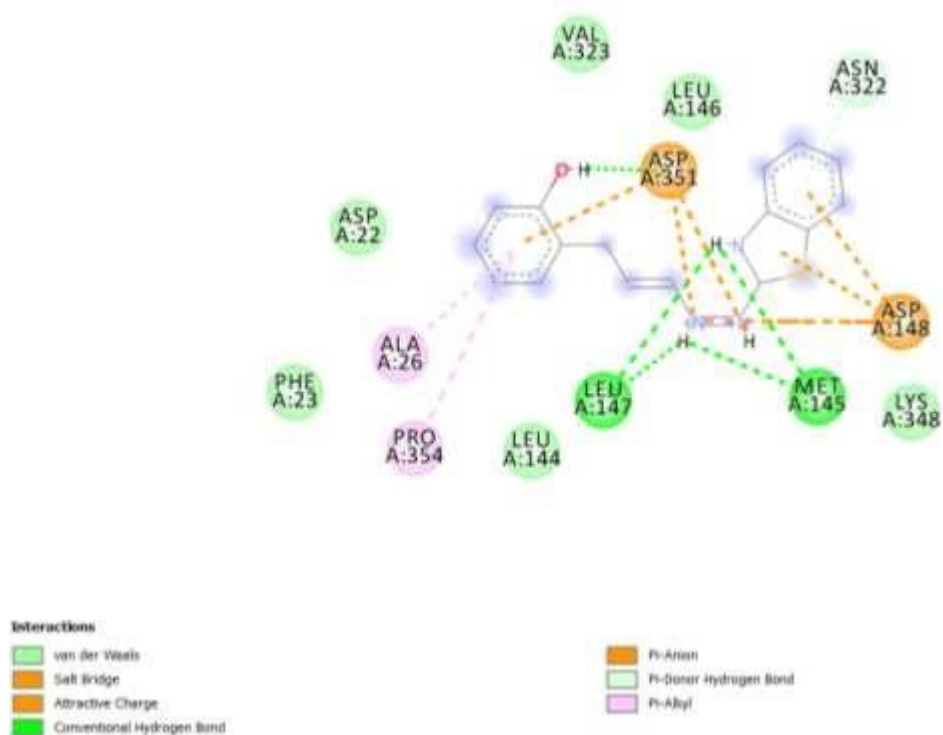


Figure 17. 2D docking pose of compound 22

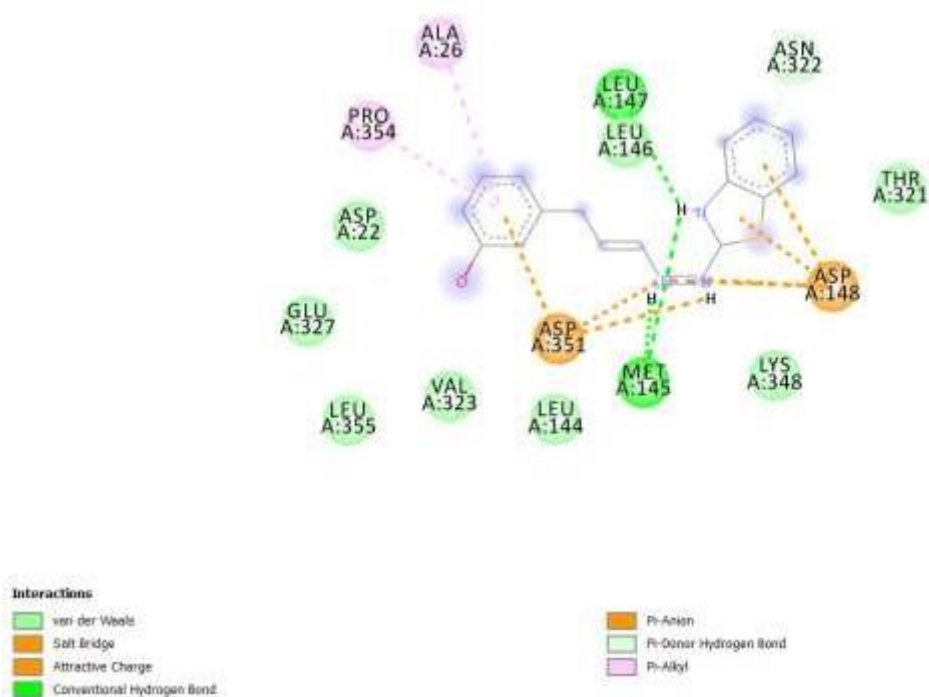


Figure 18. 2D docking pose of compound 23

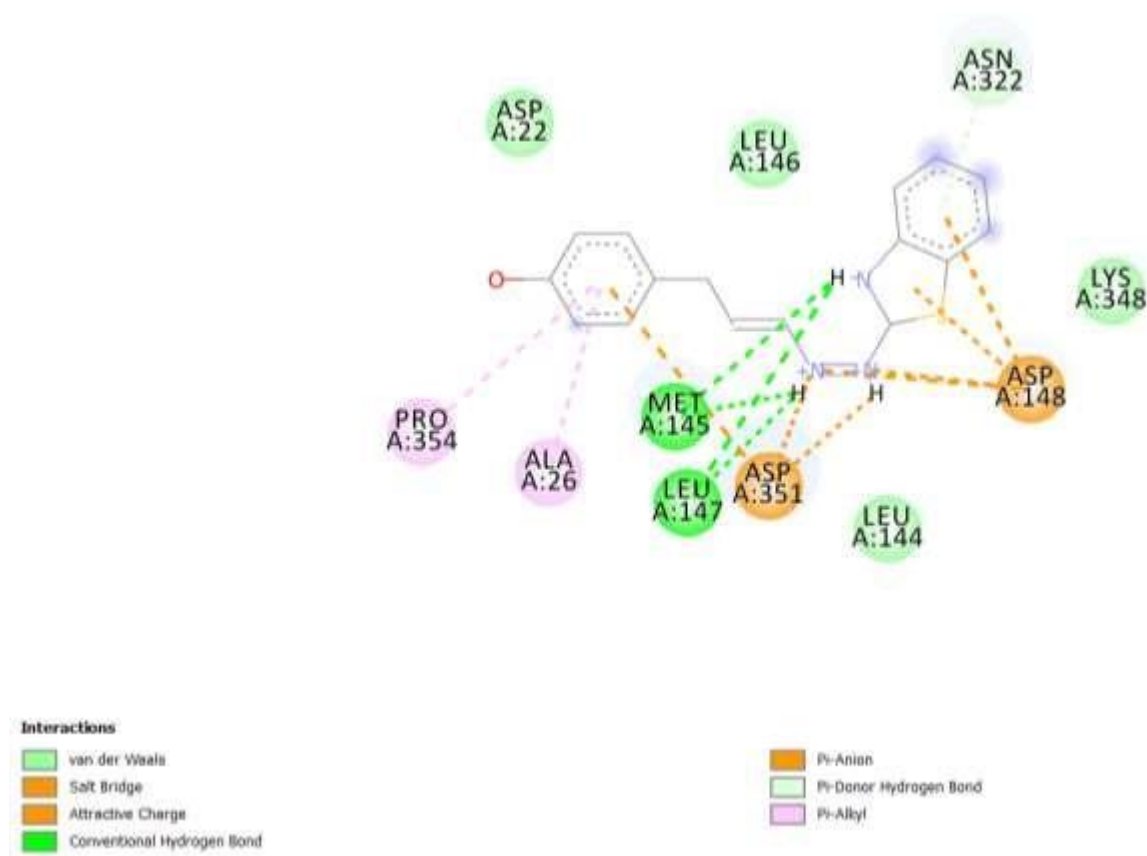


Figure 19. 2D docking pose of compound 24

6.2. Synthetic work

The substituted benzothiazole derivatives are prepared by the reaction of 2-Hydrazino- 1,3-benzothiazole and hydroxy-benzotriazole was successively added to the corresponding substituted benzoic acid in N,N-dimethylformamide (DMF). The mixture was cooled to 0 °C in an ice bath with stirring and then 1-ethyl-3-(3-dimethylaminopropyl)carbodiimide hydrochloride was added and all the compounds and intermediates were purified by successive recrystallization from ethanol. The IR spectrum of the final synthesized compounds showed absorption bands around 2850 – 2950 shows the presence of CH stretching alkane group, the peak 2030 shows presence of CH stretching aromatic and the peak at 1489–1464 cm^{-1} for CH_2 , 1379–1344 cm^{-1} for CH_3 , and 800–700 cm^{-1} for aromatic rings. These compounds also exhibited appropriate peaks at corresponding ppm in their ^1H NMR spectra. The ^1H NMR spectra of the synthesized compounds revealed a singlet signal a signal at 7.5-8.5 for H of aromatic ring. The ^{13}C NMR spectra of synthesized compounds revealed a signal at 160 – 175 for carbonyl carbon, and a signal at 120 – 145 for aromatic carbon. The corresponding molecular ion peaks in the LC–MS spectra were in conformity with the assigned structures. All the synthesized compounds were subjected to in vitro anti-bacterial studies.

6.2.1. Characterization of synthesized compounds

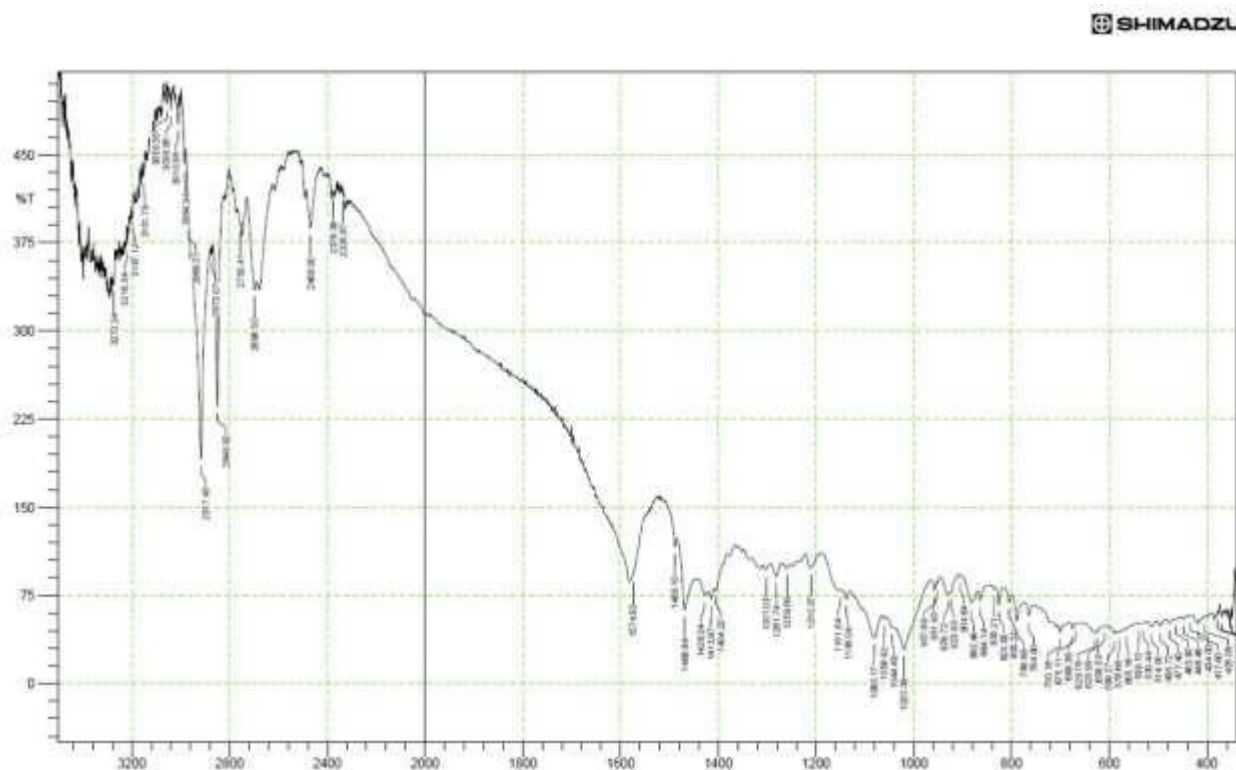


Figure 20. IR spectra for compound 5b

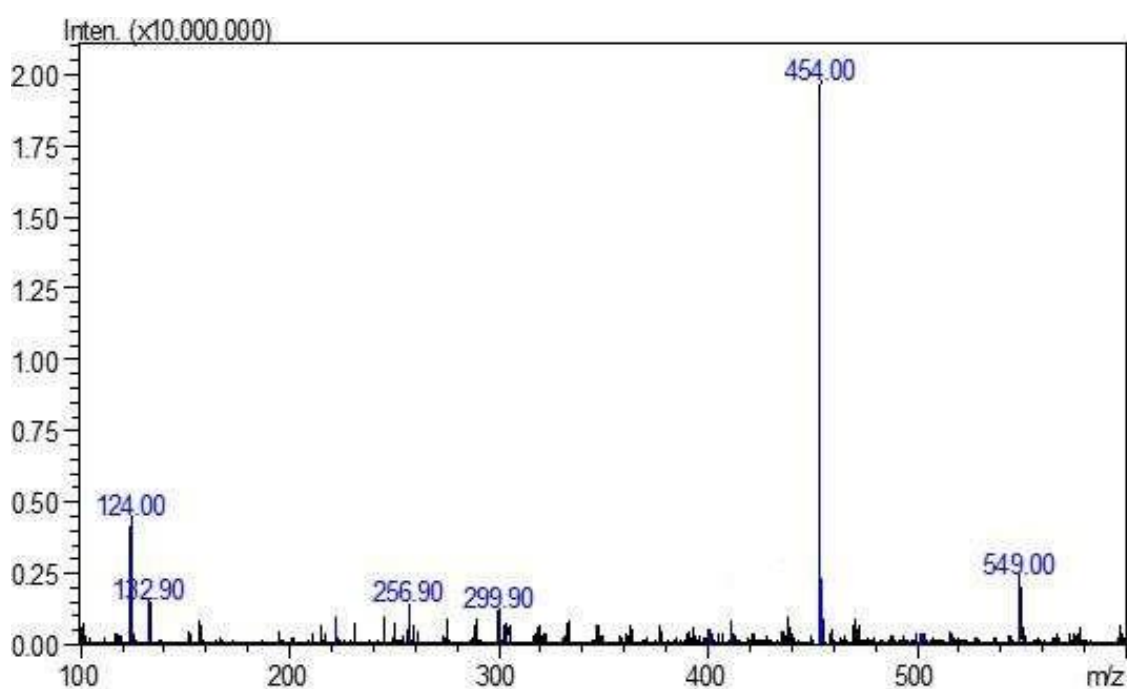


Figure 21. Mass spectra for compound 5b

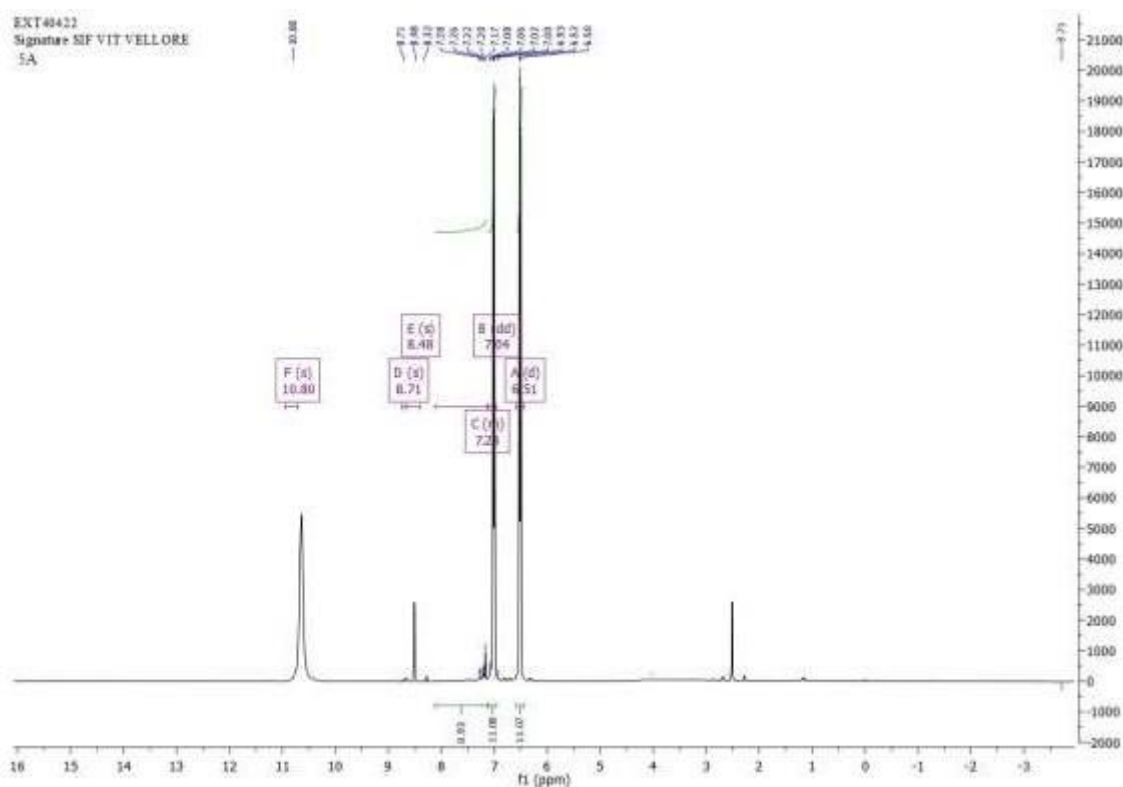


Figure 22. ^1H NMR spectra for compound 5b

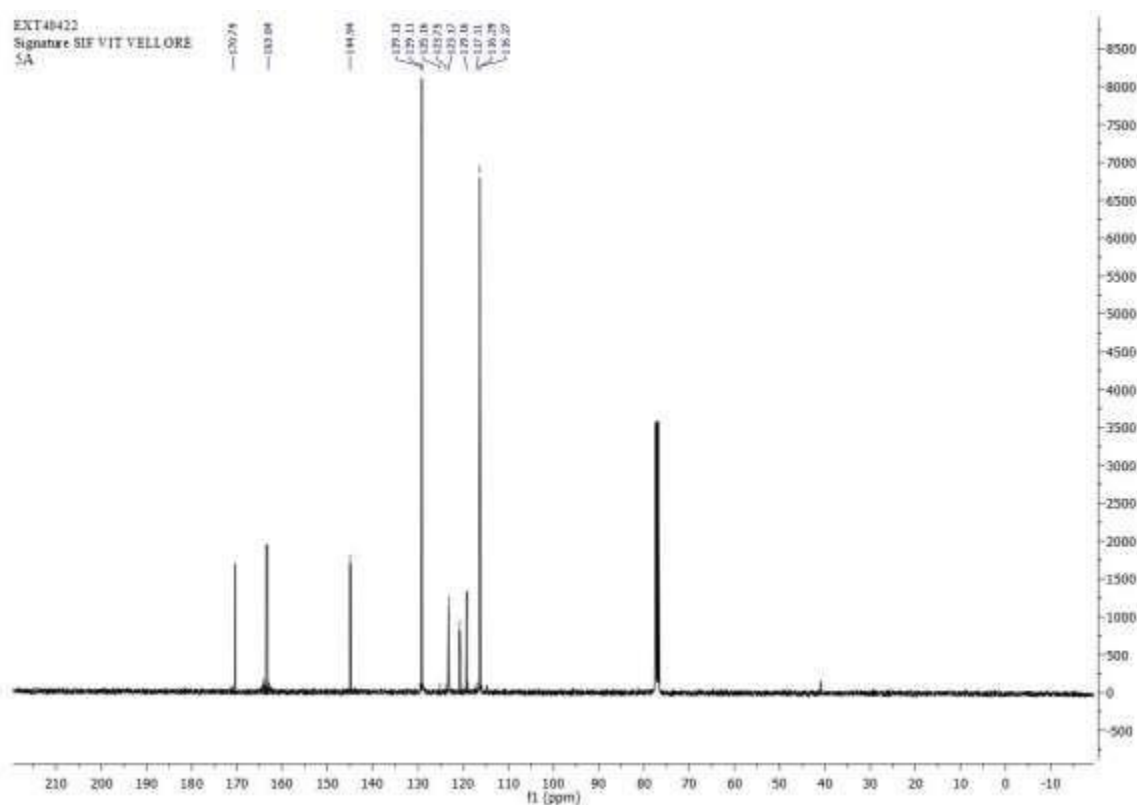


Figure 23. ^{13}C NMR spectra for compound 5b

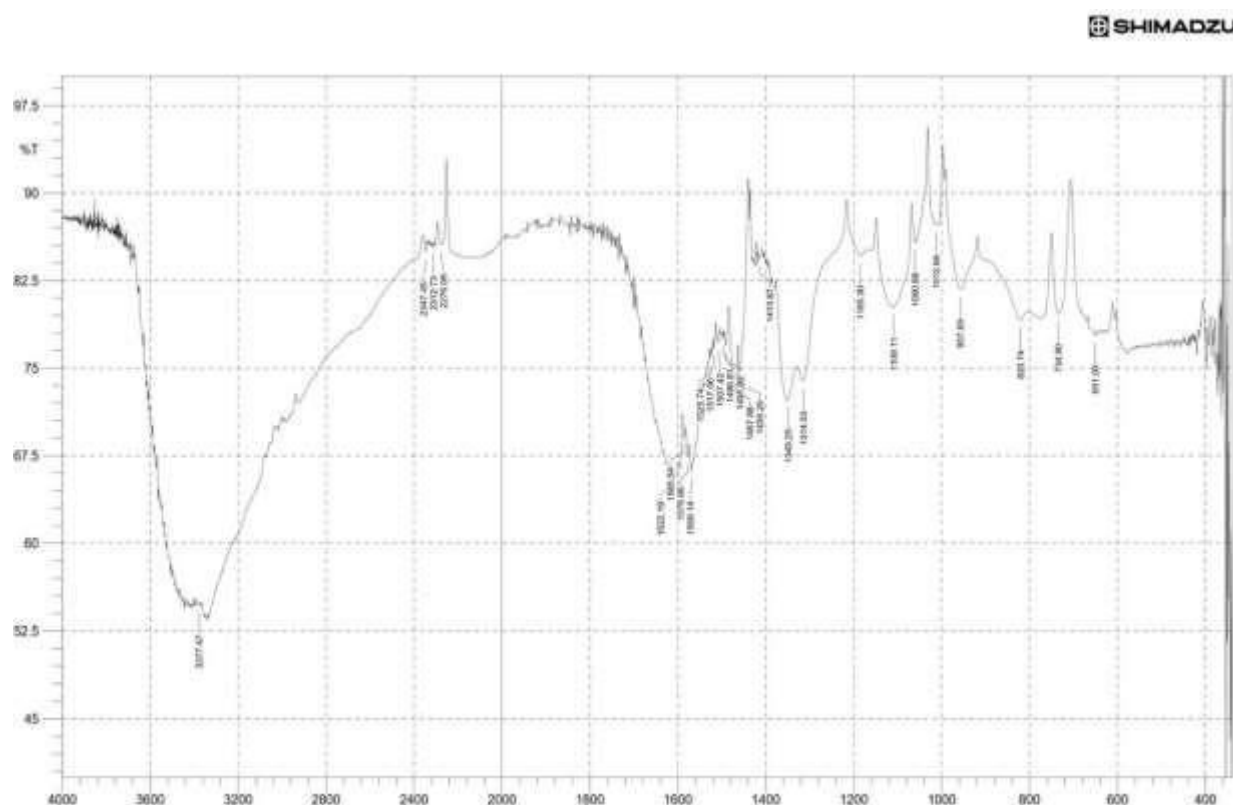


Figure 24. IR spectra for compound 6b

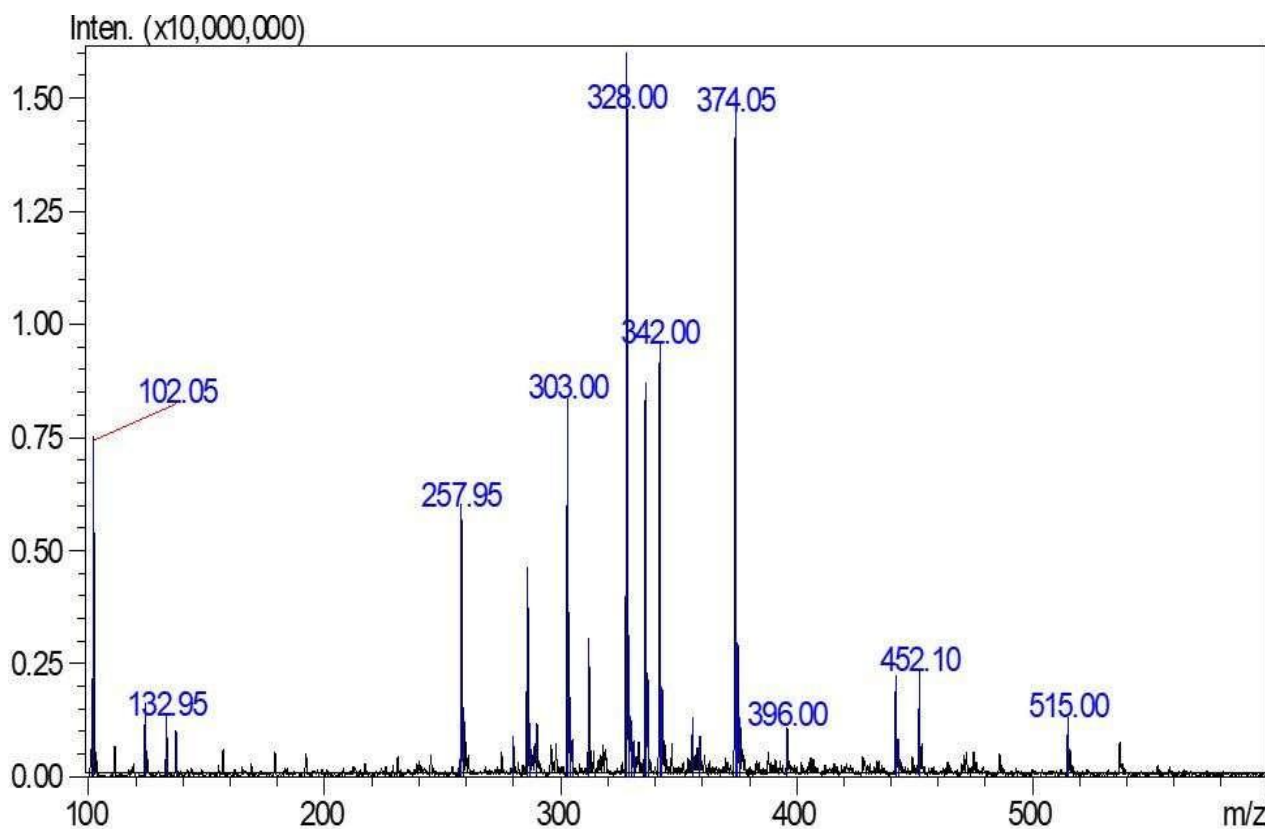


Figure 25. Mass spectra for compound 6b

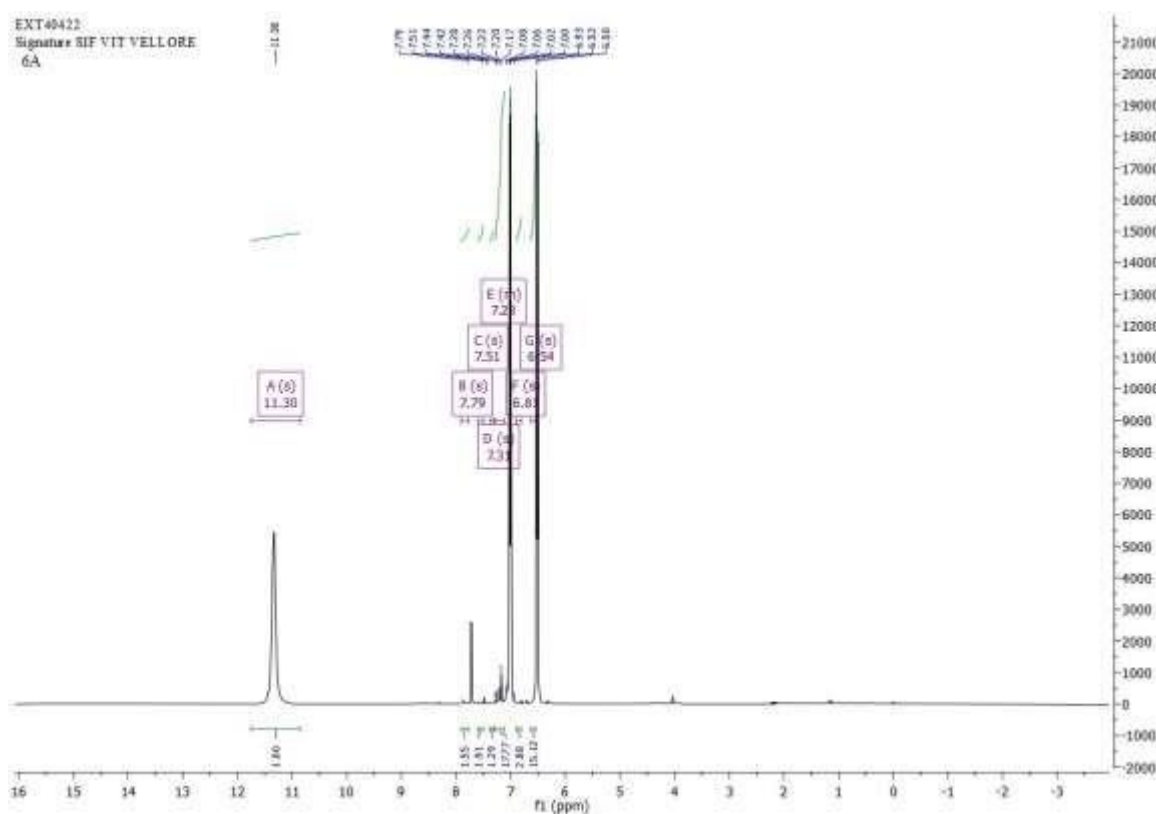
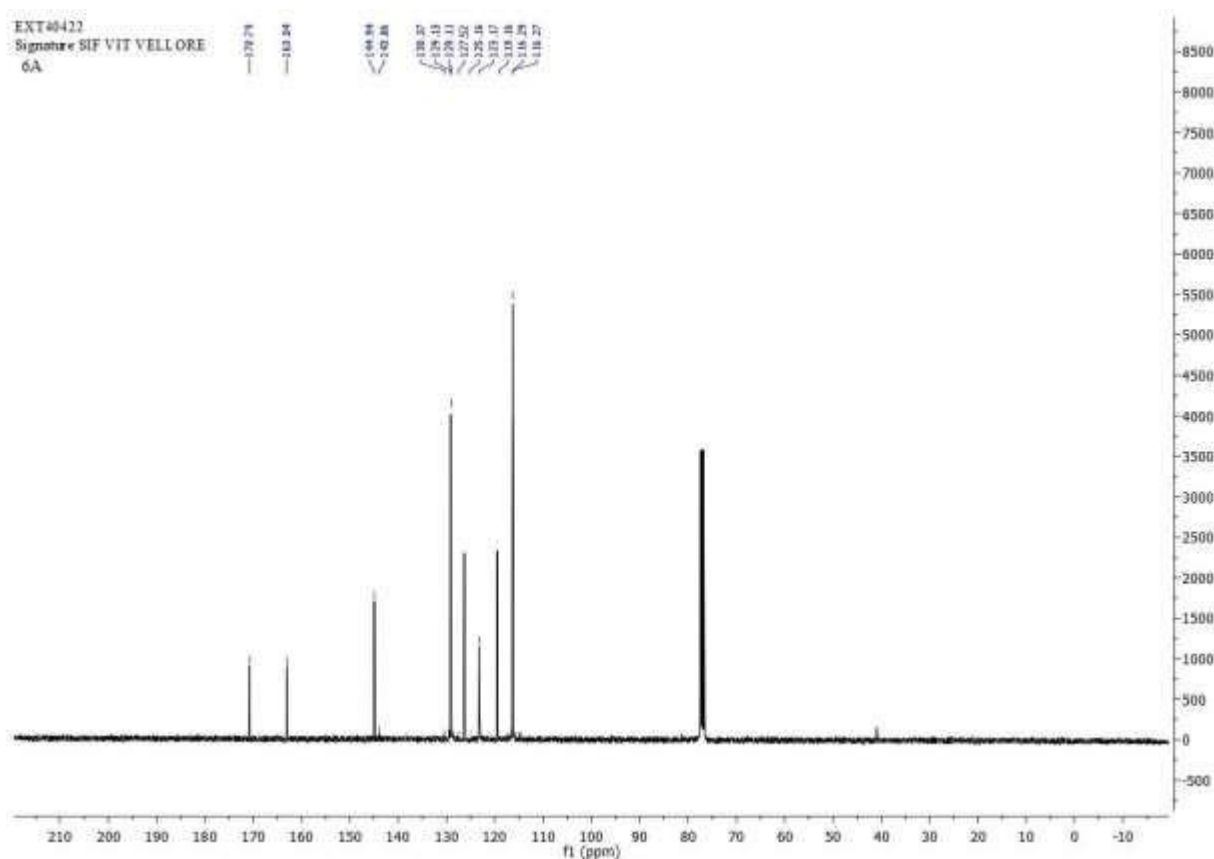


Figure 26. ^1H NMR spectra for compound 6b



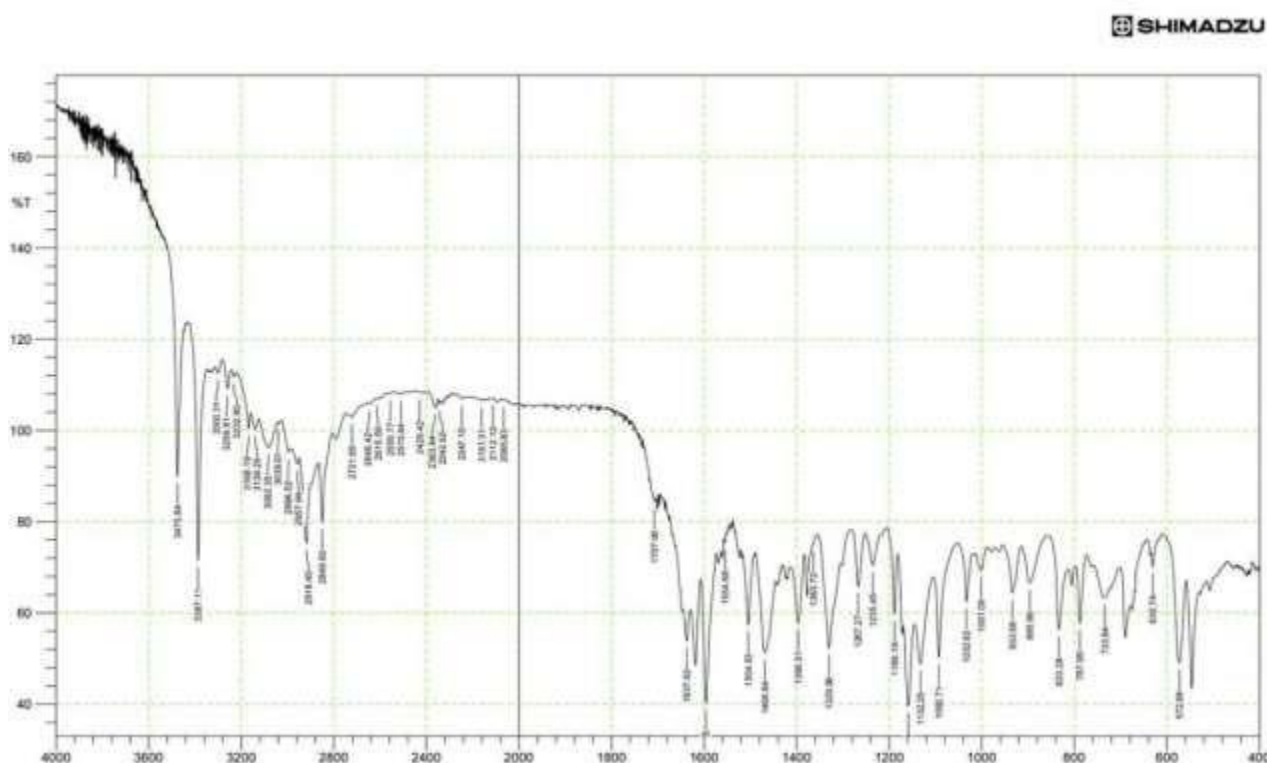


Figure 28. IR spectra for compound 7b

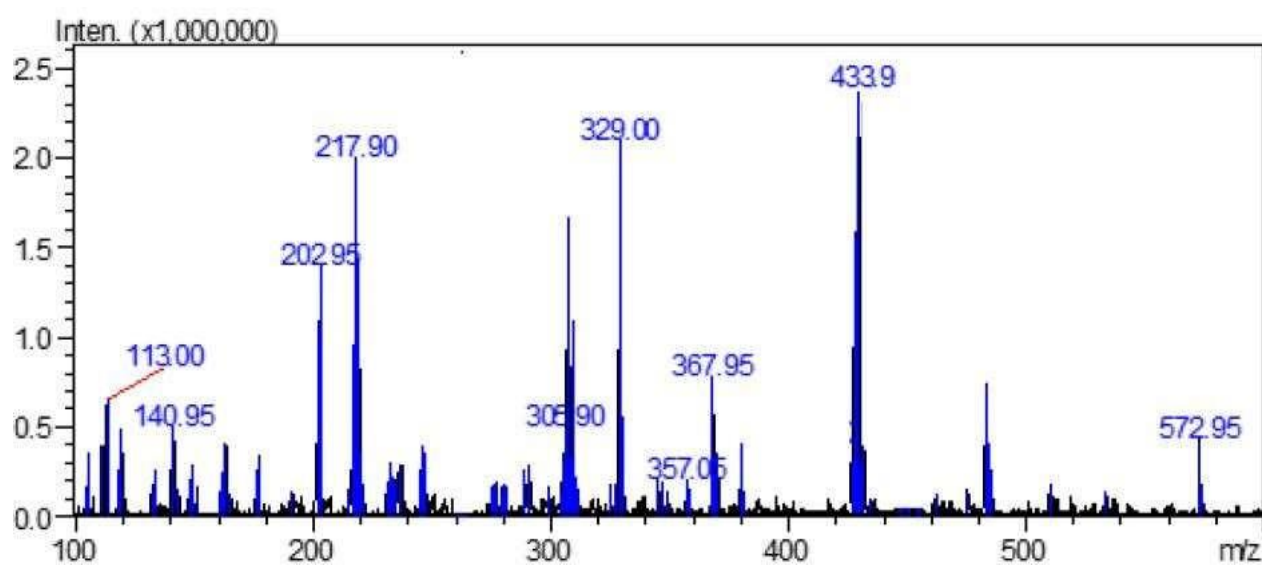


Figure 29. Mass spectra for compound 7b

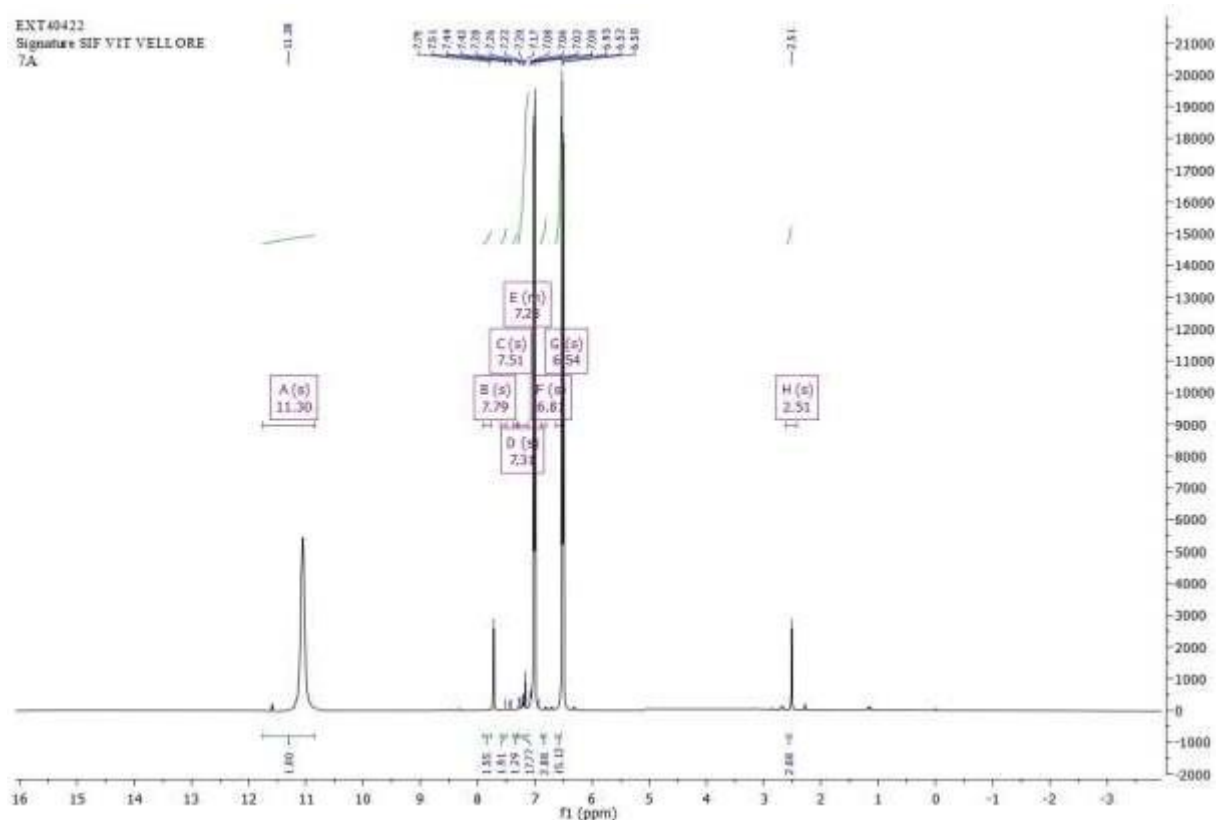


Figure 30. ^1H NMR spectra for compound 7b

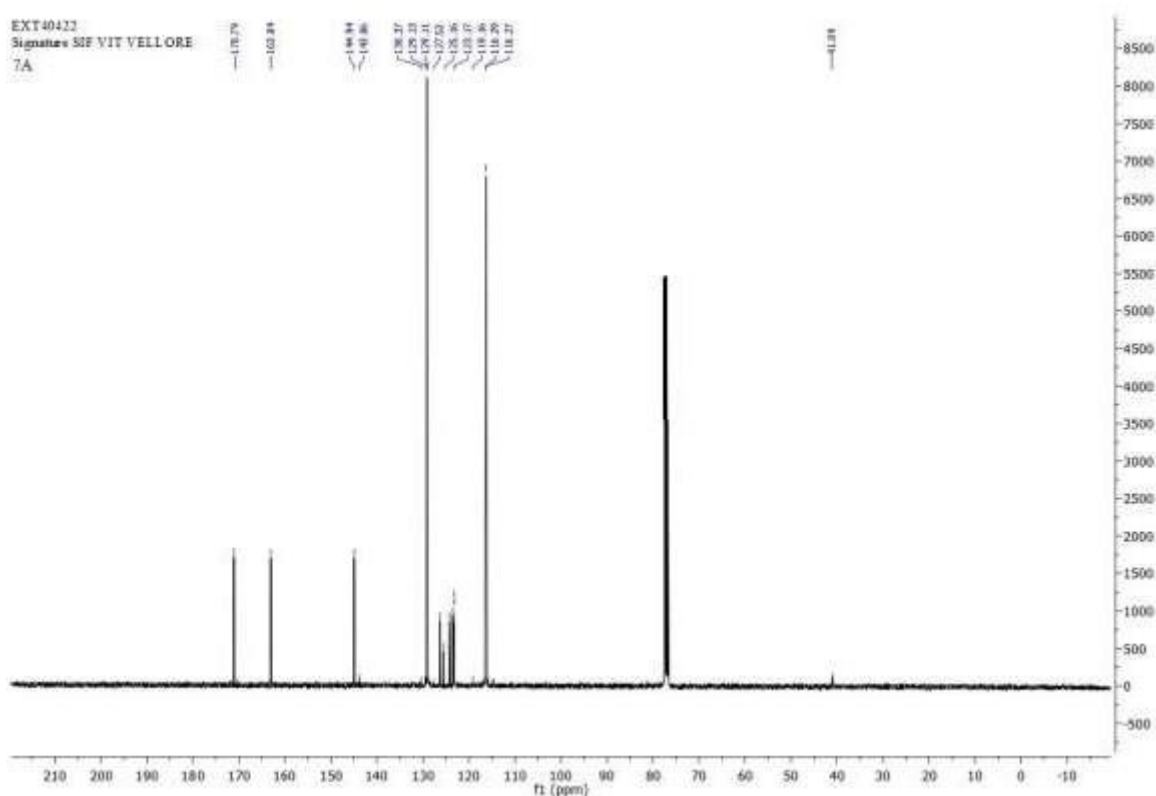


Figure 31. ^{13}C NMR spectra for compound 7b

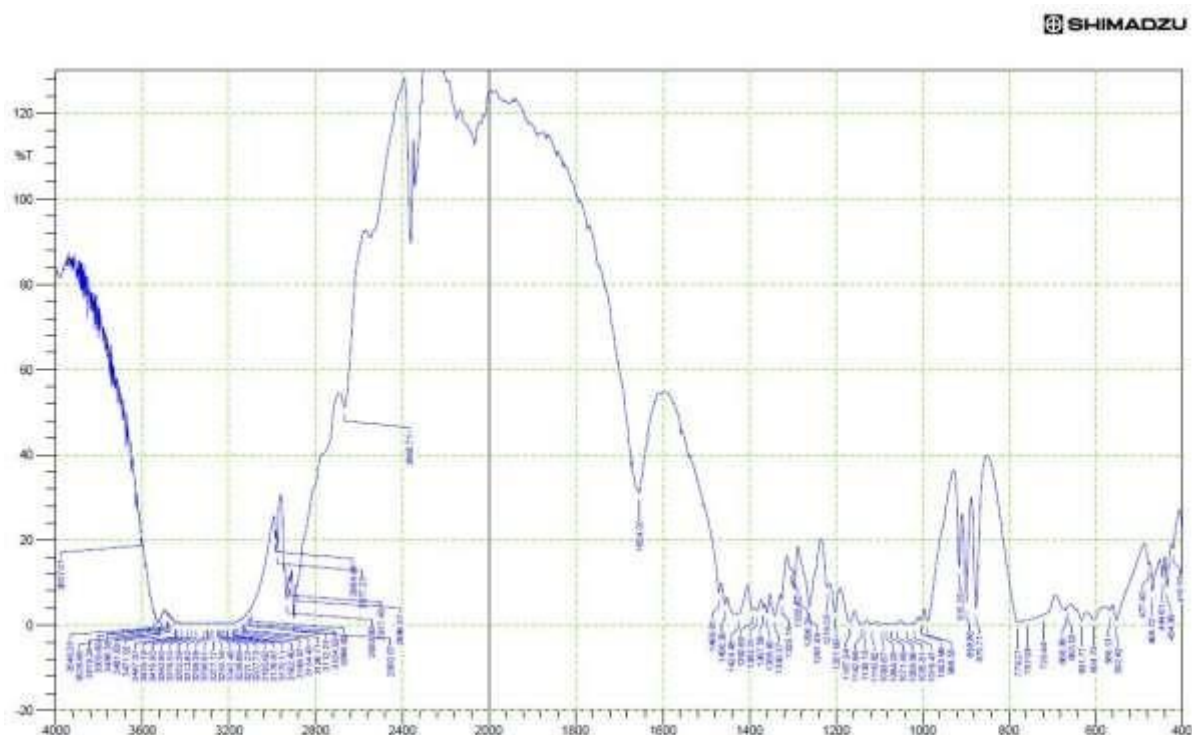


Figure 32. IR spectra for compound 14b

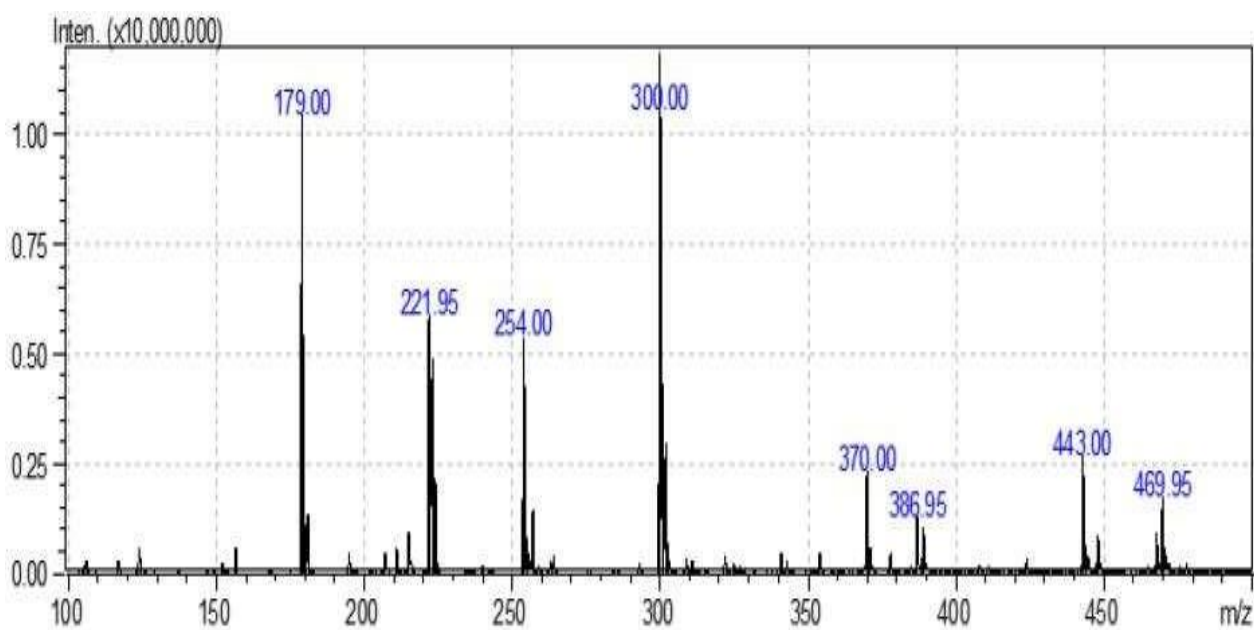


Figure 33. Mass spectra for compound 14b

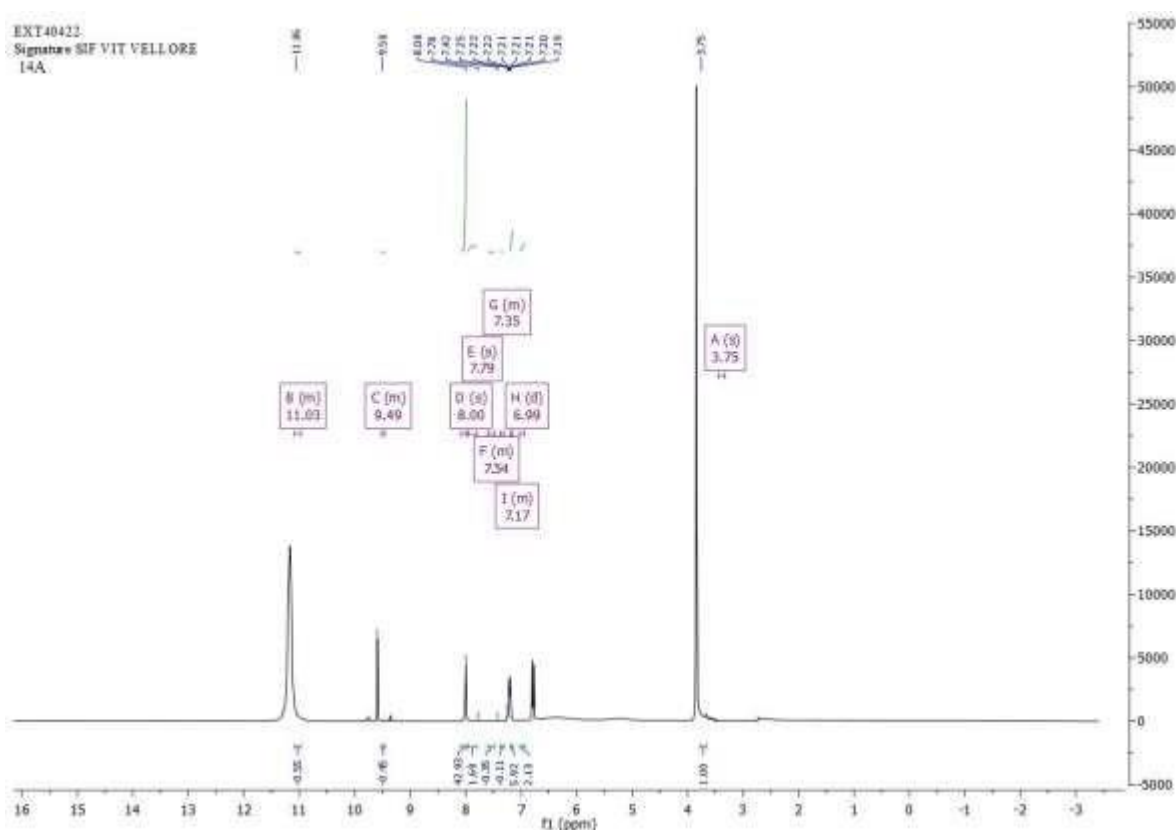


Figure 34. ^1H NMR spectra for compound 14b

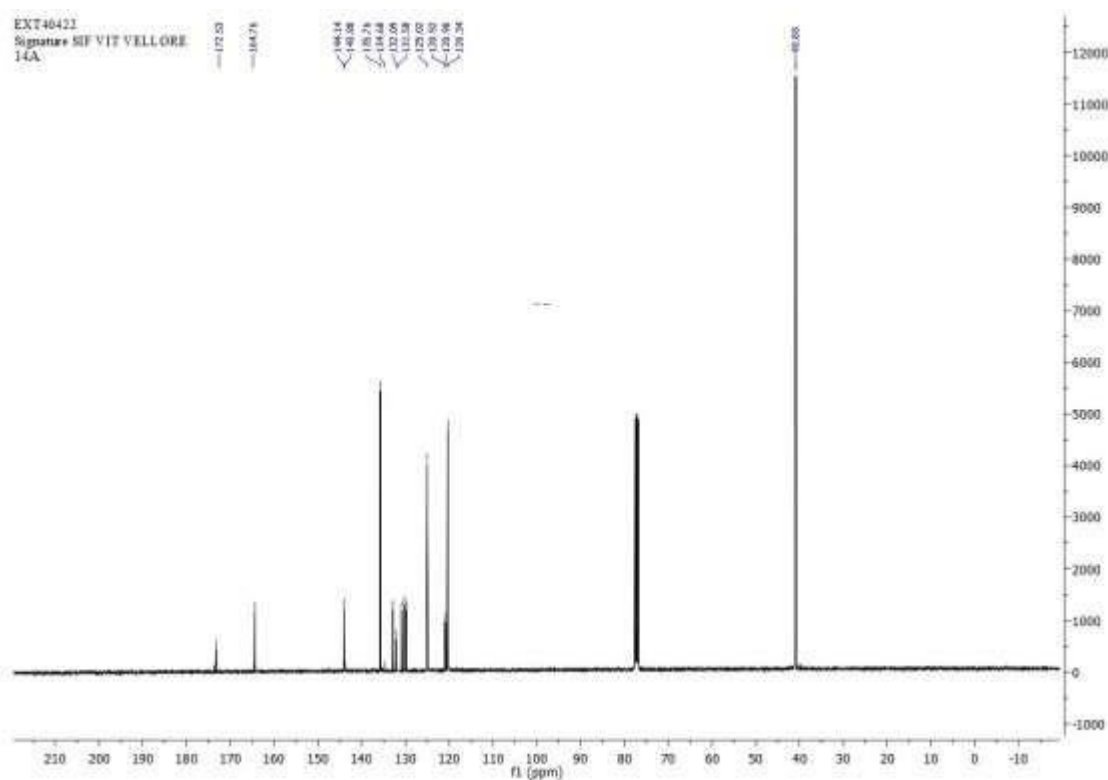


Figure 35. ^{13}C NMR spectra for compound 14b

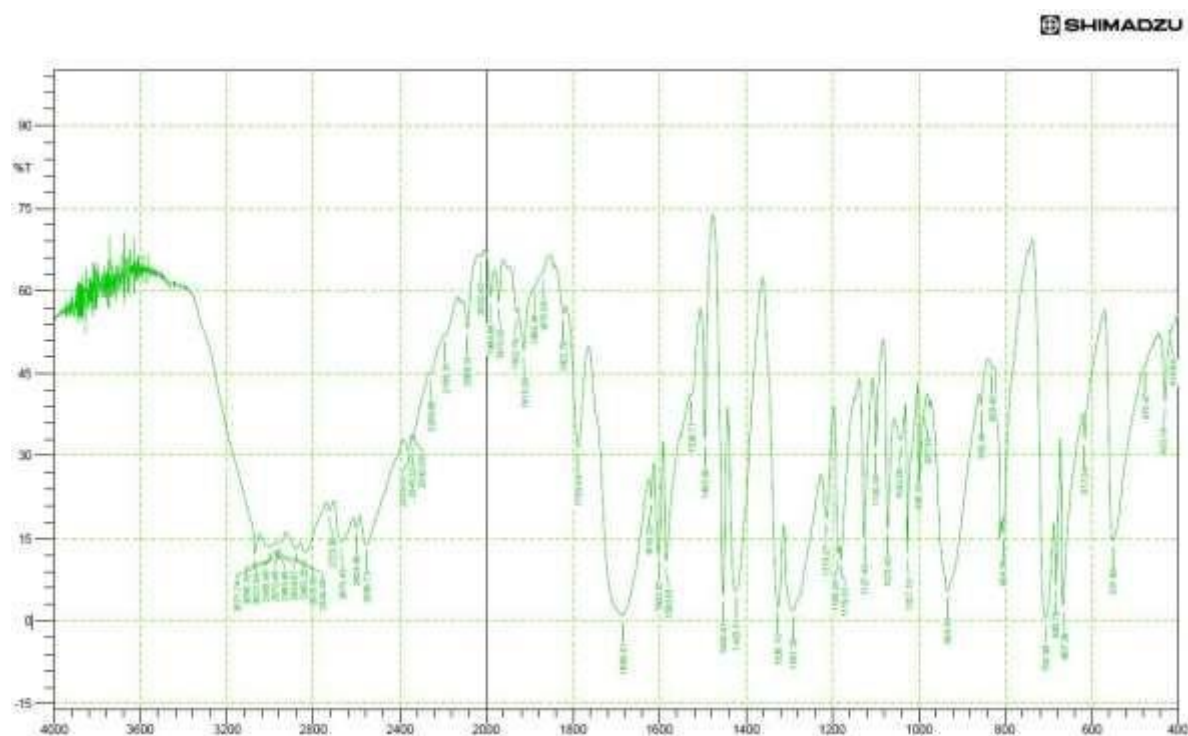


Figure 36. IR spectra for compound 17b

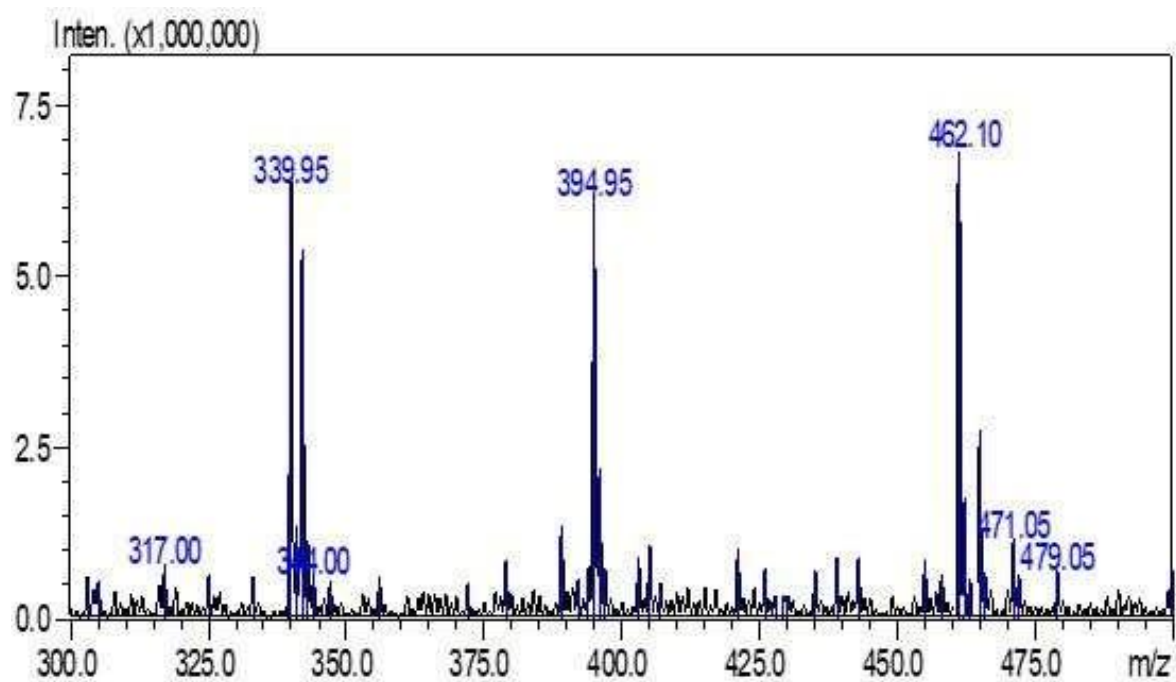


Figure 37. Mass spectra for compound 17b

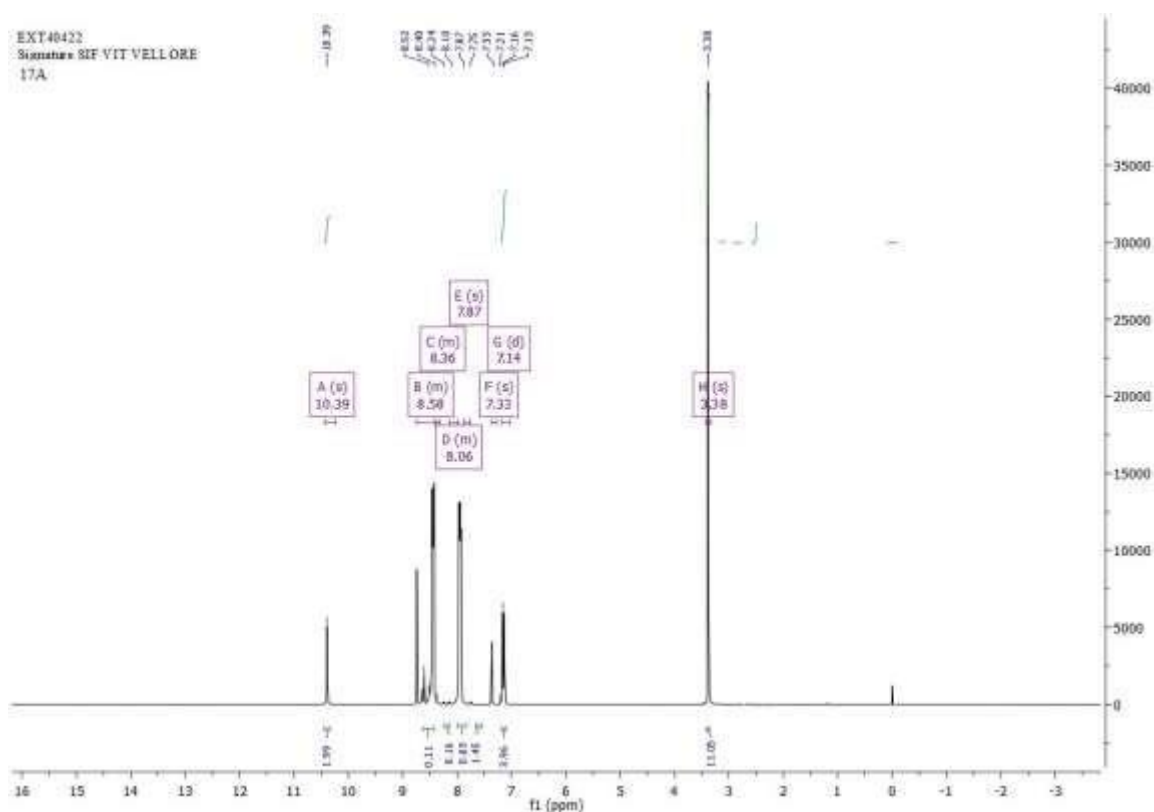


Figure 38. ^1H NMR spectra for compound 17b

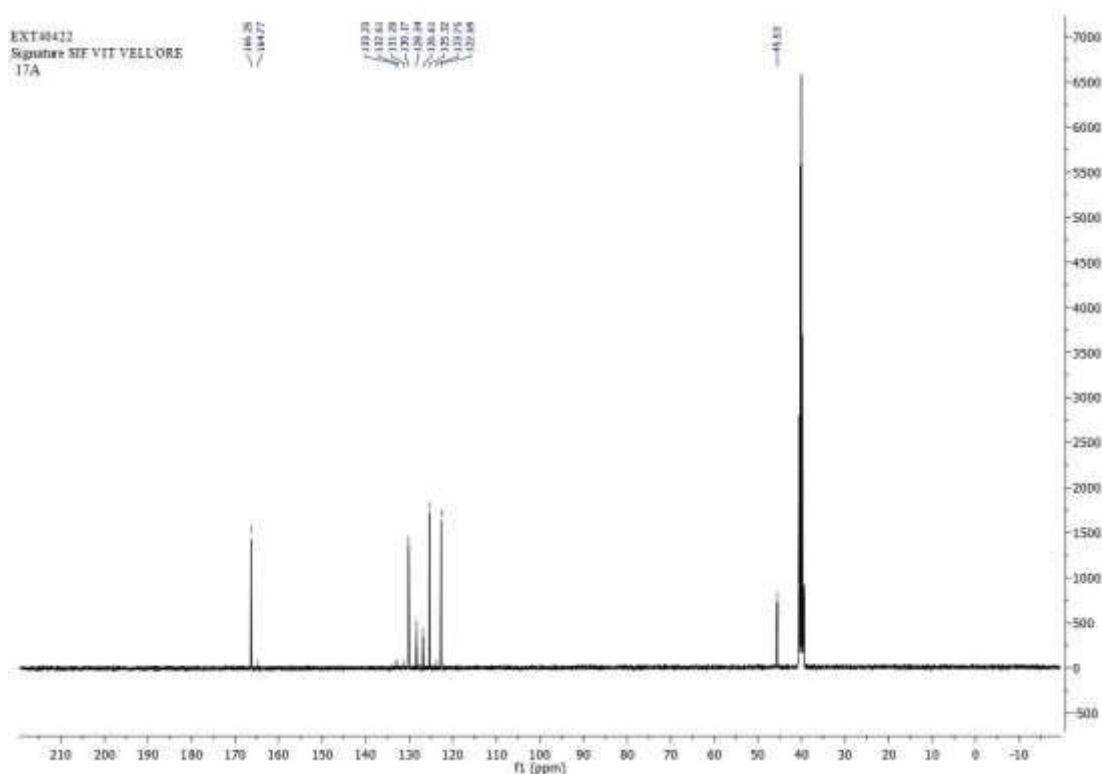


Figure 39. ^{13}C NMR spectra for compound 17b

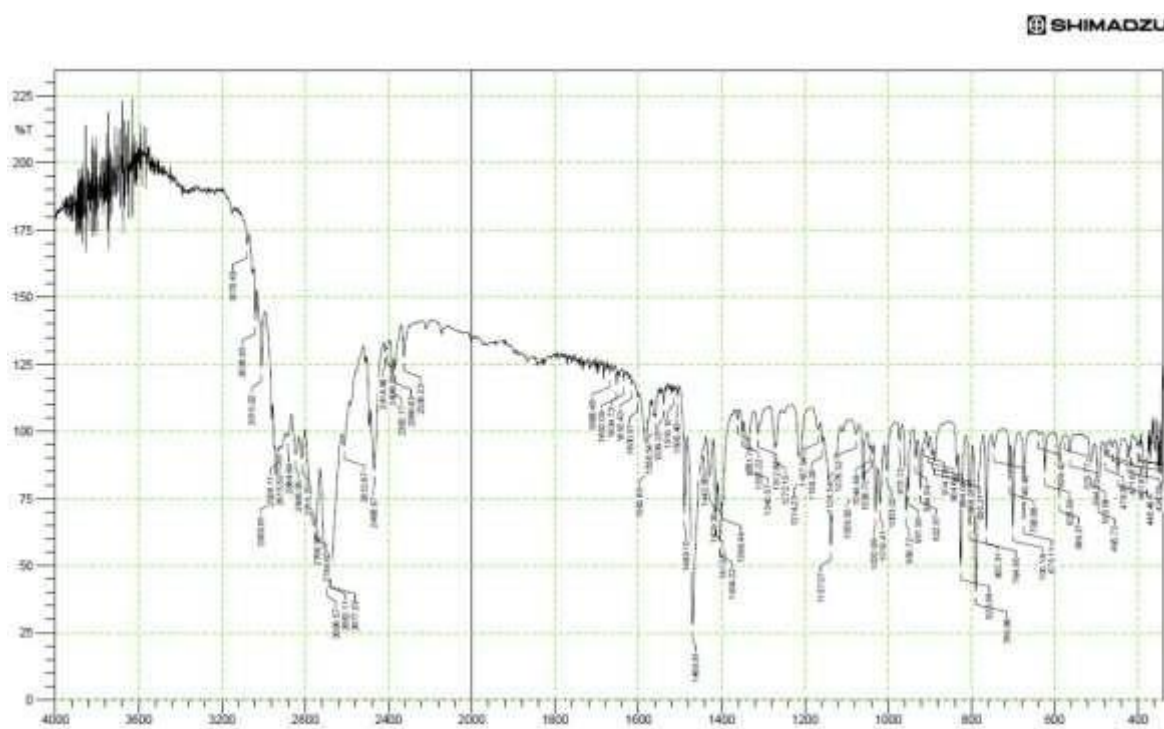


Figure 40. IR spectra for compound 18b

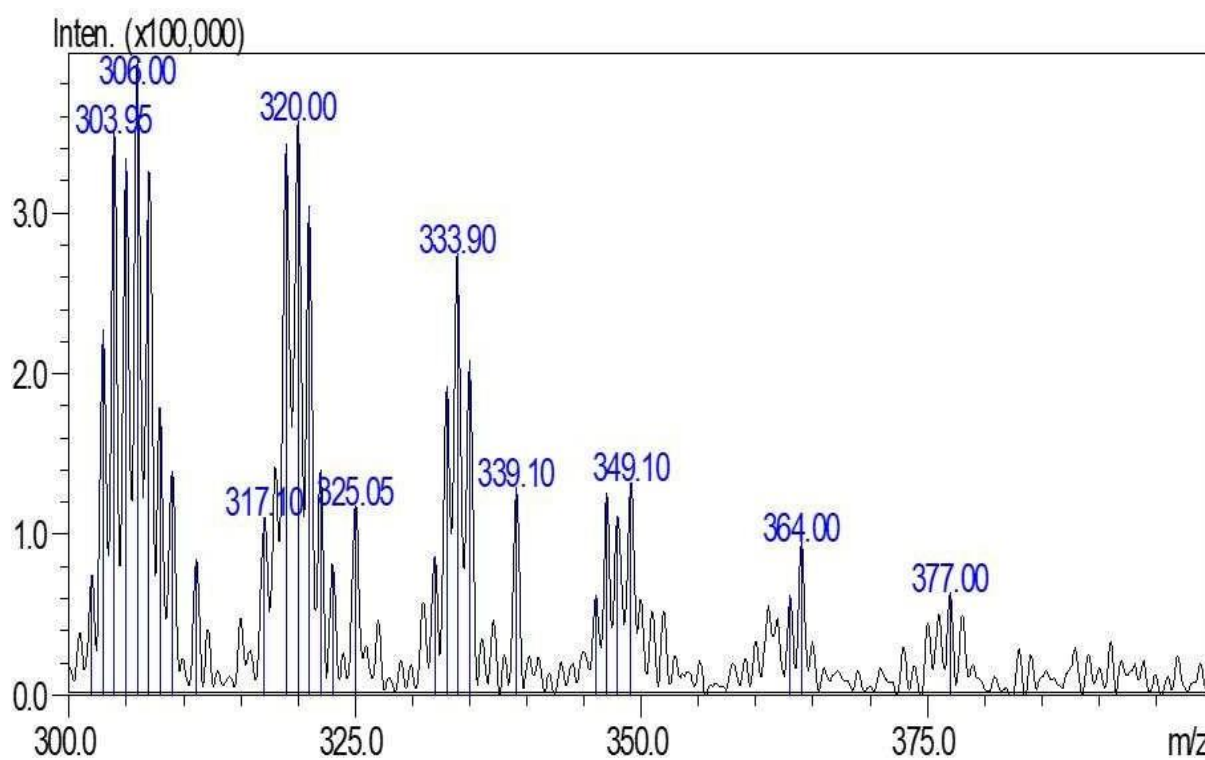


Figure 41. Mass spectra for compound 18b

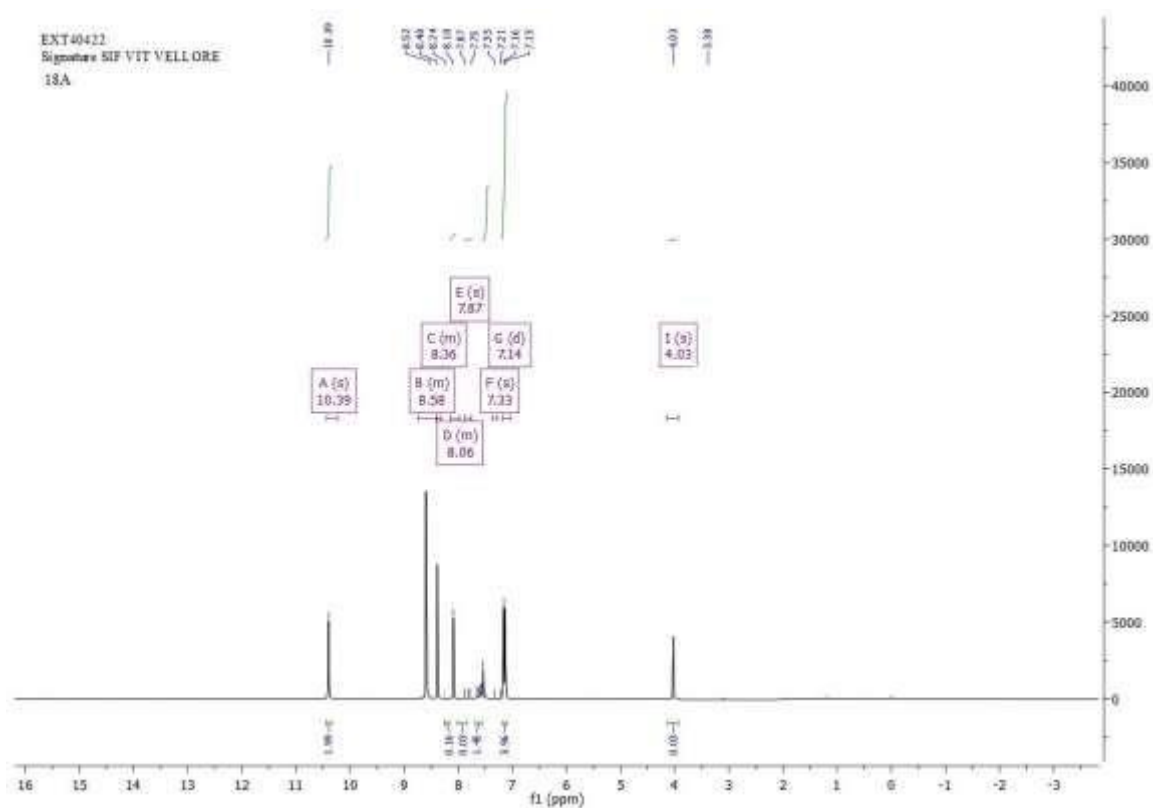


Figure 42. ^1H NMR spectra for compound 18b

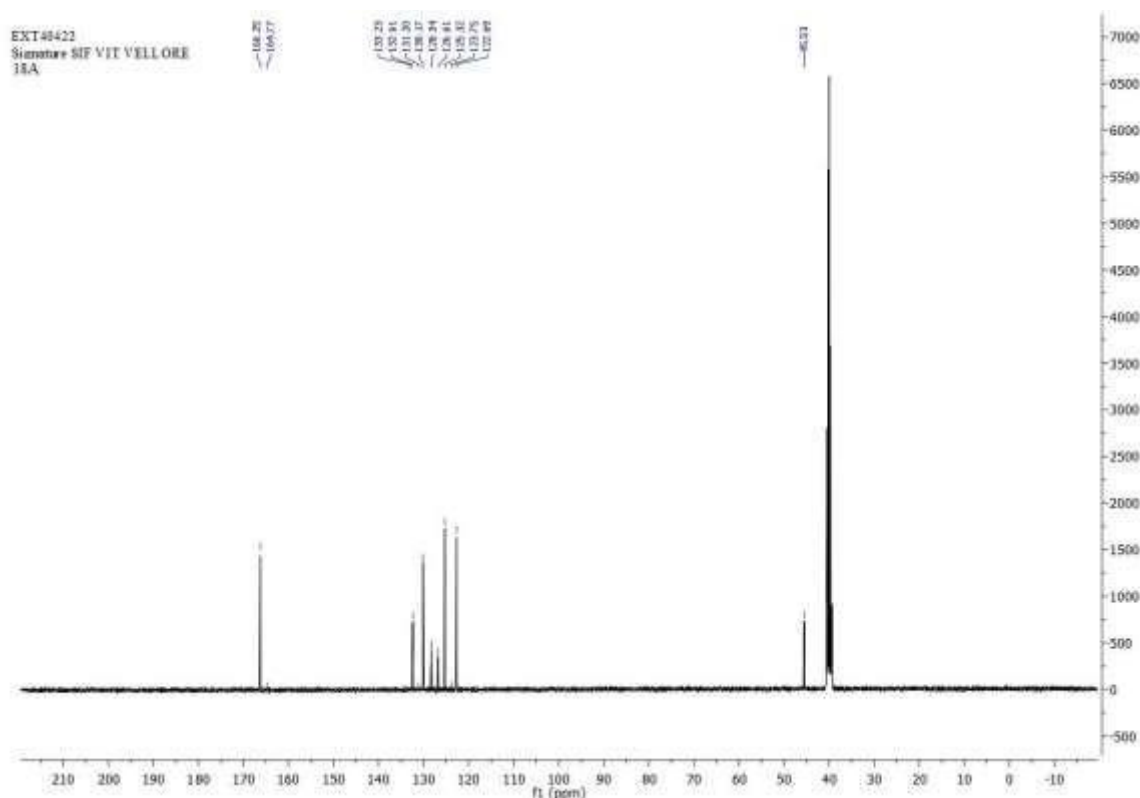


Figure 43. ^{13}C NMR spectra for compound 18b

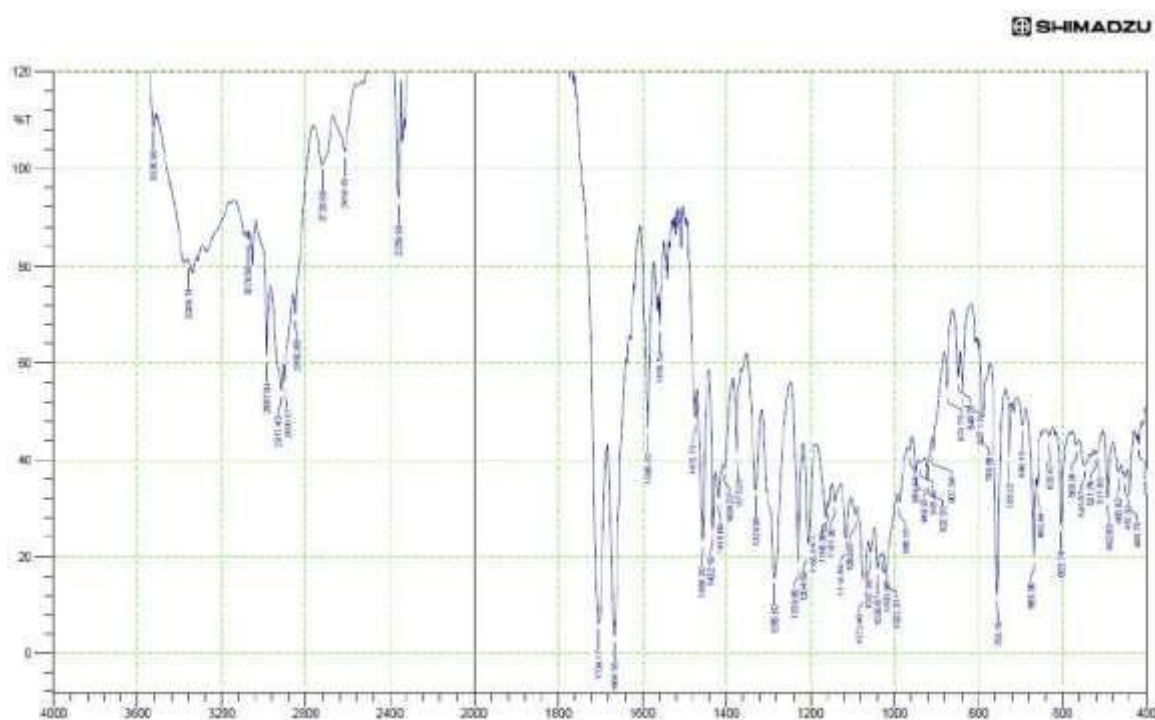


Figure 44. IR spectra for compound 21b

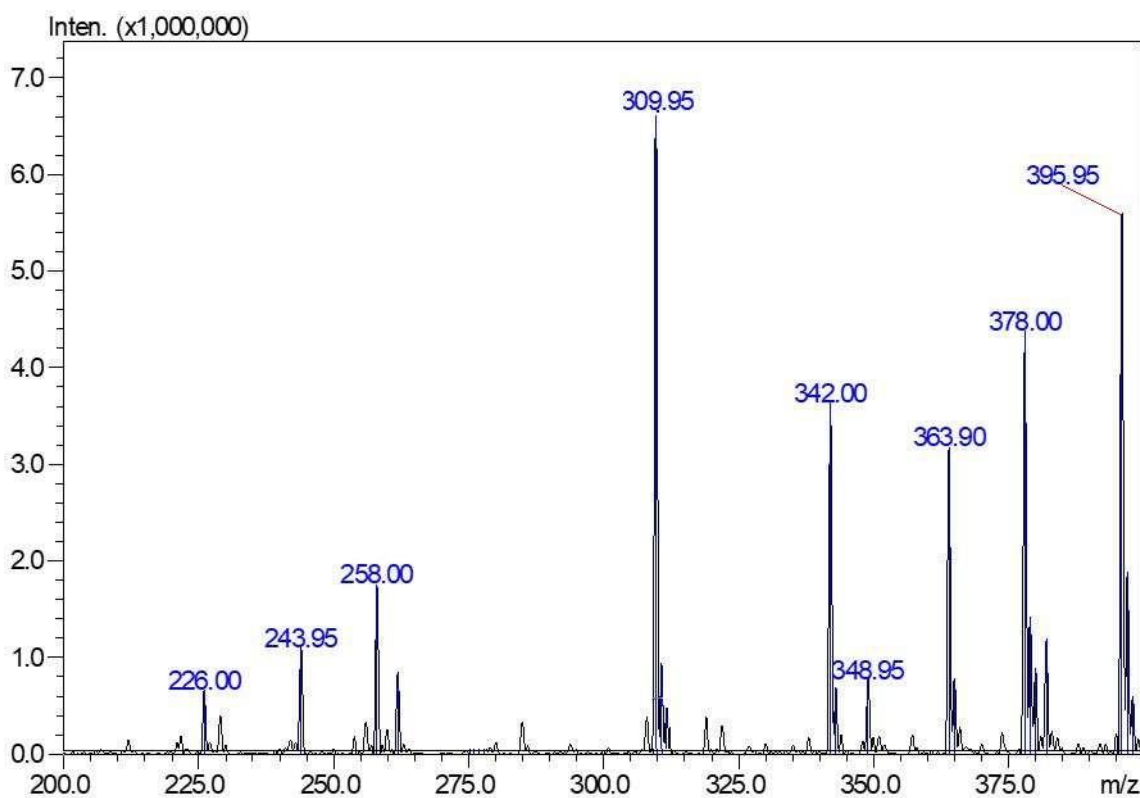


Figure 45. Mass spectra for compound 21b

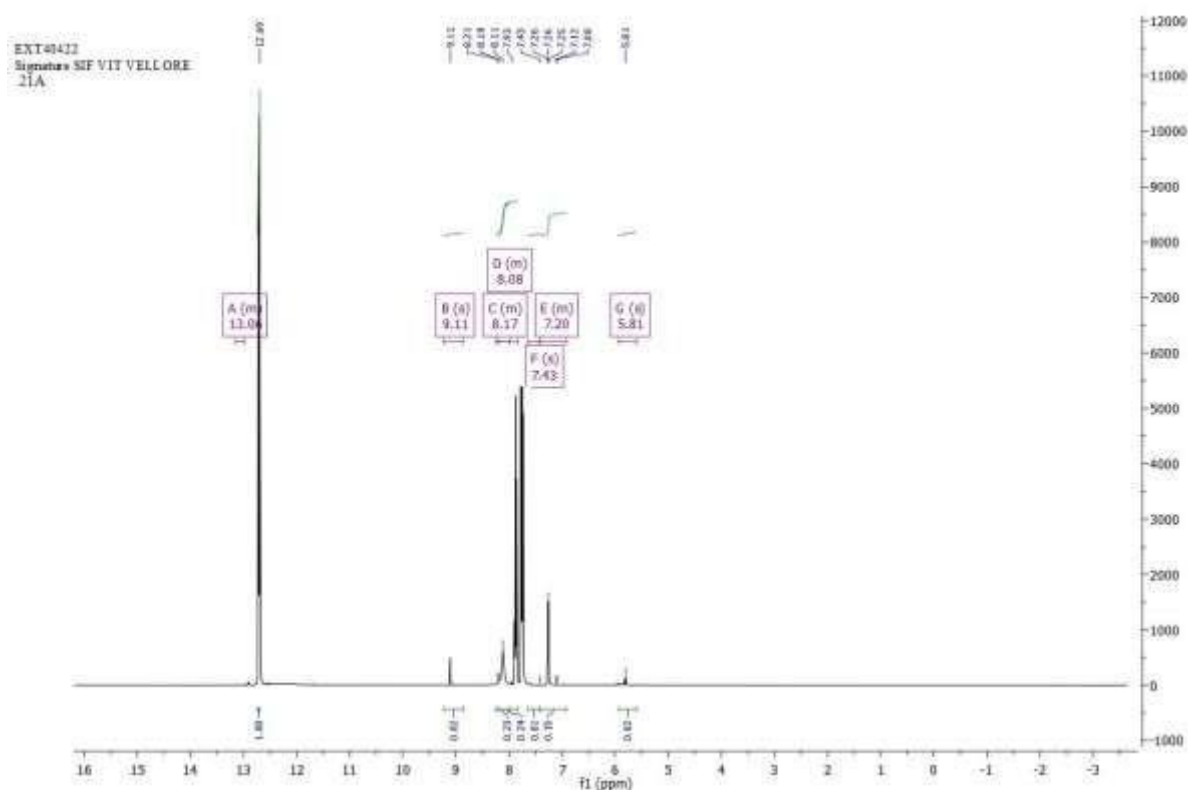


Figure 46. ^1H NMR spectra for compound 21b

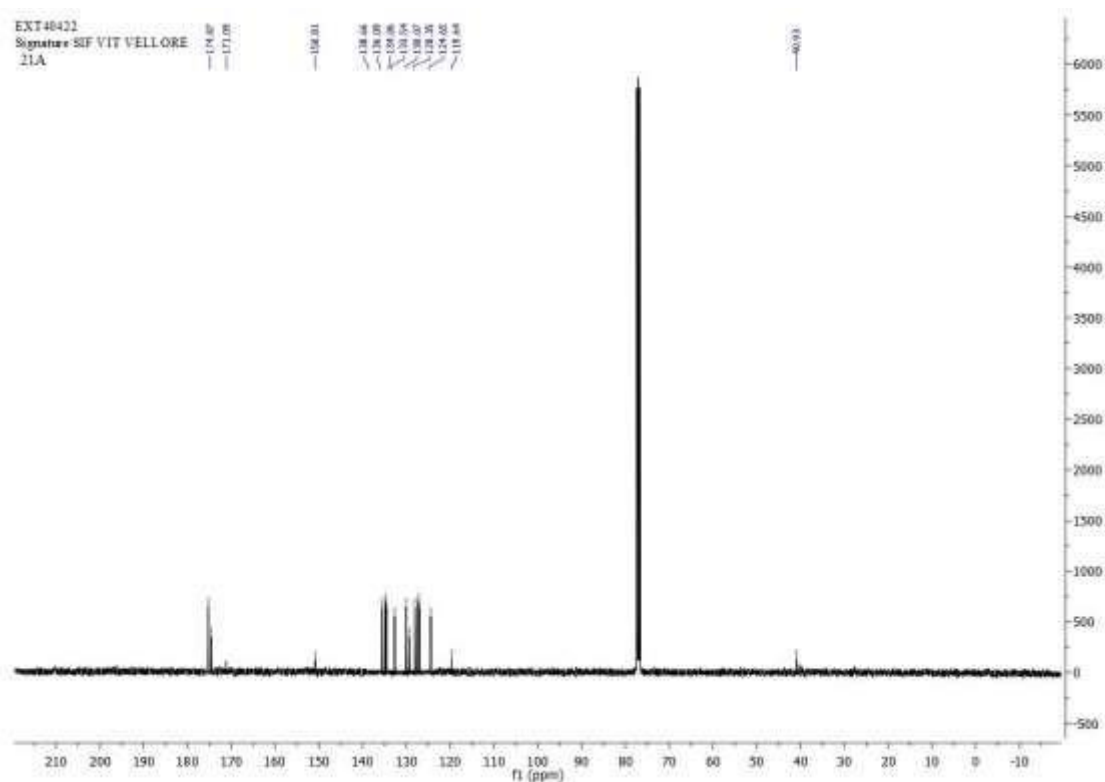


Figure 47. ^{13}C NMR spectra for compound 21b

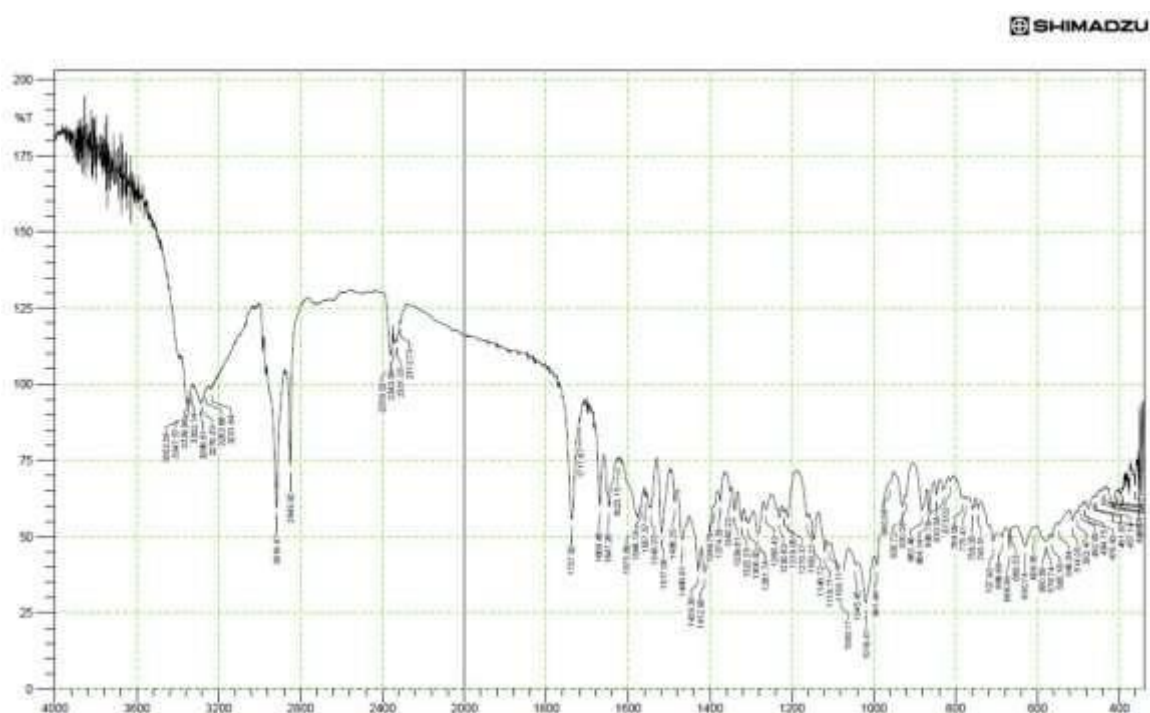


Figure 47. IR spectra for compound 22b

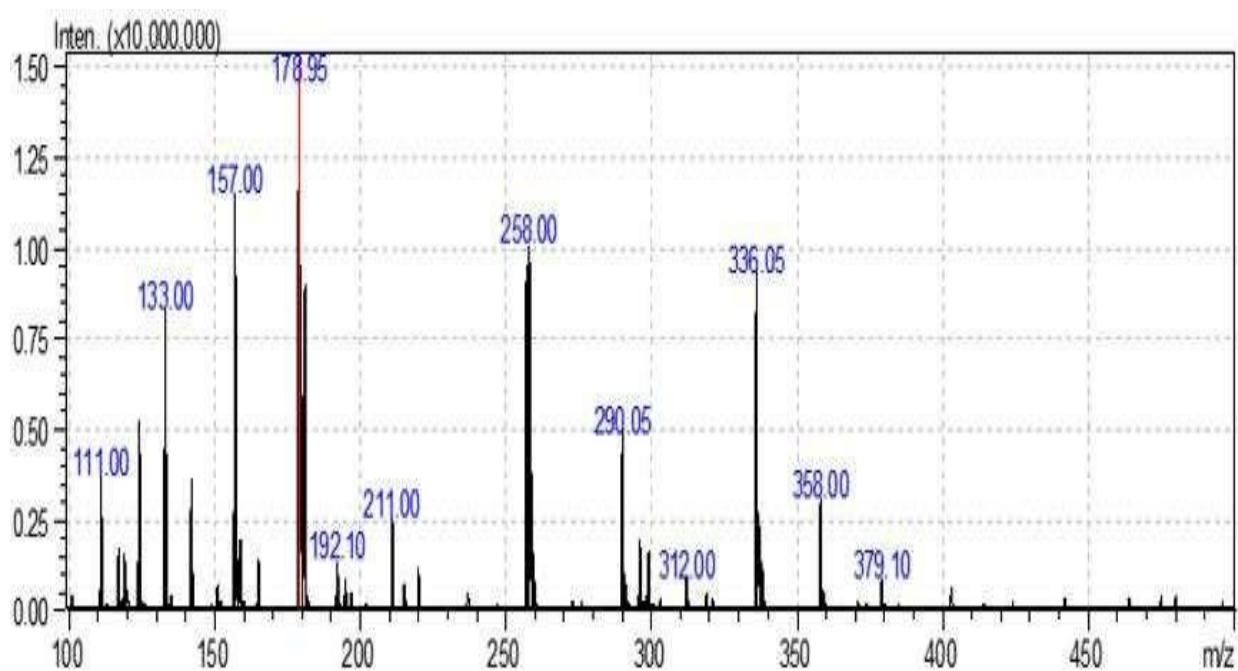


Figure 48. Mass spectra for compound 22b

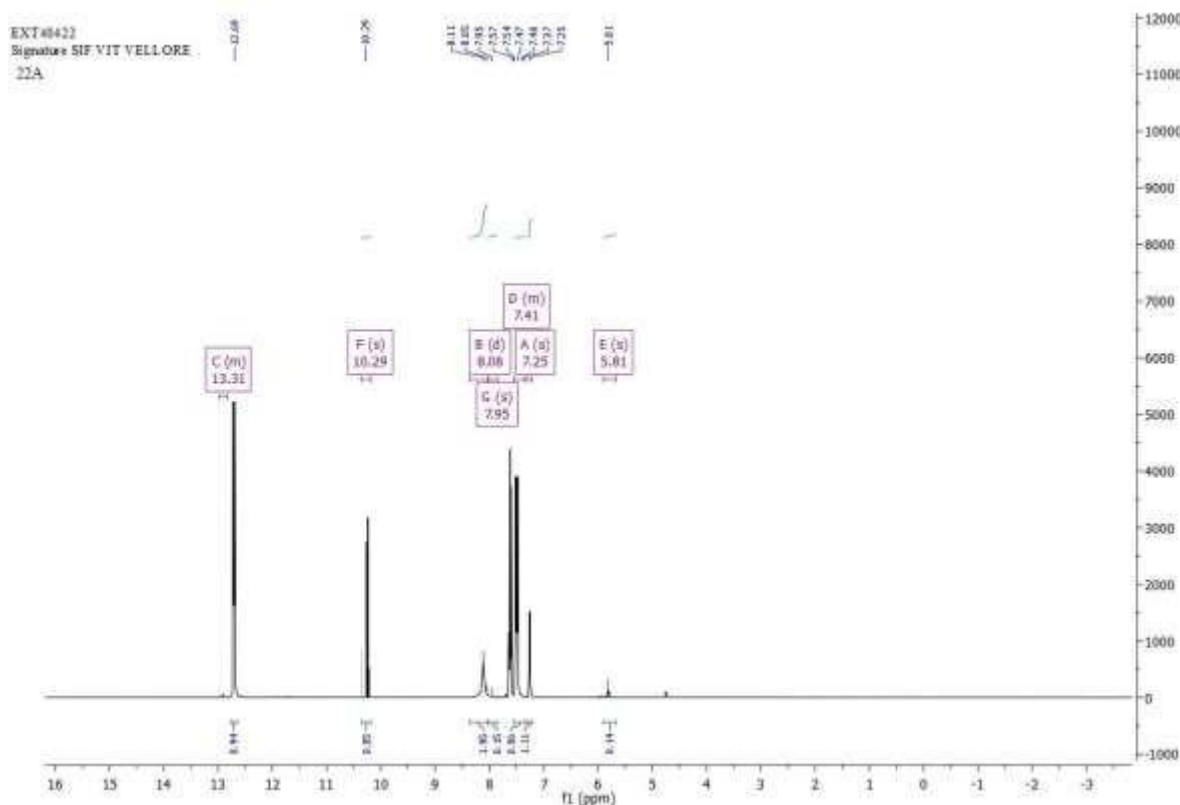


Figure 49. ^1H NMR spectra for compound 22b

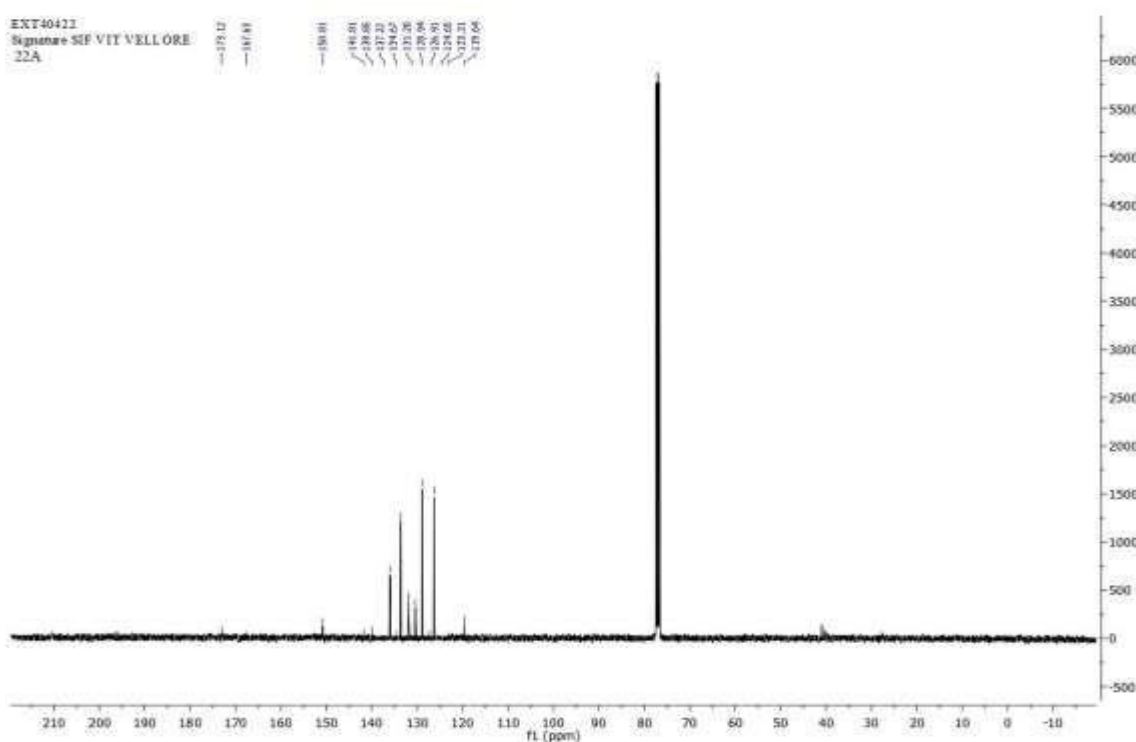


Figure 50. ^{13}C NMR spectra for compound 22b

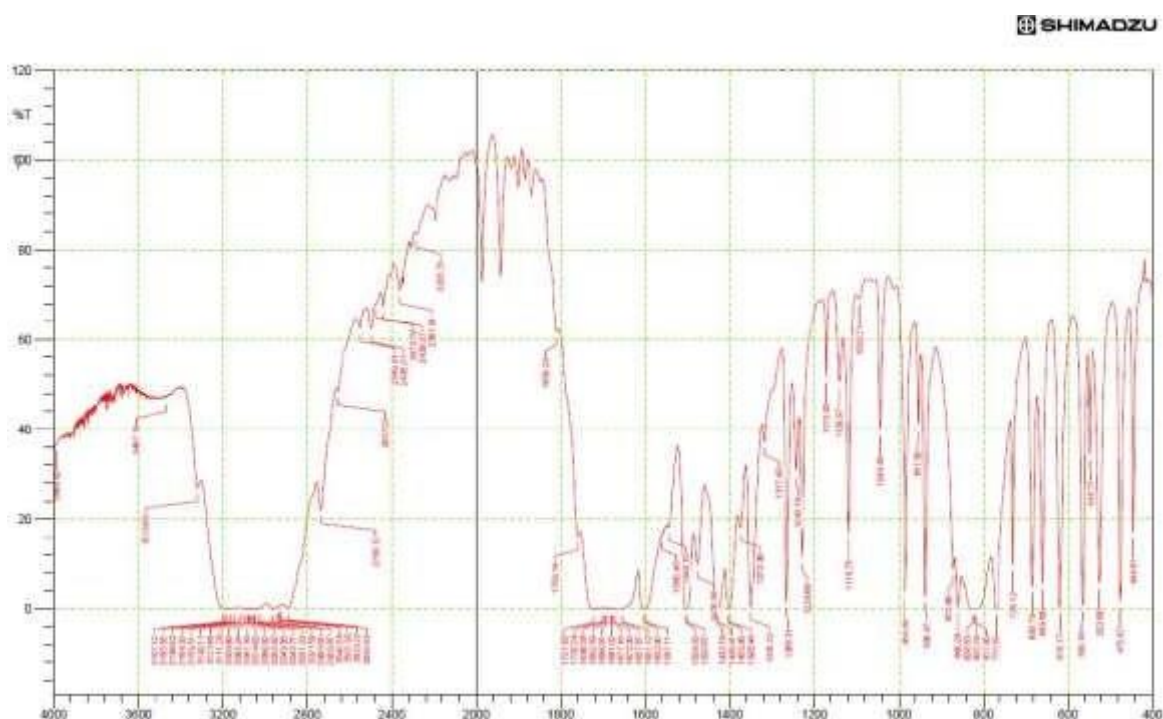


Figure 51. IR spectra for compound 23b

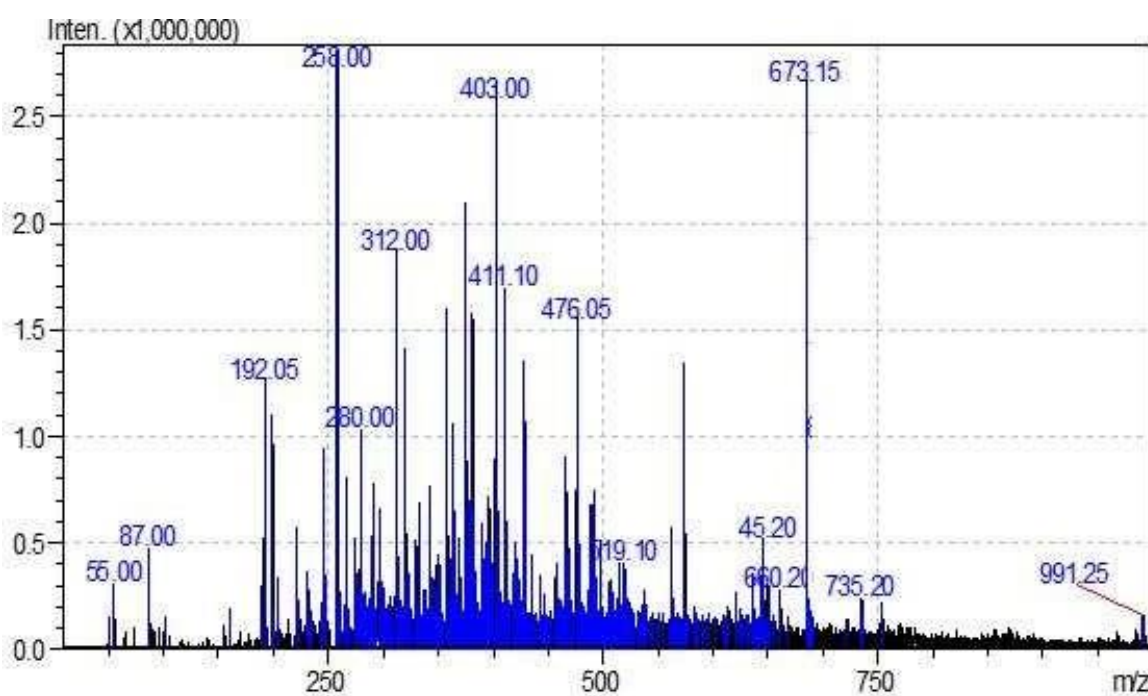


Figure 52. Mass spectra for compound 23b

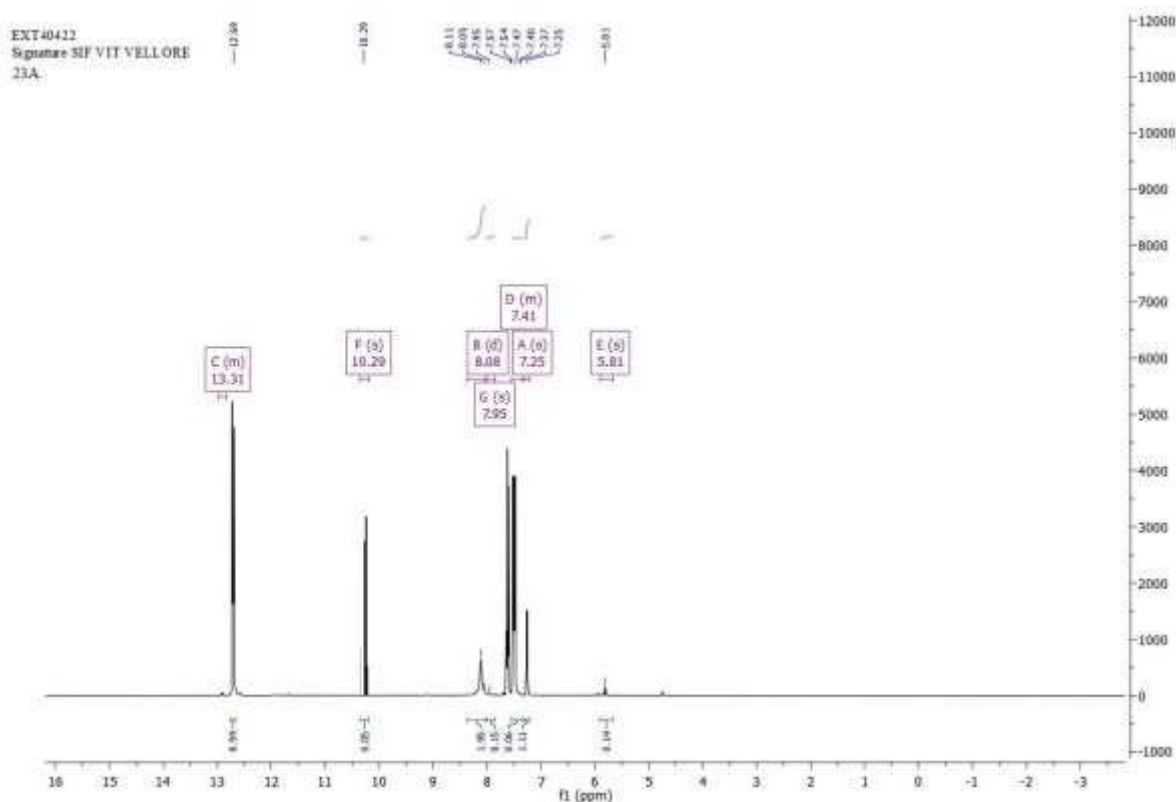


Figure 53. ^1H NMR spectra for compound 23b

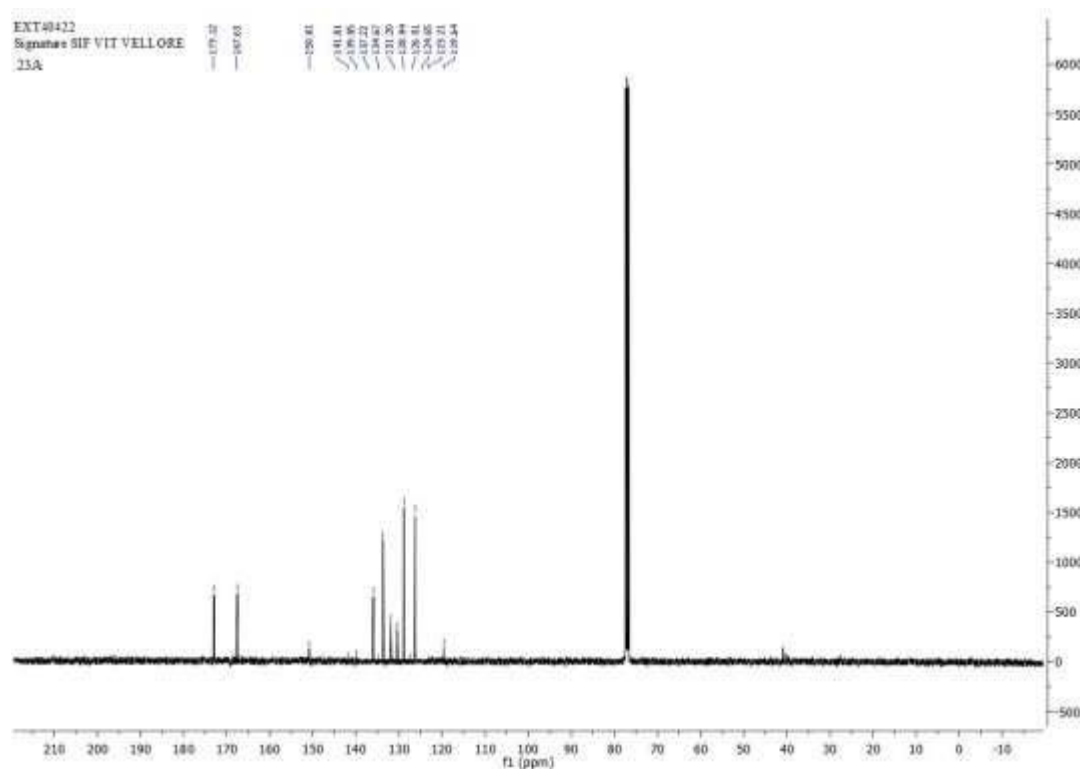


Figure 54. ^{13}C NMR spectra for compound 23b

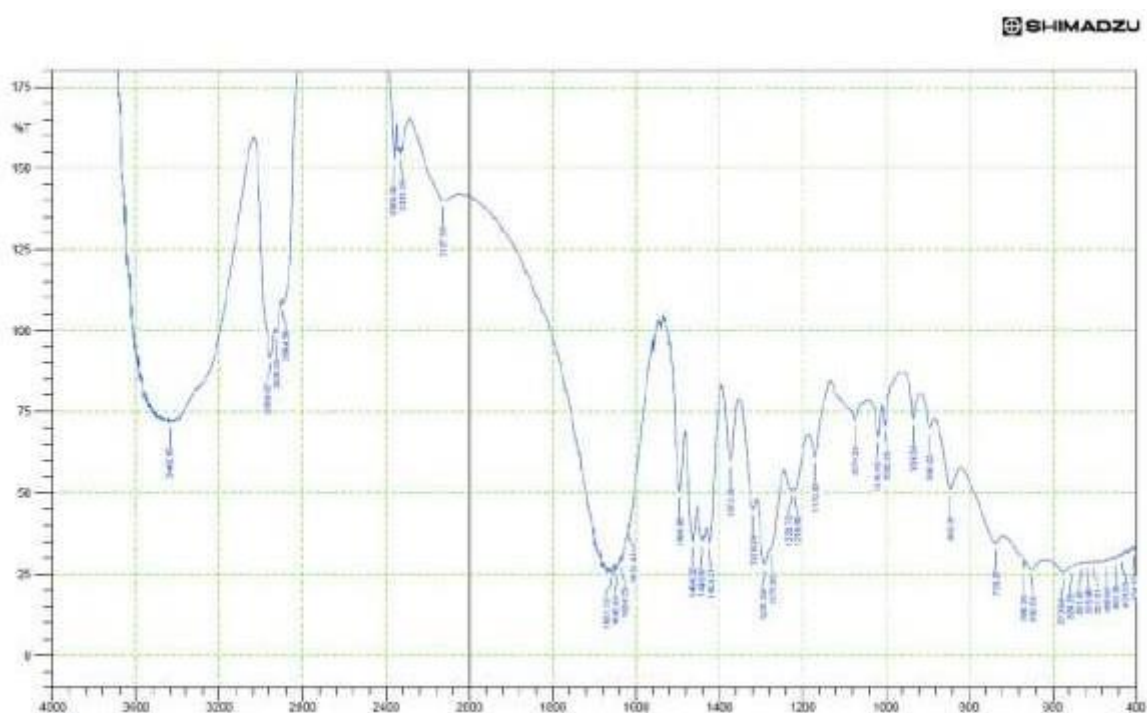


Figure 55. IR spectra for compound 24b

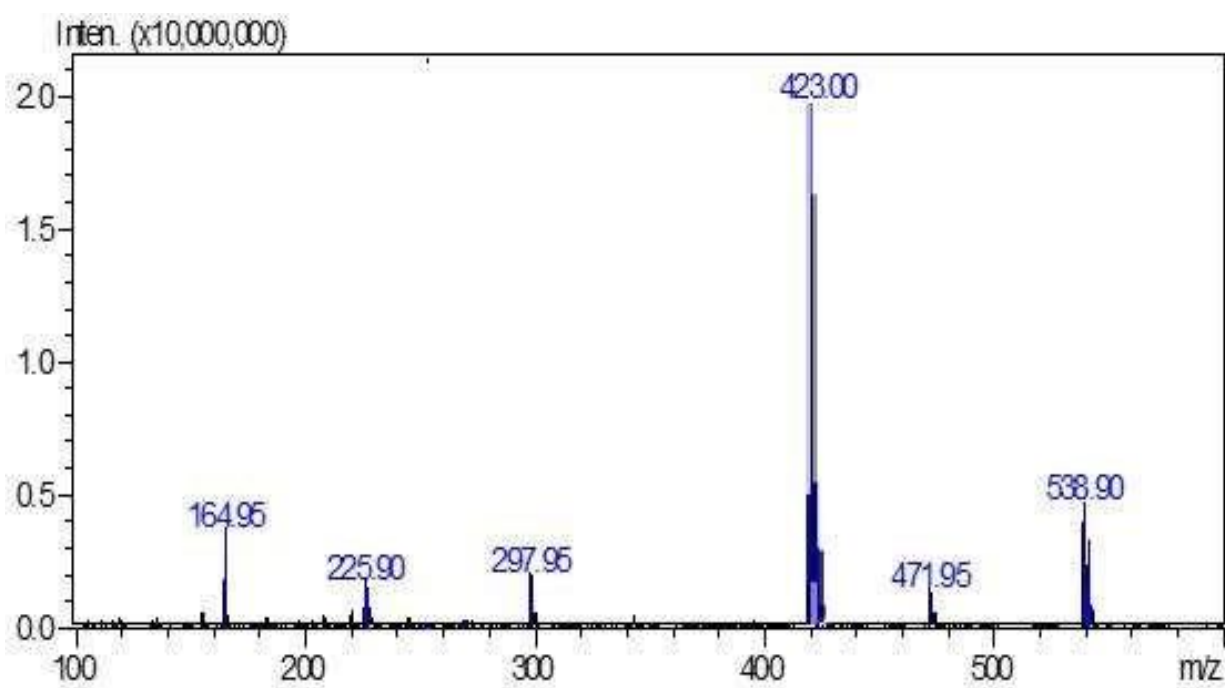


Figure 56. Mass spectra for compound 24b

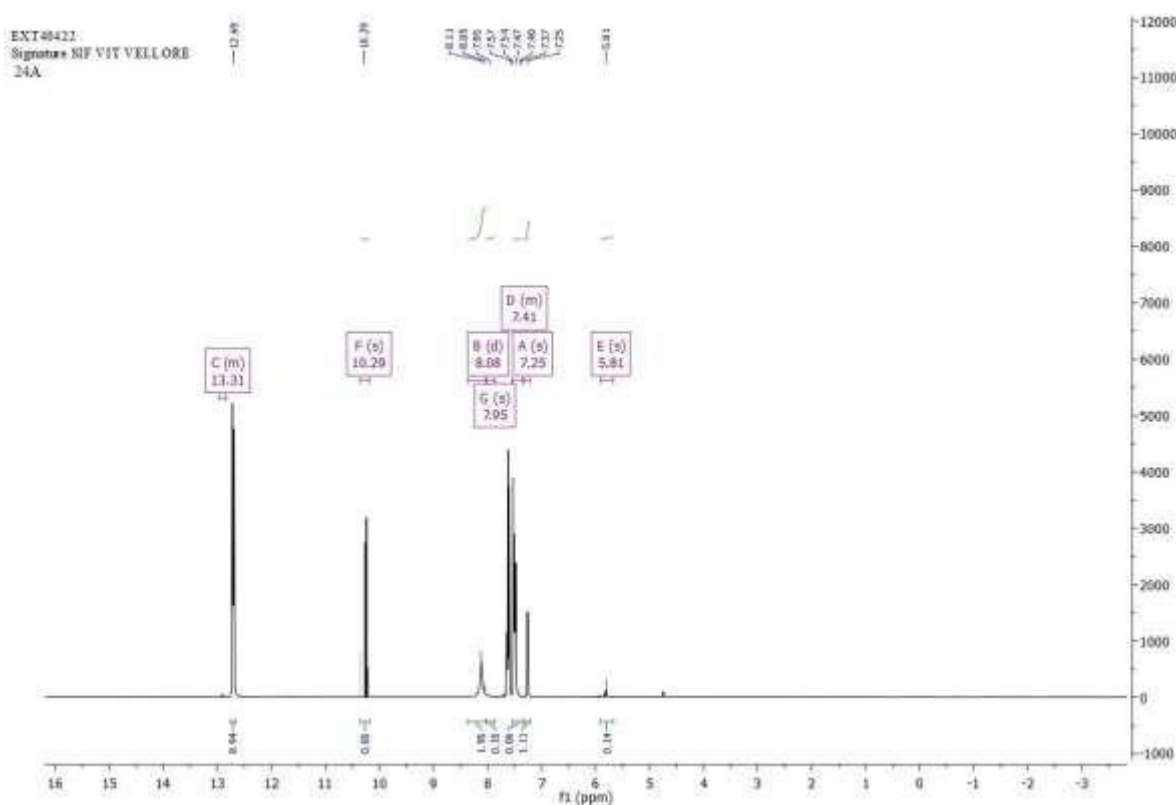


Figure 57. ^1H NMR spectra for compound 24b

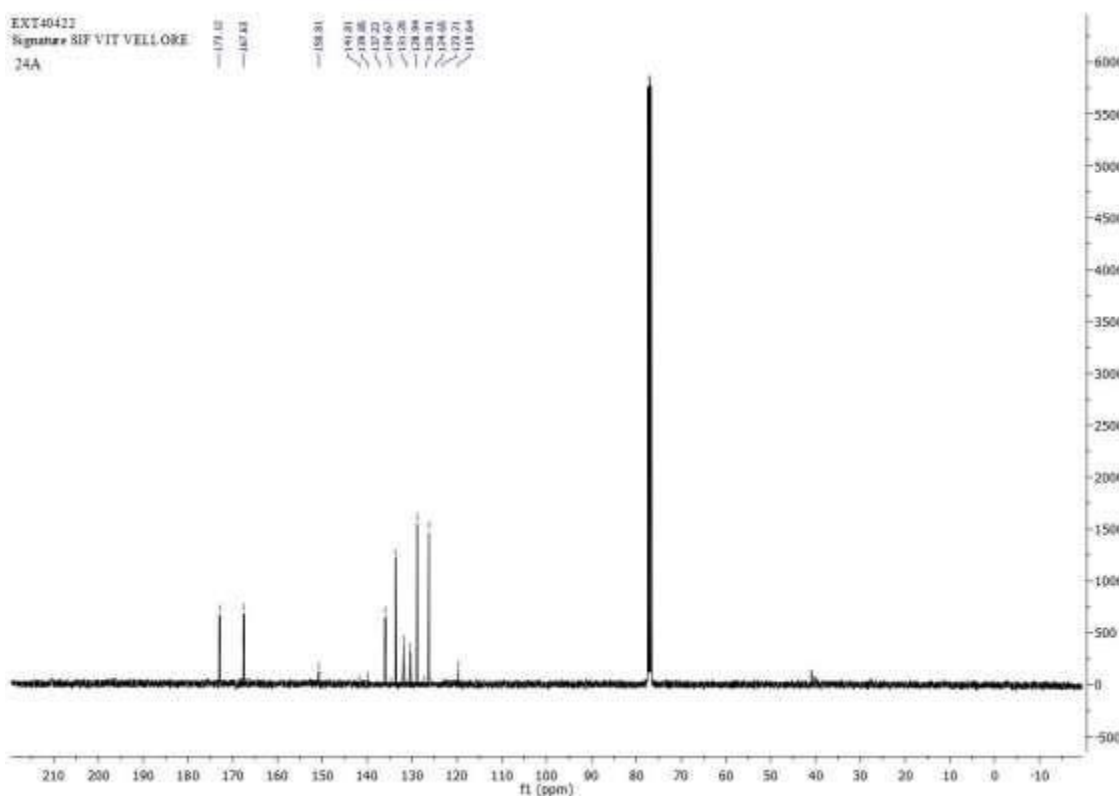
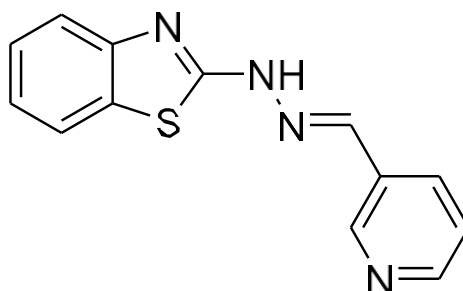


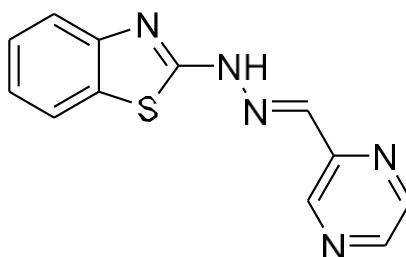
Figure 58. ^{13}C NMR spectra for compound 24b

6.2.2.(E)-2-(2-(pyridin-3-ylmethylene)hydrazineyl)benzo[d]thiazole (5b)



Chemical Formula	: C ₁₃ H ₁₀ N ₄ S
Color	: White solid
MP	: 156 – 161 ^o C
Mass	Actual mass: 254 Found mass: 256 (M+2)
IR KBr pellet (cm⁻¹)	3272 (NH stretching amine); 3038 (CH stretching aromatic); 2917 (CH stretching alkane); 1434 (C - N bending); 836 (aromatic ring)
¹H NMR (400 MHz, CDCl₃) δ	: 10.80 (s, 1H), 8.71 (s, 1H), 8.48 (s, 1H), 8.11 (m, 1H), 7.04 (dd, J = 25.4, 8.4 Hz, 1H), 6.51 (d, J = 8.4 Hz, 2H).
¹³C NMR (101 MHz, CDCl₃) δ	: 170.79, 163.04, 144.94, 129.13, 129.11, 125.16, 123.75, 123.17, 119.16, 117.11, 116.29, 116.27
Elemental Analysis	C, 61.40; H, 3.96; N, 22.03; S, 12.61

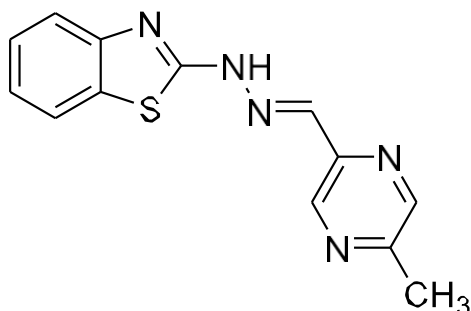
6.2.4. (E)-2-(2-(pyrazin-2-ylmethylene)hydrazineyl)benzo[d]thiazole (6b)



Chemical Formula	: C ₁₂ H ₉ N ₅ S
Color	: White solid
MP	: 162 – 165 ^o C
Mass	Actual mass: 255 Found mass: 257 (M+1)
IR KBr pellet (cm⁻¹)	3377 (NH stretching amine); 2317 (CH stretching aromatic); 2347 (CH stretching alkane); 1459 (C - N bending); 820 (aromatic ring)
¹H NMR (400 MHz, CDCl₃) δ	: 11.30 (s, 1H), 7.79 (s, 2H), 7.51 (s, 2H), 7.31 (s, 1H), 7.28 – 7.11 (m, 2H), 6.81 (s, 1H), 6.54 (s,

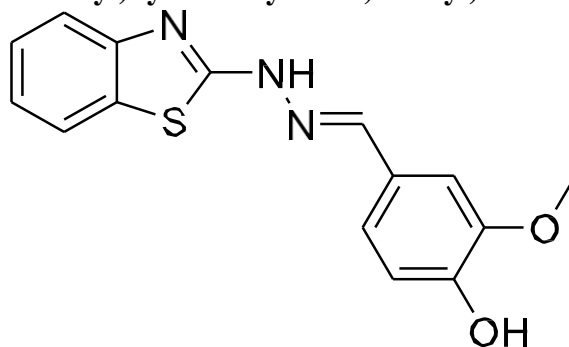
	2H).
¹³ C NMR (101 MHz, CDCl ₃) δ	170.79, 163.04, 144.94, 143.86, 130.37, 129.13, 129.11, 127.52, 125.16, 123.17, 119.16, 116.29, 116.27.
Elemental Analysis	C, 56.46; H, 3.55; N, 27.43; S, 12.56

6.2.5. (E)-2-(2-((5-methylpyrazin-2-yl)methylene)hydrazineyl)benzo[d]thiazole (7b)



Chemical Formula	: C ₁₃ H ₁₁ N ₅ S
Color	: White solid
MP	: 176 – 179°C
Mass	Actual mass: 269 Found mass: 269
IR KBr pellet (cm ⁻¹)	3071 (NH stretching amine); 3006 (CH stretching aromatic); 2878 (CH stretching alkane); 1423 (C - N bending); 855 (aromatic ring)
¹ H NMR (400 MHz, CDCl ₃) δ	11.30 (s, 1H), 7.79 (s, 1H), 7.51 (s, 2H), 7.31 (s, 4H), 7.28 (m, 2H), 6.81 (s, 1H), 6.54 (s, 2H), 2.51 (s, 2H).
¹³ C NMR (101 MHz, CDCl ₃) δ	170.79, 163.04, 144.94, 143.86, 130.37, 129.13, 129.11, 127.52, 125.16, 123.17, 119.16, 116.29, 116.27, 41.09.
Elemental Analysis	C, 57.98; H, 4.12; N, 26.00; S, 11.90

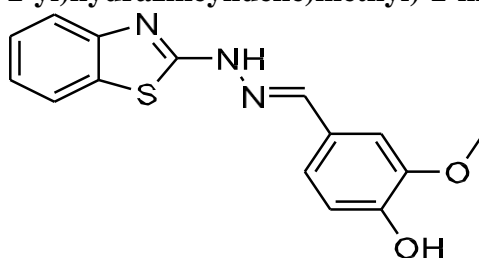
6.2.6. (E)-4-((2-(benzo[d]thiazol-2-yl)hydrazineylidene)methyl)-2-methoxyphenol (14b)



Chemical Formula	: C ₁₅ H ₁₃ N ₃ O ₂ S
Color	: White solid

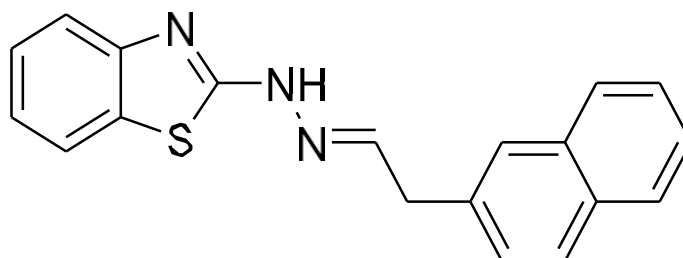
MP	: 157 – 161 ^o C
Mass	Actual mass: 299 Found mass: 300 (M+1)
IR KBr pellet (cm⁻¹)	3071 (NH stretching amine); 3006 (CH stretching aromatic); 2878 (CH stretching alkane); 1423 (C - N bending); 855 (aromatic ring)
¹H NMR (400 MHz, CDCl₃) δ	11.09 (m, 1H), 9.52 (m, 1H), 8.00 (s, 3H), 7.79 (s, 1H), 7.60 (m, 1H), 7.38 (m, 1H), 7.19 (m, 1H), 6.99 (d, J = 7.7 Hz, 1H), 3.75 (s, 3H).
¹³C NMR (101 MHz, CDCl₃) δ	172.53, 164.76, 144.14, 143.88, 135.76, 134.68, 132.09, 131.58, 125.02, 120.92, 120.90, 120.34, 40.88.
Elemental Analysis	C, 60.19; H, 4.38; N, 14.04; O, 10.69; S, 10.71

6.2.7.(E)-4-((2-(benzo[d]thiazol-2-yl)hydrazineylidene)methyl)-2-methoxyphenol (14b)



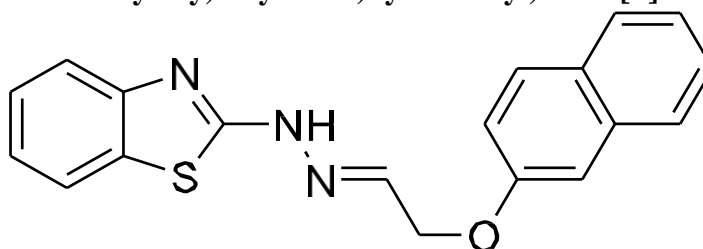
Chemical Formula	: C ₁₅ H ₁₃ N ₃ O ₂ S
Color	: White solid
MP	: 157 – 161 ^o C
Mass	Actual mass: 299 Found mass: 300 (M+1)
IR KBr pellet (cm⁻¹)	3307 (NH stretching amine); 3021 (CH stretching aromatic); 2900 (CH stretching alkane); 1424 (C - N bending); 875 (aromatic ring)
¹H NMR (400 MHz, CDCl₃) δ	11.09 (m, 1H), 9.52 (m, 1H), 8.00 (s, 3H), 7.79 (s, 1H), 7.60 (m, 1H), 7.38 (m, 1H), 7.19 (m, 1H), 6.99 (d, J = 7.7 Hz, 1H), 3.75 (s, 3H).
¹³C NMR (101 MHz, CDCl₃) δ	172.53, 164.76, 144.14, 143.88, 135.76, 134.68, 132.09, 131.58, 125.02, 120.92, 120.90, 120.34, 40.88.
Elemental Analysis	C, 60.19; H, 4.38; N, 14.04; O, 10.69; S, 10.71

6.2.8. (E)-2-(2-(2-(naphthalen-2-yl)ethylidene)hydrazineyl)benzo[d]thiazole (17b)



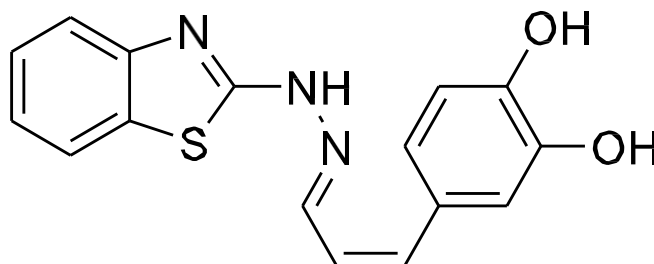
Chemical Formula	: C ₁₅ H ₁₃ N ₃ O ₂ S
Color	: White solid
MP	: 172 – 174°C
Mass	Actual mass: 317 Found mass: 317
IR KBr pellet (cm⁻¹)	3071 (NH stretching amine); 3006 (CH stretching aromatic); 2878 (CH stretching alkane); 1423 (C - N bending); 855 (aromatic ring)
¹H NMR (400 MHz, DMSO) δ	10.39 (s, 1H), 8.7 (m, 1H), 8.40 (m, 1H), 7.98 (m, 1H), 7.87 (s, 1H), 7.33 (s, 1H), 7.14 (d, J = 11.1 Hz, 2H), 3.38 (s, 1H).
¹³C NMR (101 MHz, DMSO) δ	166.25, 164.77, 133.23, 132.61, 131.20, 130.17, 128.34, 126.61, 125.32, 123.75, 122.69, 45.53.
Elemental Analysis	C, 71.90; H, 4.76; N, 13.24; S, 10.10

6.2.9. (E)-2-(2-(2-(naphthalen-2-yloxy)ethylidene)hydrazineyl)benzo[d]thiazole (18b)



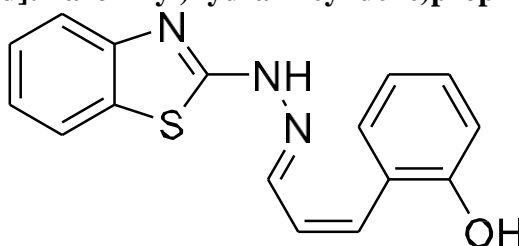
Chemical Formula	: C ₁₉ H ₁₅ N ₃ OS
Color	: White solid
MP	: 176 – 180°C
Mass	Actual mass: 333 Found mass: 333
IR KBr pellet (cm⁻¹)	3078 (NH stretching amine); 3038 (CH stretching aromatic); 2884 (CH stretching alkane); 1404 (C - N bending); 825 (aromatic ring)
¹H NMR (400 MHz, DMSO) δ	10.39 (s, 1H), 8.75 (m, 1H), 8.40 (m, 1H), 8.14 (m, 1H), 7.87 (s, 1H), 7.33 (s, 1H), 7.14 (d, J = 11.1 Hz, 2H), 4.03 (s, 2H), 3.38 (s, 1H).
¹³C NMR (101 MHz, DMSO) δ	166.25, 164.77, 133.23, 132.61, 131.20, 130.17, 128.34, 126.61, 125.32, 123.75, 122.69, 45.53.
-Elemental Analysis	C, 68.45; H, 4.53; N, 12.60; O, 4.80; S, 9.62.

6.2.10. 4-((1Z,3E)-3-(2-(benzo[d]thiazol-2-yl)hydrazineylidene)prop-1-en-1-yl)benzene- 1,2-diol (21b)

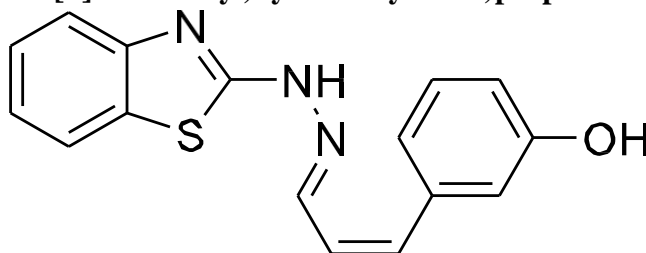


Chemical Formula	: C ₁₆ H ₁₃ N ₃ O ₂ S
Color	: White solid
MP	: 158 – 162°C
Mass	Actual mass: 311 Found mass: 310 (M-1)
IR KBr pellet (cm⁻¹)	3369 (NH stretching amine); 3076 (CH stretching aromatic); 2917 (CH stretching alkane); 1432 (C - N bending); 845 (aromatic ring)
¹H NMR (400 MHz, CDCl₃) δ	13.14 (m, 1H), 9.11 (s, 1H), 8.24 (m, 1H), 8.19 (m, 1H), 7.43 (s, 3H), 7.42 (m, 1H), 5.81 (s, 2H).
¹³C NMR (101 MHz, CDCl₃) δ	174.87, 171.09, 150.81, 138.66, 136.09, 134.06, 133.54, 130.07, 128.35, 124.65, 119.64, 40.93.
Elemental Analysis	C, 61.72; H, 4.21; N, 13.50; O, 10.28; S, 10.30

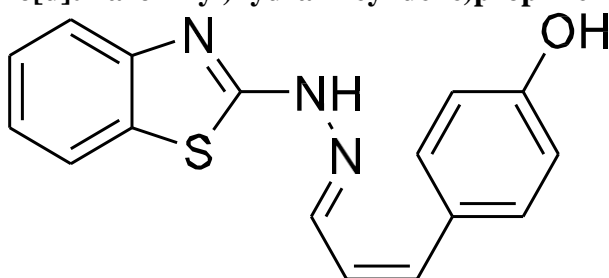
6.2.11. 2-((1Z,3E)-3-(2-(benzo[d]thiazol-2-yl)hydrazineylidene)prop-1-en-1-yl)phenol (22b)



Chemical Formula	: C ₁₆ H ₁₃ N ₃ OS
Color	: White solid
MP	: 161 – 164°C
Mass	Actual mass: 295 Found mass: 312 (M+1+16)
IR KBr pellet (cm⁻¹)	3352 (NH stretching amine); 3231 (CH stretching aromatic); 2916 (CH stretching alkane); 1412 (C - N bending); 846 (aromatic ring)
¹H NMR (400 MHz, CDCl₃) δ	13.38 (m, 1H), 10.29 (s, 1H), 8.08 (d, J = 26.6 Hz, 2H), 7.95 (s, 1H), 7.54 (m, 1H), 7.25 (s, 2H), 5.81 (s, 2H).
¹³C NMR (101 MHz, CDCl₃) δ	173.12, 167.63, 150.81, 141.81, 139.85, 137.22, 134.67, 131.20, 128.94, 126.91, 124.65, 123.21, 119.64.
Elemental Analysis	C, 65.07; H, 4.44; N, 14.23; O, 5.42; S, 10.85

6.2.12. 3-((1Z,3E)-3-(2-(benzo[d]thiazol-2-yl)hydrazineylidene)prop-1-en-1-yl)phenol (23b)


Chemical Formula	: C ₁₆ H ₁₃ N ₃ OS
Color	: White solid
MP	: 172 – 176 ^o C
Mass	Actual mass: 295 Found mass: 312 (M+1+16)
IR KBr pellet (cm⁻¹)	3467 (NH stretching amine); 3019 (CH stretching aromatic); 2890 (CH stretching alkane); 1403 (C - N bending); 817 (aromatic ring)
¹H NMR (400 MHz, CDCl₃) δ	13.38 (m, 1H), 10.29 (s, 1H), 8.08 (d, J = 26.6 Hz, 2H), 7.95 (s, 1H), 7.54 (m, 1H), 7.25 (s, 2H), 5.81 (s, 2H).
¹³C NMR (101 MHz, CDCl₃) δ	173.12, 167.63, 150.81, 141.81, 139.85, 137.22, 134.67, 131.20, 128.94, 126.91, 124.65, 123.21, 119.64.
Elemental Analysis	C, 65.07; H, 4.44; N, 14.23; O, 5.42; S, 10.85

6.2.13. 4-((1Z,3E)-3-(2-(benzo[d]thiazol-2-yl)hydrazineylidene)prop-1-en-1-yl)phenol (24b)


Chemical Formula	: C ₁₆ H ₁₃ N ₃ OS
Color	: White solid
MP	: 172 – 176 ^o C
Mass	Actual mass: 295 Found mass: 297 (M+2)
IR KBr pellet (cm⁻¹)	3440 (NH stretching amine); 2908 (CH stretching aromatic); 2874 (CH stretching alkane); 1423 (C - N bending); 845 (aromatic ring)
¹H NMR (400 MHz, CDCl₃) δ	13.38 (m, 1H), 10.29 (s, 1H), 8.08 (d, J = 26.6 Hz, 2H), 7.95 (s, 1H), 7.54 (m, 1H), 7.25 (s, 2H), 5.81 (s, 2H).
¹³C NMR (101 MHz, CDCl₃) δ	173.12, 167.63, 150.81, 141.81, 139.85, 137.22, 134.67, 131.20, 128.94, 126.91, 124.65, 123.21,

	119.64.
Elemental Analysis	C, 65.07; H, 4.44; N, 14.23; O, 5.42; S, 10.85

6.3. Determination of Minimum inhibitory concentration (MIC)

Antibacterial activity of synthesized compounds was evaluated by broth microdilution method (CLSI 2007) using Mueller Hinton medium (Hi-media). The MIC value of tested compounds is presented, respectively in **Table 2** and compared with the standard drugs ciprofloxacin. All the tested compounds exhibited variable activity against the tested Gram- positive and Gram-negative bacterial strains. Among all tested compounds **17, 18, 22 and 23** exhibited maximum activity against *S. aureus* NCIM 5021 and *S. epidermidis* NCIM 2493 with MIC of 45 – 50 μ M. against *S. aureus* NCIM 5022 compared to the standard drugs ciprofloxacin (MIC 6.3 μ M). Based on the study the compound 17 and 18 which is substituted with a bulky group like naphthalene ring produce a significant MIC value compared with standard drug.

Table 2. Minimum inhibitory concentration of tested compounds

Compound	Minimum inhibitory concentration (μ M)*	
	<i>Staphylococcus aureus</i> NCIM 5021	<i>Staphylococcus epidermidis</i> NCIM 2493
5b	112.72 \pm 0.74	112.36 \pm 0.68
6b	168.43 \pm 0.81	83.54 \pm 0.98
7b	>420	210.84 \pm 0.8
14b	218.00 \pm 0.76	217.29 \pm 1.19
17b	45.01 \pm 0.89	45.11 \pm 0.82
18b	48.04 \pm 0.25	31.17 \pm 0.7
21b	207.42 \pm 0.49	104.545 \pm 0.91
22b	54.29 \pm 0.59	54.29 \pm 0.67
23b	56.97 \pm 0.25	52.55 \pm 0.62
24b	92.84 \pm 0.09	105.53 \pm 0.21
Ciprofloxacin	6.18 \pm 0.82	6.33 \pm 0.52

*Values are mean \pm SEM ($n = 3$).

6.4. Determination of Minimum Bactericidal Concentration (MBC)

MBC of tested compounds is reported in Table 3. It is evident that all the tested compounds except compound 23 are bactericidal (MBC/MIC ≥ 2) against *S. aureus* NCIM 5021 and the compound 23 possesses bacteriostatic activity on selected strain. In the case of *S. epidermidis*, the compounds 5b, 7b, 17b, 18b, 22b, 23b, and 24b possess the bactericidal activity and remaining compound have bacteriostatic activity on selected strain. This study was compared with a reference drug ciprofloxacin.

Table 3. Represents minimum bactericidal concentration (MBC) and MBC/MIC ratio of title molecules against selected bacterial strains

Compound	MBC & MBC: MIC	<i>Staphylococcus aureus</i> NCIM 5021	<i>Staphylococcus epidermidis</i> NCIM 2493
5b	MBC	43.23 \pm 1.4	44.45 \pm 0.54

	MBC: MIC	2	2
6b	MBC	47.49±0.25	87.68±0.54
	MBC: MIC	2	4
7b	MBC	91.33±1.25	191.81±0.2
	MBC: MIC	2	2
14b	MBC	42.21±1.4	86.80±0.25
	MBC: MIC	2	4
17b	MBC	21.17±0.54	39.08±0.97
	MBC: MIC	2	2
18b	MBC	15.06±0.54	30.53±0.25
	MBC: MIC	2	2
21b	MBC	19.36±0.54	38.22±0.25
	MBC: MIC	2	4
22b	MBC	93.77±0.54	191.8±0.2
	MBC: MIC	2	2
23b	MBC	87.68±0.97	93.77±0.25
	MBC: MIC	4	2
24b	MBC	37.43±0.54	37.43±1.4
	MBC: MIC	2	2
Ciprofloxacin	MBC	2.1±0.45	1.9±0.78
	MBC: MIC	1	<1

7. SUMMARY AND CONCLUSION

- In the present work we designed the novel set of benzothiazole molecule as MurD inhibitors.
- All the designed compounds were subjected to molecular docking studies using discovery studio software.
- Based on docking score all the compounds show significant docking score among them compound 5, 6, 7, 14, 17, 18, 21, 22, 23, and 24 shows top ten compound. Further we selected these compounds for synthesis in conventional method.
- We performed hydroxybenzotriazole (HOBt) and 1-(3- dimethylaminopropyl)-3- ethylcarbodiimide hydrochloride (EDCI) mediated synthesis of a series of N'-(1,3- benzothiazol-2-yl)-substituted aryl/aralkyl hydrazides.
- High yields (80-95%) were obtained under relatively milder reaction conditions using N,N-dimethylformamide and acetone as solvent.
- All our synthesized compounds were purified by column chromatography and characterized by FT-IR, ¹H-NMR, ¹³C-NMR and HRMS spectral data.
- In the ¹H-NMR spectra splitting patterns for the aromatic protons were observed to be in agreement with the substitution pattern of respective compounds.
- In the ¹³C-NMR spectrum of synthesized compounds the carbonyl carbon of benzamide, azomethine carbon of benzothiazole and aromatic SP² hybridized carbon signals appeared in the expected region.
- The MIC value of all the synthesized compounds was evaluated by broth microdilution method using Mueller Hinton medium.

- Tested compounds showed variable activity against the tested Gram-positive and Gram-negative bacterial strains. Compounds 17, 18, 22, and 23 showed high activity against *S. aureus* and *S. epidermidis* and also exhibited bactericidal activity against this strain in MBC determination. The whole study was compared with Ciprofloxacin.
- Based on above binding this study may be concluded as the substitution in the benzothiazole molecules blocks the activity of MurD enzyme in bacterial organism.

REFERENCES

1. Jacobs MR. Worldwide trends in antimicrobial resistance among common respiratory tract pathogens in children. *Pediatr Infect Dis J*. 2003;22:109-19.
2. Outtersen K. Testimony of Kevin Outtersen (Boston University School of Law) to the House Energy and Commerce Committee, September 19, 2014. Boston Univ. School of Law, Public Law Research Paper. 2014:14-51.
3. The World Bank. Current health expenditure (% of GDP).
4. <https://data.worldbank.org>. Antimicrobial Resistance Centre. Economic, social and political sciences.
5. Boston Consulting Group. Report for the German Guard Initiative. Breaking through the Wall—enhancing research and development of antibiotics inscience and industry. Global Union for Antibiotics Research and Development (GUARD) Initiative. Boston Consulting Group; 2015.
6. Mahin G, Hamed K. Role of Biotechnology in Cancer Control. *Int. J. Sci. Res*. 2015;5:180 – 185.
7. Aaron JS, John O, Dino Prato. Immunotherapy in Cancer Treatment. *Open J. Med. Microbiol*. 2014;4:178 - 191.
8. Akulapalli S. History of Cancer, Ancient and Modern Treatment Methods. *J. Cancer Sci. Ther*. 2009;1(2):1948 – 5956.
9. Yapeng, H, Liwu F. Targeting cancer stem cells: a new therapy to cure cancer patients. *Am. J. Cancer Res*. 2012;2(3):340 - 356.
10. Anant NB, Rohit M, Abdullah F, Amit V, Dwarakanath BS. Cancer biomarkers - Current perspectives. *Indian J. Med. Res*. 2010;132:129 - 149.
11. Tokajian S. New epidemiology of *Staphylococcus aureus* infections in the Middle East. *Clin Microbiol Infect* 2014; 20:624–8.
12. Boucher HW, Corey GR. Epidemiology of methicillin-resistant *Staphylococcus aureus*. *Clin Infect Dis* 2008; 46(Suppl 5):344–9.
13. Haddadin A, Fappiano S, Lipsett P. Methicillin resistant *Staphylococcus aureus*(MRSA) in the intensive care unit. *Postgrad Med J* 2002; 78:385–92.
14. Jarvis WR, Jarvis AA, Chinn RY. National prevalence of methicillin-resistant *Staphylococcus aureus* in inpatients at United States health care facilities, 2010. *Am J Infect Control* 2012; 40:194–200.
15. Dulon M, Haamann F, Peters C, Schablon A, Nienhaus A. MRSA prevalence in European healthcare settings: a review. *BMC Infect Dis* 2011; 11:138.
16. Wilson J, Elgohari S, Livermore DM, Cookson B, Johnson A, Lamagni T, et al. Trends among pathogens reported as causing bacteraemia in England, 2004–2008. *Clinical Microbiology and Infection* 2010; 17:451–8.
17. Simner PJ, Zhanel GG, Pitout J, Tailor F, McCracken M, Mulvey MR, et al. Prevalence and

- characterization of extended-spectrum b-lactamase- and AmpC b-lactamase- producing *Escherichia coli*: results of the CANWARD2007–2009 study. *Diagnostic Microbiology and Infectious Disease* 2011; 69:326–34.
18. Lu PL, Liu YC, Toh HS, Lee YL, Liu YM, Ho CM, et al. Epidemiology and antimicrobial susceptibility profiles of Gram-negative bacteria causing urinary tract infections in the Asia-Pacific region: 2009–2010 results from the Study for Monitoring Antimicrobial Resistance Trends (SMART). *Int J Antimicrob Agents* 2012; 40(Suppl):S37–43.
19. Livermore DM. Fourteen years in resistance. *International Journal of Antimicrobial Agents* 2012; 39:283–94.
20. Yang Q, Zhang H, Wang Y, Xu Y, Chen M, Badal RE, et al. A 10 year surveillance of antimicrobial susceptibility of *Escherichia coli* and *Klebsiella pneumoniae* in community- and hospital-associated intra-abdominal infections in China. *J Med Microbiol* 2013; 62:1343–9.
21. Lee JC, Lee NY, Lee HC, Huang WH, Tsui KC, Chang CM, et al. Clinical characteristics of urosepsis caused by extended-spectrum b-lactamase-producing *Escherichia coli* or *Klebsiella pneumoniae* and their emergence in the community. *J Microbiol Immunol Infect* 2012; 45:127–33.
22. Hawser SP, Bouchillon SK, Hoban DJ, Badal RE, Hsueh PR, Paterson DL. Emergence of high levels of extended-spectrum-b-lactamase-producing Gram-negative bacilli in the Asia-Pacific region: data from the Study for Monitoring Antimicrobial Resistance Trends (SMART) program, 2007. *Antimicrob Agents Chemother* 2009; 53: 3280–4.
23. Hausdorff WP, Feikin DR, Klugman KP. Epidemiological differences among pneumococcal serotypes. *Lancet Infect Dis* 2005; 5:83–93.
24. Kim SH, Song JH, Chung DR, Thamlikitkul V, Yang Y, Wang H, et al. Changing trends in antimicrobial resistance and serotypes of *Streptococcus pneumoniae* isolates in Asian countries: an Asian Network for Surveillance of Resistant Pathogens (ANSORP) study. *Antimicrob Agents Chemother* 2012; 56:1418–26.
25. Lynch JP 3rd, Clark NM, Zhanel GG. Evolution of antimicrobial resistance among Enterobacteriaceae (focus on extended spectrum beta-lactamases and carbapenemases). *Expert Opin Pharmacother*. 2013; 14:199–210.
26. Nathan JJ, Taib NM, Desa MNM, Masri SN, Yasin RM, Jamal F, et al. Prevalence of macrolide resistance and in vitro activities of six antimicrobial agents against clinical isolates of *Streptococcus pneumoniae* from a multi-center surveillance in Malaysia. *Med J Malaysia* 2013; 68:119–24.
27. Jenkins SG, Farrell DJ. Increase in pneumococcus macrolide resistance, United States. *Emerg Infect Dis* 2009; 15:1260–4.
28. Ghoshal U, Garg A, Tiwari DP, Ayyagari A. Emerging vancomycin resistance in enterococci in India. *Indian J Pathol Microbiol* 2006; 49:620–2.
29. Blair JM, Webber MA, Baylay AJ, Ogbolu DO, Piddock LJ. Molecular mechanisms of antibiotic resistance. *Nat Rev Microbiol*. 2015; 13:42–51.
30. Voulgari E, Poulou A, Koumaki V, Tsakris A. Carbapenemase producing Enterobacteriaceae: now that the storm is finally here, how will timely detection help us fight back? *Future Microbiol*. 2013; 8:27–39.
31. Johnson AP, Woodford N. Global spread of antibiotic resistance: the example of New Delhi metallo-beta-lactamase (NDM)-mediated carbapenem resistance. *J Med Microbiol*. 2013; 62:499–513.
32. Woodford N, Turton JF, Livermore DM. Multiresistant Gram-negative bacteria: the role of high-risk

- clones in the dissemination of antibiotic resistance. *FEMS Microbiol Rev.* 2011; 35:736–755.
33. Chuanchuen R, Karkhoff-Schweizer RR, Schweizer HP. High-level triclosan resistance in *Pseudomonas aeruginosa* is solely a result of efflux. *Am J Infect Control.* 2003; 31:124–127.
34. Zhu L, Lin J, Ma J, Cronan JE, Wang H. Triclosan resistance of *Pseudomonas aeruginosa* PAO1 is due to FabV, a triclosan-resistant enoyl-acyl carrier protein reductase. *Antimicrob Agents Chemother.* 2010; 54:689–698.
35. Floyd JL, Smith KP, Kumar SH, Floyd JT, Varela MF. LmrS is a multidrug efflux pump of the major facilitator superfamily from *Staphylococcus aureus*. *Antimicrob Agents Chemother.* 2010; 54:5406–5412.
36. Rm H, Liao ST, Huang CC, Huang YW, Yang TC. An inducible fusaric acid tripartite efflux pump contributes to the fusaric acid resistance in *Stenotrophomonas maltophilia*. *PLoS One.* 2012; 7:e51053.
37. Kim C, Mwangi M, Chung M, Milheirico C, de Lencastre H, Tomasz A. The mechanism of heterogeneous beta-lactam resistance in MRSA: key role of the stringent stress response. *PLoS One.* 2013; 8:e82814.
38. Ogawa W, Onishi M, Ni R, Tsuchiya T, Kuroda T. Functional study of the novel multidrug efflux pump KexD from *Klebsiella pneumoniae*. *Gene.* 2012; 498:177–182.
39. Liu YY, Wang Y, Walsh TR, et al. Emergence of plasmid-mediated colistin resistance mechanism MCR-1 in animals and human beings in China: a microbiological and molecular biological study. *Lancet Infect Dis.* 2016; 16:161–168.
40. Arias M. JM; Arias, CA Mechanisms of Antibiotic Resistance. *Microbiol. Spectr.* 2016; 2:1-37.
41. Nikaido H. Multidrug resistance in bacteria. *Annu Rev Biochem.* 2009; 78: 119–46.
42. Bryan LE, Kwan S Mechanisms of aminoglycoside resistance of anaerobic bacteria and facultative bacteria grown anaerobically *Antimicrob Chemother* 1981; 8 Suppl D: 1–8.
43. Schaechter M, Engleberg NC, DiRita VJ et al. Schaechter's Mechanisms of Microbial Disease. Lippincott Williams & Wilkins, Philadelphia: 2007.
44. Alanis AJ. Resistance to antibiotics: are we in the post-antibiotic era? *Arch Med Res* 2005; 36:697–705.
45. Abee T, Kovacs AT, Kuipers OP et al. Biofilm formation and dispersal in Gram-positive bacteria. *Curr Opin Biotechnol* 2011; 22:172–9.
46. Donlan RM. Biofilms: microbial life on surfaces. *Emerg Infect Dis* 2002; 8:881–90.
47. Gilbert P, Collier PJ, Brown M. Influence of growth rate on susceptibility to antimicrobial agents: biofilms, cell cycle, dormancy, and stringent response. *Antimicrobial agents and chemotherapy* 1990; 34:1865.
48. Wood TK, Knabel SJ, Kwan BW. Bacterial persister cell formation and dormancy. *Appl Environ Microbiol* 2013; 79:7116–21.
49. Holmes AH, Moore LS, Sundsfjord A, et al. Understanding the mechanisms and drivers of antimicrobial resistance. *Lancet.* 2016; 387:176–187.
50. Stokes HW, Gillings MR. Gene flow, mobile genetic elements and the recruitment of antibiotic resistance genes into Gram-negative pathogens. *FEMS Microbiol Rev.* 2011; 35:790–819.
51. Laxminarayan R, Duse A, Wattal C, et al. Antibiotic resistance—the need for global solutions. *Lancet Infect Dis.* 2013; 13(12):1057–1098.
52. Wellington EM, Boxall AB, Cross P, et al. The role of the natural environment in the emergence of

- antibiotic resistance in Gram-negative bacteria. *Lancet Infect Dis.* 2013; 13(2):155–165.
53. Lewis DA. The role of core groups in the emergence and dissemination of antimicrobial-resistant *N. gonorrhoeae*. *Sex Transm Infect.* 2013; 89(Suppl 4):47–51.
54. Chamchod F, Ruan S. Modeling methicillin-resistant *Staphylococcus aureus* in hospitals: transmission dynamics, antibiotic usage and its history. *Theor Biol Med Model.* 2012; 9:25.
55. Anderson ES, Lewis MJ. Drug resistance and its transfer in *Salmonella typhimurium*. *Nature.* 1965; 206(984):579–583.
56. Molbak K. Spread of resistant bacteria and resistance genes from animals to humans – the public health consequences. *J Vet Med B Infect Dis Vet Public Health.* 2004; 51:364–369.
57. Humphrey TJ, Jorgensen F, Frost JA, et al. Prevalence and subtypes of ciprofloxacin-resistant *Campylobacter* spp. in commercial poultry flocks before, during, and after treatment with fluoroquinolones. *Antimicrob Agents Chemother.* 2005; 49:690–698.
58. Kristiansson E, Fick J, Janzon A, et al. Pyrosequencing of antibiotic-contaminated driver sediments reveals high levels of resistance and gene transfer elements. *PLoS One.* 2011; 6:17038.
59. Van Heijenoort J. Recent advances in the formation of the bacterial peptidoglycan monomer unit. *Natural product reports.* 2001; 18:503-19.
60. Silver LL. Does the cell wall of bacteria remain a viable source of targets for novel antibiotics? *Biochemical pharmacology* 2006; 71:996-1005.
61. El Zobeiry A, Sanschagrin F, Levesque RC. Structure and function of the Mur enzymes: development of novel inhibitors. *Molecular microbiology* 2003; 47:1-2.
62. Bouhss A, Mengin-Lecreulx D, Blanot D, van Heijenoort J, Parquet C. Invariant amino acids in the Mur peptide synthetases of bacterial peptidoglycan synthesis and their modification by site-directed mutagenesis in the UDP-MurNAc: L-alanine ligase from *Escherichia coli*. *Biochemistry* 1997; 36:11556-63.
63. Walsh AW, Falk PJ, Thanassi J, Discotto L, Pucci MJ, Ho HT. Comparison of the D-glutamate-adding enzymes from selected gram-positive and gram-negative bacteria. *Journal of bacteriology.* 1999 Sep; 181:5395-401.
64. Bertrand JA, Auger G, Fanchon E, Martin L, Blanot D, Van Heijenoort J, Dideberg O. Crystal structure of UDP-N-acetylmuramoyl-L-alanine:D-glutamate ligase from *Escherichia coli*. *The EMBO journal.* 1997; 16:3416-25.
65. Bertrand JA, Fanchon E, Martin L, Chantalat L, Auger G, Blanot D, van Heijenoort J, Dideberg O. “Open” structures of MurD: domain movements and structural similarities with folylpolyglutamate synthetase. *Journal of molecular biology.* 2000; 301:1257-66.
66. Perdih Perdih A, Kotnik M, Hodoscek M, Solmajer T. Targeted molecular dynamics simulation studies of binding and conformational changes in *E. coli* MurD. *PROTEINS: Structure, Function, and Bioinformatics.* 2007; 68:243-54.
67. Jacobs MR. Worldwide trends in antimicrobial resistance among common respiratory tract pathogens in children. *Pediatr Infect Dis J.* 2003; 22:S109-19.
68. R. Frlan, A. Kovac, D. Blanot, S. Gobec, S. Pecar, A. Obreza. Design and Synthesis of Novel N-Benzylidenesulfonohydrazide Inhibitors of MurC and MurD as Potential Antibacterial Agents. *Molecules*, **2008**, 12 – 32.
69. Sova M, Kovač A, Turk S, Hrast M, Blanot D, Gobec S. Phosphorylated hydroxyethylamines as novel inhibitors of the bacterial cell wall biosynthesis enzymes MurC to MurF. *Bioorganic*

- chemistry. 2009; 37:217-22.
70. Tomasic T, Zidar N, Rupnik V, Kovač A, Blanot D, Gobec S, Kikelj D, Mašič LP. Synthesis and biological evaluation of new glutamic acid-based inhibitors of MurD ligase. *Bioorganic & Medicinal Chemistry Letters*. 2009; 19:153-7.
71. Tomašić T, Kovač A, Simčič M, Blanot D, Grdadolnik SG, Gobec S, Kikelj D, Mašič LP. Novel 2-thioxothiazolidin-4-one inhibitors of bacterial MurD ligase targeting D- Glu-and diphosphate-binding sites. *European journal of medicinal chemistry*. 2011; 46:3964-75.
72. K. Osmana, D. Evangelopoulosb, C. Basavannacharya, A. Guptab, T.D. McHughc, S. Bhaktab, S. Gibbons. An antibacterial from *Hypericum acmosepalum* inhibits ATP- dependent MurE ligase from *Mycobacterium tuberculosis*. *International Journal of Antimicrobial Agents* 39 (2012) 124– 129.
73. Barreateau H, Sosič I, Turk S, Humljan J, Tomašić T, Zidar N, Hervé M, Boniface A, Peterlin-Mašič L, Kikelj D, Mengin-Lecreulx D. MurD enzymes from different bacteria: evaluation of inhibitors. *Biochemical pharmacology*. 2012; 84:625-32.
74. Y. Yang, A. Severin, R. Chopra, G. Krishnamurthy, G. Singh, William Hu, D. Keeney,
75. K. Svenson, P.J. Petersen, P. Labthavikul, D.M. Shlaes, B.A. Rasmussen, A.A. Failli,
76. J.S. Shumsky, K.M.K. Kutterer, A. Gilbert, T.S. Mansour. 3,5-Dioxypyrazolidines, Novel Inhibitors of UDP-NAcetylenolpyruvylglucosamine Reductase (MurB) with Activity against Gram-Positive Bacteria. *Antimicrobial agents and chemotherapy*, 2006, 556–564.
77. Novak A, Testen A, Bezenšek J, Grošelj U, Hrast M, Kasunič M, Gobec S, Stanovnik B, Svete J. Synthesis of pyrazolo [1, 2-a] pyrazole-based peptide mimetics. *Tetrahedron*. 2013; 69:6648-65.
78. A. Perdih, M. Hrast, H. Barreateau, S. Gobec, G. Wolber, T. Solmajer. Inhibitor Design Strategy Based on an Enzyme Structural Flexibility: A Case of Bacterial MurD Ligase. *J. Chem. Inf. Model*. 2014, 54, 1451–1466.
79. Perdih A, Wolber G, Solmajer T. Molecular dynamics simulation and linear interaction energy study of d-Glu-based inhibitors of the MurD ligase. *Journal of computer-aided molecular design*. 2013; 27:723-38.
80. Sarkar S. Design, Synthesis, and Evaluation of Antitubercular Activity of Novel Benzothiazole-Containing an Azetidinone Ring. *Istanbul; Istanbul J Pharm*. 2018; 48 (2): 28-31
81. P. Sai Harshita, CH. Supriya, S. Sravanthi, V. Jyothi, S.R. Peddi1, V. Manga, V. Saddanapu, T. Saritha Jyostna. Design synthesis and biological evaluation of dithiocarbamate substituted 2-aminobenzothiazole derivatives as proviral integration site of moloney murine leukaemia virus 1 kinase inhibitors. *Indian J Pharm Sci* 2020;82(6):1015-1024.
82. Rakesh Kumar Paul, MA azam, Srikanth Jupudi. Synthesis, Molecular Docking and Antibacterial Activity of Some Novel Pyridin-2-yl-Carbamodithioates. *FABAD J. Pharm. Sci.*,2020, 45, 1, 9-18.